UAB
Universitat Autònoma de Barcelona

High resolution cardiovascular magnetic resonance as a tool in evaluating the efficacy of P2Y12 receptor antagonists to preserve cardiac microcirculation and limit adverse left ventricular remodelling post myocardial infarction

Doctoral thesis by

MONIKA RADIKĖ

High resolution cardiovascular magnetic resonance as a tool in evaluating the efficacy of P2Y12 receptor antagonists to preserve cardiac microcirculation and limit adverse left ventricular remodelling post myocardial infarction

DOCTORAL THESIS

Doctoral student:
Monika Radikė

Supervisors:
Dr Gemma Vilahur García
Dr Alberto Hidalgo Pérez
Prof Lina Badimon Maestro

Tutor:
Prof Joan Cinca Cuscullola

PhD Program in Medicine
Department of Medicine
Universitat Autònoma de Barcelona (UAB)

2023

Cover artwork by Jorūnė Emilija Valaikaitė, 2022.

Certification

Dr Gemma Vilahur García
Cardiovascular Program-ICCC, Research Institute Hospital de la Santa Creu i Sant Pau, Barcelona, Spain
CiberCV, Institute Carlos III, Madrid, Spain

Dr Alberto Hidalgo Pérez
Department of Radiology
Hospital de la Santa Creu i Sant Pau,
Barcelona, Spain

Prof Lina Badimón Maestro
Cardiovascular Program-ICCC, Research Institute Hospital de la Santa Creu i Sant Pau, Barcelona, Spain
CiberCV, Institute Carlos III, Madrid, Spain
Cardiovascular Research Chair, UAB, Barcelona, Spain
Institut de Recerca, IIB-Sant Pau and Hospital Santa Creu i Sant Pau

Prof Joan Cinca Cuscullola
Department of Cardiology, Hospital de la Santa Crei i Sant Pau,
Barcelona, Spain
Research Institute Hospital de la Santa Creu i Sant Pau, Barcelona, Spain

Certify:

That Monika Radikė (née Aržanauskaitė), licenced physician and radiology specialist, has undertaken the following doctoral project under their supervision:

"High resolution cardiovascular magnetic resonance as a tool in evaluating the efficacy of P2Y12 receptor antagonists to preserve cardiac microcirculation and limit adverse left ventricular remodelling post myocardial infarction"

These studies have been completed by the below date, with the final presented project revised and approved for thesis defence.

2023

Acknowledgements

How do you thank so many people?

Some years ago, when I was a medical student, my uncle emailed me a photograph from his holiday trip to Barcelona, with a note along the lines of "Maybe you will be among them one day". The photograph – now sadly lost – showed a group of doctors enjoying a sunny break on the steps of the modernist Sant Pau Hospital. The background was unmistakable: red bricks, ornate decorations, green garden leaves and a blue sky. Little did I know that my path would eventually take me to the very same place for several very rewarding endeavours, including this incredible opportunity to learn from researchers who by exploring the possibilities of cardiovascular science contribute to people's health with a rarely found level of enthusiasm and professionalism.

A finished dissertation thesis would be impossible without considerable support. Sant Pau Hospital, apart from their outstanding clinical work, is a treasured knowledge hub, where many ideas arise and flourish. I could not have wished for a better team and supporters in this journey and am very grateful.

- Gemma Vilahur, apart from being an excellent supervisor, has quickly become a role model for me in daily work – research and beyond.
- Alberto Hidalgo, one of the first cardiac imaging connoisseurs I met has been extremely supportive in all radiology-related aspects of the project.
- Lina Badimón, for her trust, supervision and always to-the-point insight.
- Joan Cinca, for his trust, support and ideas that make one postulate new possibilities boldly.
- Javier Esposito and Ada Nuñez: without their dedication, none of the scans would be available for this project.

List of Abbreviations

ACS – acute coronary syndrome
AK – adenosine kinase
ADP – adenosine diphosphate
AMP – adenosine monophosphate
AMPK – AMP-activated protein kinase
AMI – acute myocardial infarction
ANT – adenine nucleotide translocator
AR – adenosine receptor
ATP – adenosine triphosphate
BP – blood pressure
CAD – coronary artery disease
Cmax – maximum serum concentration
CMR – cardiovascular magnetic resonance
Cox – cyclooxygenase
CYP – cytochrome P
CypD – cyclophilin D
CVD – cardiovascular disease
DAPT – dual antiplatelet therapy
ECG – electrocardiography
EGE – early gadolinium enhancement
FWHM – full width half maximum
HDL – high-density lipoprotein
HR – heart rate
IFNy – interferon gamma
IHD – ischaemic heart disease
IMH – intramyocardial haemorrhage
LAD – left anterior descending
LDL – low-density lipoprotein
LGE – late gadolinium enhancement
LV – left ventricle
LVEDV – left ventricular end diastolic volume

LVEF – left ventricular ejection fraction

LVESV – left ventricular end systolic volume

LVSV – left ventricular stroke volume

mPTP – mitochondrial permeability transition pore

MVO – microvascular obstruction

NO – nitric oxide

PKC – protein kinase C

PKG – cGMP-dependent protein kinase

RAS – renin-angiotensin system

ROS – reactive oxygen species

RV – right ventricle

RVEDV – right ventricular end diastolic volume

RVEF – right ventricular ejection fraction

RVESV – right ventricular end systolic volume

RVSV – right ventricular stroke volume

MI – myocardial infarction

MMPs – matrix metalloproteinases

NSTEMI – non-ST-segment elevation myocardial infarction

TGF-β – transforming growth factor-beta

TF – tissue factor

TXA_2 – thromboxane A2

STEMI – ST-segment elevation myocardial infarction

VDAC – voltage-dependent anion channel

VSMC – vascular smooth muscle cells

vWf – von Willebrand factor

TABLE OF CONTENTS

Abstract

Background: Cardiovascular disease, which includes ischaemic heart disease, remains the leading cause of death worldwide. Despite advances in the context of revascularisation, to date there are no cardioprotective strategies capable of reducing infarct size, the main prognostic marker of mortality and hospitalization for heart failure. The search for new therapeutic strategies capable of reducing cardiac damage after infarction is needed. Platelet P2Y12 receptor inhibitors have been shown to exert cardioprotective effects beyond their antiplatelet properties. In fact, ticagrelor has been shown to reduce infarct size through adenosine-dependent mechanisms. Adenosine is a protective molecule that is released during myocardial ischemia due to the hydrolysis of adenosine triphosphate to adenosine monophosphate by apyrases, and its subsequent conversion to adenosine. We hypothesise that intravenous administration of a recombinant human apyrase (AZD3366) in ticagrelor-treated animals will decrease infarct-induced myocardial damage to a greater extent than single administration of ticagrelor.

Design: Pigs were treated with loading doses of ticagrelor and subsequently had an acute myocardial infarction (AMI) induced by balloon occlusion of the left anterior descending artery. Prior to reperfusion, pigs received intravenously: 1) vehicle; 2) 1 mg/kg AZD3366; or 3) 3 mg/kg AZD3366. After reperfusion, animals received maintenance doses of ticagrelor for the next 42 days. An untreated control group also underwent AMI induction. Myocardial function and damage were then assessed by cardiovascular magnetic resonance (CMR) imaging at days 3 and 42 post-AMI. At day 42 the animals were sacrificed, and histological and molecular analyses of the infarcted heart were performed. Two additional studies were performed. The first aimed to determine the optimal ischaemia time to induce sufficient myocardial damage, and the second one aimed to validate the interoperability of two computer programs to analyse CMR data.

Results: Intravenous administration of a soluble recombinant apyrase (AZD3366) prior reperfusion on top of ticagrelor exerts additive and synergistic cardioprotective effects to those observed with ticagrelor alone. Furthermore, we demonstrate that 90 min of ischaemia induces necrotic and microvascular damage and cardiac remodelling amenable to therapeutic intervention. Moreover, although different computer programs can be used to analyse CMR data, it is especially important to use the same program to reliably monitor infarct size over time.

Resumen

Contexto: Las enfermedades cardiovasculares, que incluyen la cardiopatía isquémica, siguen siendo la principal causa de muerte en todo el mundo. A pesar de los avances en el contexto de la revascularización, a fecha de hoy, no existen estrategias cardioprotectoras capaces de reducir el tamaño de infarto, el principal determinante pronóstico de mortalidad y hospitalización por insuficiencia cardíaca. Es necesario la búsqueda de nuevas estrategias terapéuticas capaces de reducir el daño cardíaco tras sufrir un infarto. Los inhibidores del receptor plaquetar P2Y12 han demostrado ejercer efectos cardioprotectores más allá de sus propiedades antiplaquetares. De hecho, se ha demostrado que el ticagrelor reduce el tamaño de infarto mediante mecanismos dependiente de adenosina. La adenosina es una molécula protectora que se libera durante la isquemia miocárdica debido a la hidrólisis del trifosfato de adenosina en monofosfato de adenosina por apirasas, y su posterior conversión a adenosina. Nuestra hipótesis es que la administración intravenosa de una apirasa recombinante humana (AZD3366) en animales tratados con ticagrelor disminuirá el daño miocárdico inducido por el infarto en mayor medida que la administración única de ticagrelor.

Diseño: Los cerdos se trataron con dosis de carga de ticagrelor y posteriormente se les indujo infarto agudo de miocardio (IAM) mediante oclusión por balón de la arteria descendiente anterior izquierda. Antes de la reperfusión, los cerdos recibieron por vía intravenosa: 1) vehículo; 2) 1 mg/kg de AZD3366; o 3) 3 mg/kg de AZD3366. Tras la reperfusión, los animales recibieron dosis de mantenimiento de ticagrelor durante los siguientes 42 días. Se realizó un grupo de control sin tratar al que también se le indujo IAM. Posteriormente se estudiaron la función y daño miocárdicos mediante resonancia magnética cardiovascular (RMC) a los días 3 y 42 post-IAM. A día 42 los animales fueron sacrificados y se

realizaron análisis histológicos y moleculares del corazón infartado. Se han realizado dos estudios adicionales. Uno para determinar el tiempo óptimo de isquemia para inducir suficiente daño miocárdico y el otro para validar la interoperabilidad de dos programas informáticos para analizar las RMCs.

Resultados: La administración intravenosa previa a la reperfusión de una apirasa recombinante soluble (AZD3366) junto a ticagrelor ejerce efectos cardioprotectores aditivos y sinérgicos a los observados con la administración única de ticagrelor. Además, demostramos que 90 min de isquemia inducen un daño necrótico y microvascular así como un remodelado cardíaco susceptibles de intervención terapéutica. Es más, a pesar de que pueden usarse programas informáticos diferentes para poder analizar los datos de RMCs, es especialmente importante usar siempre el mismo programa para poder monitorizar de manera fiable el tamaño de infarto de manera seriada.

1. Introduction

1.1. Acute myocardial infarction in the context of public health

Cardiovascular diseases (CVDs) have been the leading cause of death in the world in the last two decades: in 2016, a total of 17.9 million people died from all causes of CVDs (coronary heart disease, cerebrovascular disease, peripheral arterial disease, rheumatic heart disease, congenital heart disease and deep vein thrombosis with pulmonary embolism) (1). In 2015, there were approximately 8.9 million deaths due to ischaemic heart disease (IHD) across the world, resulting in being the number one cause of death worldwide; less prevalent disease groups were stroke, hypertensive heart disease, among others. Geographically, in Europe, IHD causes an estimate of 1.74 million deaths yearly out of 3.9 million deaths caused by CVDs (2). In the United States of America, CVDs caused 840,768 deaths in 2016 (3).

Moreover, likely due to public health policies such as immunisation and adoption of lifestyle including diet from the West, atherosclerotic cardiovascular disease patterns have been changing worldwide, contributing to an epidemiological transition: Dai et al. found that the age-standardised rate of IHD-related deaths was 116.9/100000 worldwide with the highest incidence and death rates in the regions of North Africa, Middle East and Central Asia, while the prevalence of CVDs has dropped by 16.1% in Western Europe and by 14.8% in high-income North America from 1990 to 2017 (**Figure 1)** (4). This means that while the population ages across regions, despite some CVD prevalence reduction in the Northern Hemisphere, CVD risk is increasing in other parts of the world.
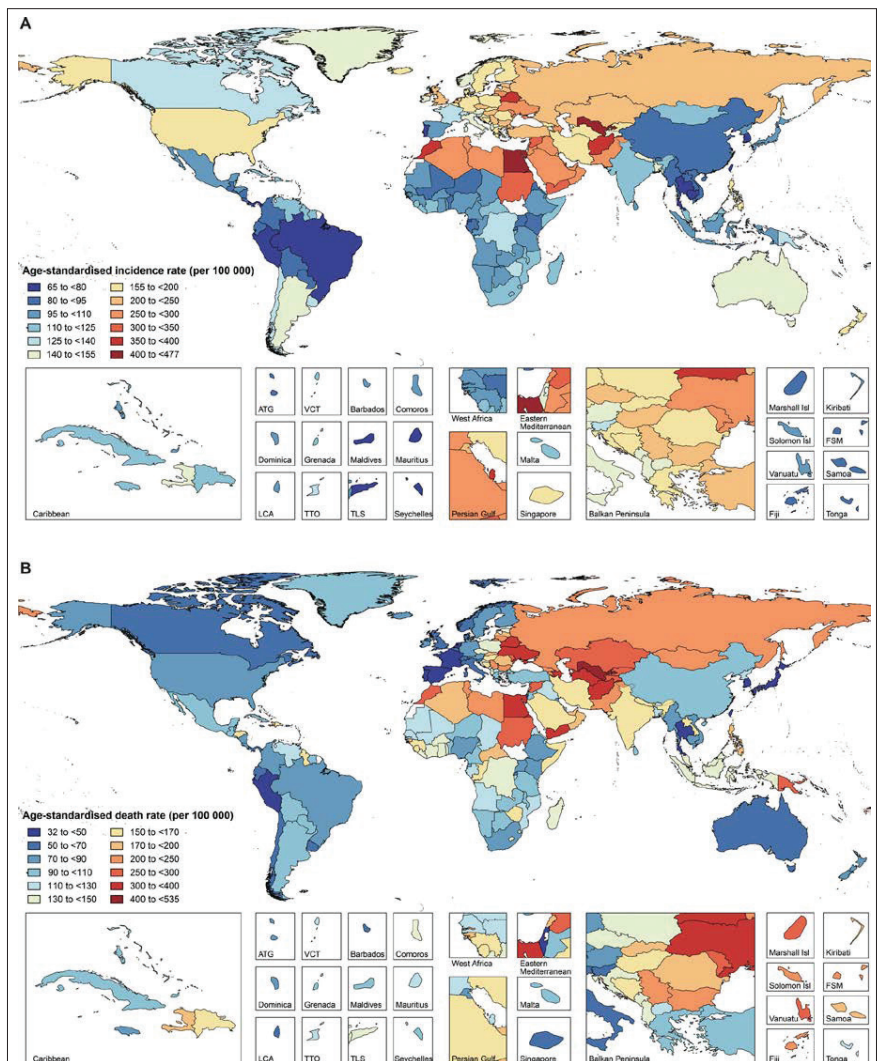
Figure 1. Age-standardised incidence (A) and death (B) rates of ischaemic heart disease across 195 countries and territories for both sexes, 2017. ATG, Antigua and Barbuda; FSM, Federated States of Micronesia; Isl, Islands; LCA, Saint Lucia; TLS, Timor-Leste; TTO, Trinidad and Tobago; VCT, Saint Vincent and the Grenadines. Reused with permission (licence number 5321951056735) from Dai et al (4).

It is worth defining the two currently used clinical / electrocardiographical patterns of acute myocardial infarction (MI) early: in acute coronary artery disease, MI, depending on the predicted transmurality of the myocardial injury and related electrocardiography (ECG) changes, can result in Non-ST-segment Elevation Myocardial Infarction (NSTEMI) or ST-segment Elevation Myocardial Infarction (STEMI), although an overlap of patterns has been recently reported (5). STEMI is considered the most severe type of ischaemic myocardial injury.

Transmural ischaemia of the myocardium in the territory of the obstructed epicardial coronary artery (or arteries) causes symptoms of an acute coronary syndrome (ACS), characteristic dynamic ECG changes with ST-segment elevation and presence of cardiac biochemical markers (6).

1.2. Atherosclerosis and atherothrombosis in acute coronary syndrome

1.2.1. Atherosclerosis

The most common causes of coronary artery obstruction are rupture or erosion of an atherosclerotic plaque with thrombus formation. Since the twentieth century, the understanding of the pathophysiology of atherosclerosis has been evolving from a concept of cholesterol storage disease in the arterial walls to the current evidence of molecular and cellular inflammation pathways and atherosclerotic plaque formation (7). The arterial wall consists of three layers: adventitia, tunica media and the intima, the latter being the innermost to the lumen (8). The adventitia is composed of collagenous connective tissue, supplied by nerve endings and vasa vasorum; it also contains mast cells (multifactorial myeloid-line mesenchymal cells involved in many immune and inflammatory processes, depending on their phenotypical expression). The tunica media is comprised of smooth muscle cells and a

collagenous extracellular matrix containing several glycoproteins and proteoglycans. Regarding the intima (sometimes called tunica intima), it is the thinnest layer, composed of endothelial cells lining the lumen on a basement membrane and a subendothelial extracellular matrix composed of collagen and elastin. While acting as a physical barrier, the endothelium also takes part in vascular functions such as vessel tone, coagulation and inflammation. The atherosclerotic plaque mainly develops in the intima.

As recently and elegantly reviewed by Libby et al. in detail (9), the pathological mechanisms can be briefly divided into the following three phases:

1) Initiation of atherosclerosis:

Long-term increase of circulating levels of low-density lipoprotein (LDL) cholesterol particles can cause intimal accumulation of LDL. Due to their phospholipid coating, these particles easily cross the cellular membrane and accumulate in the intima. The current line of thought, based on experimental data, is that after oxidation and other modifications, the LDL particles can become pro-inflammatory and immunogenic and thus promote atherosclerosis (10). This results in endothelial cell activation (expression of adhesion molecules) and the release on chemoattractant mediators that induce monocyte recruitment and attachment to the endothelium and further transmigration into the intima. There, monocytes differentiate into macrophages and, after engulfing oxidized LDL particles, turn into foam cells. T-lymphocytes also contribute, although to a lesser extent, to cellular regulation and can mediate smooth muscle cell migration into the intima. In addition, LDL particles can aggregate and incorporate into the vascular smooth muscle cells (VSMC), where, similarly as in macrophages/foam cells, contribute to the atherosclerosis progression (11).

2) Progression of atherosclerosis:

Both foam cells and lipid-rich VSMC initially contribute to plaque growth since they contribute to cellular proliferation and the synthesis of extracellular matrix components (collagen, elastin, proteoglycans and glycosaminoglycans). While the extracellular matrix thickens the intima, its protective effect of fibrous cap formation is negatively influenced by activated-macrophage derived matrix metalloproteinases (MMPs), and likely by impaired collagen synthesis due to the effect of interferon gamma (IFNy), as well (9). The thin fibrous cap is thus less effective in preventing plaque rupture to occur.

In the growing plaque, defective cellular division and ineffective efferocytosis (clearance of the apoptotic cells) result in an intra-intimal core of dead lipid-enriched macrophages and VSMC.

Depending on their type, T-cells differ in their effect on atherosclerotic plaque progression: T helper-1 cells promote atherosclerosis progression whereas T helper-2 cells can reduce inflammation, VSMC proliferation and promote collagen synthesis via transforming growth factor-beta (TGF-β) secretion. The adventitial vasa vasorum also a contains lymphatic network, which can drain some of the plaque components to the lymph nodes, activating T and B cells and modulate further immune responses via cytokines. Additionally, a relationship between clonal haematopoiesis and cardiovascular risk has been recently reported, further supporting the role of leucocytes in atherosclerosis progression (12,13).

Eventually, the lipid-rich necrotic core of the plaque may become calcified. There are two main patterns of calcification: larger calcium accumulations are seen as more stable plaques, while microscopic or spotty (of lower density) calcifications are associated with vulnerable plaques (14,15).

3) Complications of atherosclerosis:

This phase covers several overlapping processes of plaque degeneration, which include plaque remodelling and plaque erosion or rupture:

- Remodelling

With time, a growing plaque expands. It firstly expands outside the lumen towards the media and adventitia (eccentric plaque), and the lumen is generally preserved. However, responding to the plaque, the vascular wall remodels by thickening of the wall via VSMC production and degradation of extracellular matrix and luminal dilatation (compensatory, positive remodelling). Conversely, negative remodelling refers to the luminal narrowing of the lumen adjacent to the plaque (**Figure 2**). The type of vascular wall remodelling has been described as an instability feature in terms of clinical presentation, with positively remodelled plaques causing more acute cardiovascular events (16,17).
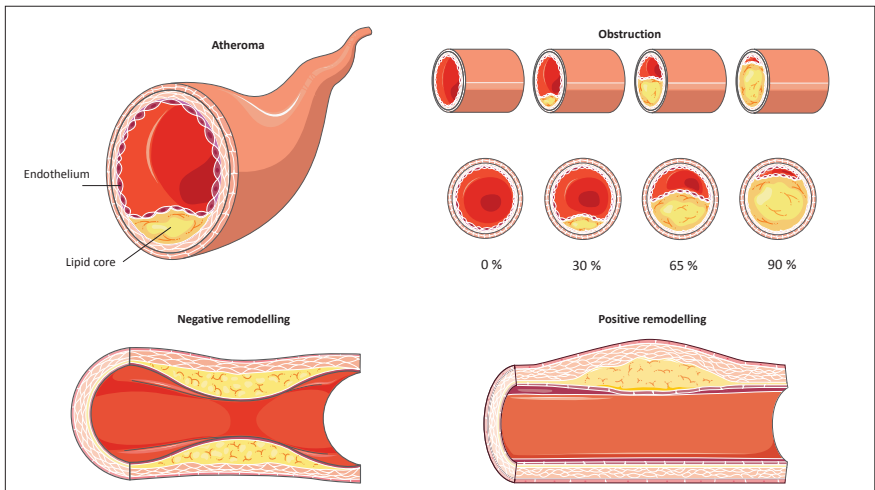
Figure 2. Atheroma and remodelling. Parts of the figure were drawn by using pictures from Servier Medical Art. Servier Medical Art by Servier is licensed under a Creative Commons Attribution 3.0 Unported License (https://creativecommons.org/licenses/by/3.0/).

Growing plaque decreases the luminal area and the luminal blood flow; this can result in ischaemia during increased demand.

- Plaque erosion and rupture:

The growing atherosclerotic plaque can rupture or erode. In a simplified classification, plaques with larger lipid-rich cores with thin fibrous caps have been defined as vulnerable due to their tendency to rupture. On the other hand, those plaques with small lipid-rich cores and thick protective fibrous caps are considered more stable. Furthermore, autopsy data have revealed that most culprit lesions in patients dying of sudden cardiac death had angiographic lumen diameter stenoses of 40% to 69%. Arbustini et al found coronary thrombi in 98% of patients dying with clinically documented acute MI, and of those thrombi, 75% were caused by plaque rupture and 25% by plaque erosion (18). It has been suggested that factors such as age <50y, current smoking, absence of coronary risk factors, lack of multi-vessel disease, reduced lesion severity, larger vessel size and nearby bifurcation are associated with plaque erosion (19).

1.2.2. Atherothrombosis

A nineteenth-century scientist and physician, Rudolf Virchow, described the three components of venous thrombosis ("abnormalities of blood vessel wall", "abnormalities of blood constituents", and "abnormalities of blood flow") (20). Although there have been significant advancements in research in thrombosis since these three pathophysiological factors are still relevant today. While venous thrombosis is more related to stasis and coagulation, the three above principles may also be applicable to arterial thrombosis. Nowadays, these principles are referred to as endothelial injury, abnormalities in platelets, coagulation and fibrinolysis pathways and altered coronary flow at peri- and stenotic regions (21).

Atherothrombosis is a multifactorial process. After an atherosclerotic plaque erodes or ruptures, platelet contribution to thrombus formation results from platelet aggregation and activation

of the coagulation cascade. This process can be resumed in the following steps (22–24):

1) Platelets' contribution to thrombus growth
- *Adhesion*: platelet membrane receptors (with the main proteins being glycoprotein Ib/V/IX and glycoprotein VI) bind to the ligands found on the vascular extracellular matrix components exposed to the blood flow including collagen, fibronectin and to the interaction with collagen-anchored von Willebrand factor (vWf). These interactions promote a firm adhesion of platelets to the vessel surface and triggers "inside-out" signals that favours platelet activation.
- *Activation*: platelet adhesion and further activation induce platelet shape change with the consequent release of its granule content rich in soluble agonists, adhesion molecules, and coagulation factors among others all of which contribute to amplify the thrombotic response. Besides, platelet activation favours TXA_2 generation through cyclooxygenase-1 (Cox-1) dependent arachidonic acid metabolism and exposes phosphatidylserine on the outer leaflet of the platelet plasma membrane providing the surface to form the prothrombinase complex (Xa, Va, phospholipid, and Ca^{2+}). The prothrombinase complex catalyses the conversion of prothrombin into thrombin through factor Xa and co-factor Va allowing platelet activation to occur. Yet, thrombin generation is mainly driven by tissue-factor mediated activation of the extrinsic coagulation pathway through interaction of factors VII and VIIa. Multiple mainly soluble platelet agonists such as adenosine diphosphate (ADP), thromboxane A2 (TXA_2), thrombin, serotonin, and epinephrine, enhance the recruitment and further activation of additional platelets into the forming thrombus. In summary, the overall "inside-out" signaling induces the activation of the GPIIb/IIIa receptor, the most abundant platelet receptor in the platelet surface.

- *Aggregation*: Activated GPIIb/IIIa binds to fibrinogen and vWF favoring platelet aggregation. Besides, GPIIb/IIIa conformational change triggers a second signal cascade ("outside-in" signals) which is pivotal for thrombus stabilization and growth.

2) Activation of the coagulation cascade

The blood coagulation system involves a sequence of reactions integrating zymogens (proteins susceptible to activation into enzymes via limited proteolysis) and co-factors (nonproteolytic enzyme activators) and involves two distinct pathways which crosstalk between them: the extrinsic, or tissue factor (TF)-dependent pathway and the intrinsic or contact activation pathway. Both pathways converge on a final common pathway activated Xa, which converts prothrombin into thrombin. During plaque rupture, flowing blood interacts with inner components of the lesions, TF being among them. The exposed TF is considered to be the initial event triggering arterial thrombosis because induces activation of the coagulation cascade and consequent formation of a fibrin monolayer covering the exposed surface where flowing platelets are further recruited (25). TF starts the extrinsic coagulation by activating the VII factor into VIIa, which in turn activates the factor X, which prompts the common pathway where thrombin (factor IIa) turns into fibrinogen, followed by fibrin (factor Ia). Activated platelets have recently been shown to play a critical role in triggering the contact/intrinsic coagulation pathway. As such, activated platelets release inorganic polyphosphates from their dense granules, which trigger the activation of factor XII, prekallikrein enhancing factor XI-related thrombin activation. Small quantities of thrombin display strong platelet-activating properties; thus, these two processes are intertwined.

1.3. Myocardial ischaemia and reperfusion injury

The myocardium consists of cardiomyocytes (containing around 80% of its volume), microvasculature fed by coronary arteries, veins and lymphatics, and the supporting connective tissue matrix. The cardiomyocytes are organised into laminar sheetlets and shear layers that change direction during contraction and form a single ventricular myocardial band (26–28). Each cardiomyocyte has 1-2 nuclei, multiple sarcomeric units containing myofibrils and an extensive network of mitochondria that synthesise adenosine triphosphate (ATP) (via oxidative phosphorylation) required for very high demands of energy that cardiomyocytes demand constantly contracting and relaxing.

In ACS, the mismatch of available oxygenated blood and myocardial demand results in myocardial metabolism alterations, leading to progressive damage of cardiomyocytes and the surrounding tissue.

During ischaemia, cardiomyocyte biology is altered: the cells move from aerobic to anaerobic metabolism, resulting in lower ATP levels, and acidosis occurs due to increased levels of lactate and hydrogen. Following low ATP levels, cellular membrane transporters are disrupted, changing the intracellular water and electrolyte balance with an increase of intracellular calcium, sodium and water molecules and a decrease of intracellular magnesium (**Figure 3).**
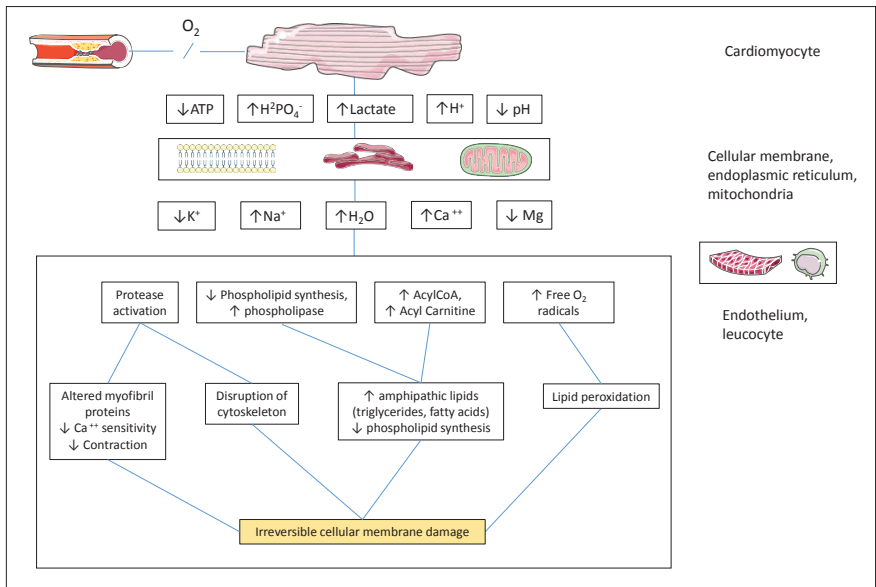
Figure 3. Cellular mechanisms resulting from an ischaemic injury. Adapted from Buja et al (licence number 5321951377666) and Gutierrez, M (29,30). Parts of the figure were drawn by using pictures from Servier Medical Art. Servier Medical Art by Servier is licensed under a Creative Commons Attribution 3.0 Unported License (https://creativecommons.org/licenses/by/3.0/).

Because of their vital role in energy metabolism, mitochondrial processes are heavily involved in cardiomyocyte injury and cellular death (**Figures 4, 5**). Mitochondria have multiple membrane channels that activate distinctly in different conditions; death channels and salvage pathways activate during cellular stress. An important channel is the mitochondrial permeability transition pore (mPTP), a voltage-dependent structure sensitive to increased intracellular calcium and oxidants. When mPTP opens, the mitochondrial membrane potential is altered, reducing ATP production, followed by an influx of water molecules into the organelle, eventually resulting in loss of function. Voltage-dependent anion channel (VDAC), the adenine nucleotide translocator (ANT), cyclophilin D (CypD) are the proteins that affect the mPTP function, accompanied by the enzyme membrane-bound ATPase (F0F1ATPase) (31).
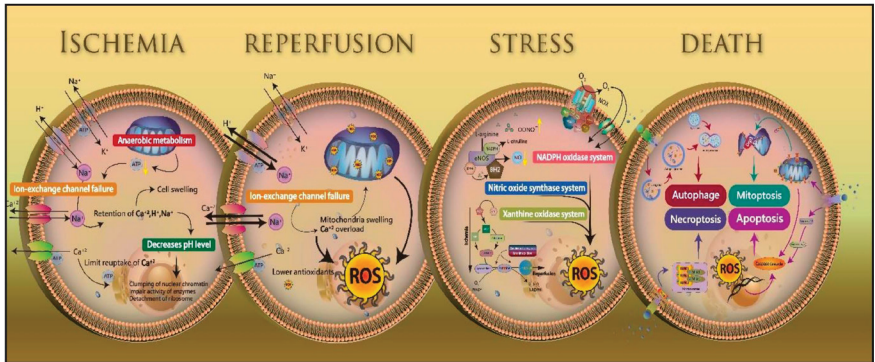
Figure 4. Mechanisms of ischaemia-reperfusion injury. Reused from Wu et al (32) under a Creative Commons CC-BY-NC-ND license. The final, published version of this article is available at https://www.karger.com/Article/FullText/489241.
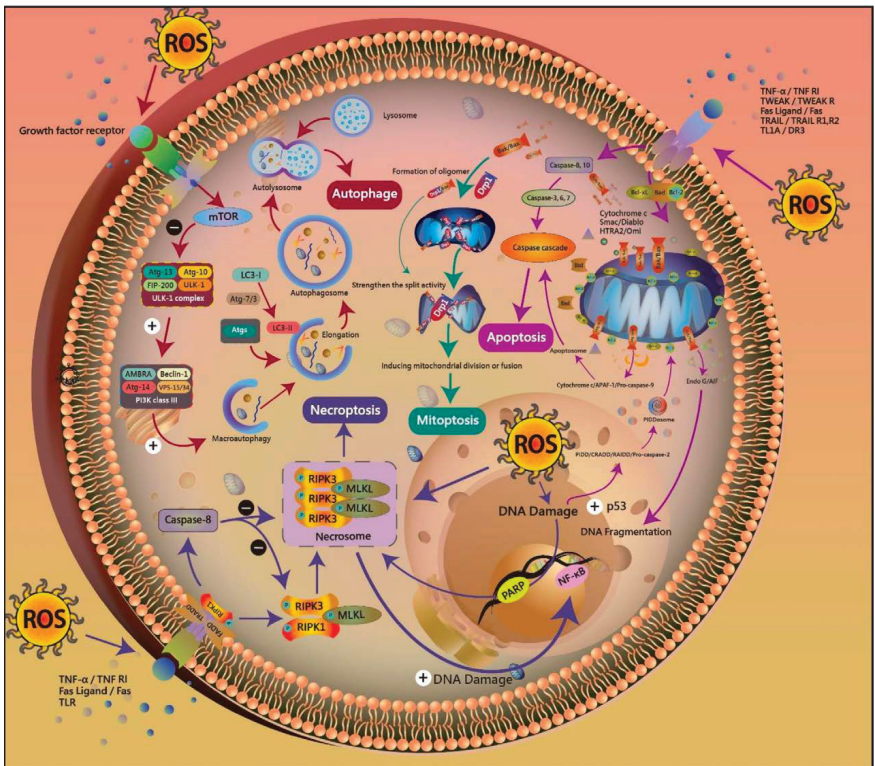
Figure 5. Cell death mechanisms of ischaemia-reperfusion injury. Reused from Wu et al (32) under a Creative Commons CC-BY-NC-ND license. The final, published version of this article is available at https://www.karger.com/Article/FullText/489241.

Cardiac damage in a reperfused AMI results from two components: the ischaemic injury and the reperfusion injury. During ischaemia and subsequent reperfusion, molecules of opioids, bradiquinine, sphyngosine and adenosine are released. Upon attaching to their corresponding receptors, they activate the enzyme protein kinase C (PKC) through two intracellular pathways: 1) mediated by AKT-eNOS-PKG and 2) mediated by PLC/PLD, where, respectively, nitric oxide (NO) and cGMP-dependent protein kinase (PKG) open mitochondrial potassium channels for potassium to enter. The cellular membrane is further affected by protease activation, a growth of phospholipase, acylcarnitine and reactive oxygen species (ROS), which eventually lead to membrane disruption, further mitochondrial damage and cellular death (29). Infarcted myocardium thus shows features of necrosis: myofibrillar contraction, intracellular oedema, rupture of sarcolemma, leucocyte infiltration and haemorrhage within the infarcted territory. Apart from necrosis, apoptosis, necroptosis, and autophagy also occur in evolving MI, resulting in a mixed pattern of cellular death (29).

The territory of the occluded coronary artery is considered to be the area at risk, which increases with the duration of ischaemia. Without reperfusion, myocardial cellular death will occur progressively, the myocardium adjacent to the immediately affected area increasingly joining the area at risk. Upon reperfusion, the potentially viable non-necrotic myocardial tissue is also affected by oxidative stress, pH alterations, increased inflammatory response, and microvascular obstruction (33,34). This phenomenon, often manifesting as myocardial stunning, microvascular dysfunction or myocyte death, is associated with greater infarct size, adverse remodelling, and worse prognosis (35–39).

Overall, the pathophysiology mechanisms of the irreversible reperfusion injury can be grouped into the cardiomyocyte- and the vascular compartments (**Figure 6**) (34).
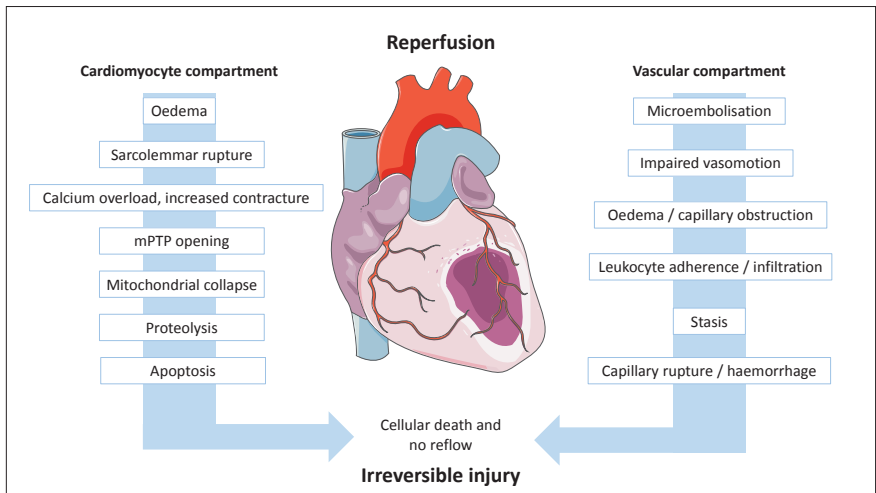
Figure 6. Mechanisms of irreversible ischaemia and reperfusion injury: cardiomyocyte and vascular compartments. Adapted from (30). Parts of the figure were drawn by using pictures from Servier Medical Art. Servier Medical Art by Servier is licensed under a Creative Commons Attribution 3.0 Unported License (https://creativecommons.org/licenses/by/3.0/).

- The cardiomyocyte compartment

After reperfusion, due to more readily available extracellular oxygen and electrolytes, aerobic mechanism, intracellular calcium overload, and intracellular hyperosmolarity develop while intracellular acidosis decreases. These factors lead to even more myofibrillar contraction, the formation of ROS and proteolysis of intracellular components, the opening of mPTP, loss of mitochondrial function and cellular death. and eventually to more necrosis (29,40). In addition, apoptosis, necroptosis and autophagy are seen in ischaemia-reperfusion injury, triggered by reperfusion (41).

- The vascular compartment

The vascular compartment is a chain of mechanisms, starting with microembolisation of the atherosclerotic and thrombotic debris at the time of reperfusion (42). This is followed by microvascular dysfunction with impaired vascular motion, excess permeability, oedema and stasis (43). Next, leucocytes, platelets and erythrocytes

migrate to the capillary bed of the previously ischaemic and now reperfused tissue (44). Eventually, there is the destruction of the capillary bed with haemorrhage (45).

The microvascular dysfunction and obstruction lead to the no-reflow phenomenon, seen in an estimated 35% of patients with STEMI in 2008 when combined diagnostic methods were used (46). Cardiac magnetic resonance imaging (CMR) is one of the most accurate tools to identify the no-reflow phenomenon (47) as discussed further.

Following reperfusion, part of the area at risk will survive to eventually function again, depending on ischaemia duration (48). This has been shown in the HORIZONS-AMI trial, where the researchers used perfusion and electrocardiographic markers: the most beneficial effect was when reperfusion occurred or was performed within 60-90 minutes from when the symptoms started (48).

1.4. Infarct size and ventricular remodelling after myocardial infarction

The size of the infarction is determined by occlusion time (49), reperfusion injury, collateral circulation, the size of the previously normally perfused territory (and as such, the area at risk). The infarction develops in a wavefront pattern, first affecting the distal (subendocardial) part of the myocardium, and, as the duration of the occlusion increases, the infarction gets gradually transmural, reaching the subepicardial part (50).

If the coronary artery is revascularised promptly, this results in a significantly better prognosis for survival: infarct size is a known prognostic marker for mortality, morbidity and development of heart failure (51).

In this regard, a key player in the development of heart failure after a myocardial injury is cardiac remodelling, which the International Forum of Cardiac Remodelling has defined as a series of injury-related changes in gene expression, molecular, cellular and interstitial processes that affect cardiac size, shape and function (52). This process is complex and not yet fully understood; it is known that depending on the severity of the injury, remodelling starts within the first few hours after the index event and continues for months. Cardiomyocytes, interstitial fibroblasts and extracellular matrix, as well as haemodynamic, neurohormonal activation and paracrine factors, have a role here (52).

The timeline of cardiac remodelling can be roughly divided into very early, early and late phases, which in addition to the severity of the injury can be affected by secondary events, cofounding factors (e.g. co-existent ischaemia), genotype and treatment (52,53) (detailed in **Table 1**). Furthermore, these phases overlap and are influenced by the temporal consideration of fibroblast/myofibroblast activity in infarcted heart – the inflammatory phase, the proliferative and the maturation phase, respectively (54,55). These responses have a positive short-term effect in stabilising cardiovascular functions after a myocardial injury. However, in the late phase, the process is considered maladaptive.

Phases of cardiac remodelling after reperfused AMI	
Very early (several hours)	Starts with the ischaemic and reperfusion injuries. Cellular death triggers an inflammatory response (recruitment of neutrophils and mononuclear cells) which activates the reparatory process and the chain of fibrosis within the injured area.
Early (hours to days)	A combined phase of *inflammatory response* and *neovascularisation*. As part of the inflammatory response, macrophages resorb the dead cells and debris of the matrix. Eventually, inflammation is signalled to suppress, and matrix preservation begins with fibroblasts differentiating into myofibroblasts which induce collagen synthesis to form the extracellular matrix and, ultimately, scar. In parallel, cells (pericytes, endothelial, VSMC) and extracellular matrix interact to start neovascularisation in response to angiogenic activation. This provides the jeopardised myocardium with oxygen and nutrients and helps the inflammatory response to form the granulation tissue. In this phase, cardiac fibrosis is reparatory and maintains the integrity of the myocardial wall.

Phases of cardiac remodelling after reperfused AMI	
Late (weeks to months)	Due to the *neurohumoral activation*, the recruited cells, including myofibroblasts, travel diffusely into the heart, involving the remote tissue. Besides, loss of myocytes in the injured area and subsequent loss of contraction result in a) a change of flows and forces within the ventricle and b) alteration of myocyte morphology in the peri-infarct and remote areas. As a result of the former, there is an excess of myofibroblasts and subsequent collagen synthesis in the remote regions (reactive fibrosis), where the tissue is already adapting to the mechanical changes. Thus, ventricular dilatation, having been compensatory in the earlier phase, together with interstitial fibrosis, is among the factors contributing to reduced contractility, impaired diastolic function and eventually heart failure.

Table 1. Phases and mechanisms of cardiac remodelling after reperfused AMI

Elevated plasma noradrenaline levels and activation of the renin-angiotensin system (RAS) are the major players amongst the neurohormonal factors in cardiac remodelling. It is known that ventricular remodelling can progress without subsequent episodes of myocardial injury (56). While elevated noradrenaline levels result in improvement of cardiovascular function at acute phase due to increased contraction and heart rate, sodium retention and maintained volume status, the steady-state cardiovascular regulation in a healthy individual is predominantly driven by the parasympathetic system, as opposed to the dominance of sympathetic regulation in heart failure (57,58). Furthermore, elevated plasma noradrenaline levels, apart from direct cardiomyocyte toxicity (59), result in overexpression of beta-1-adrenergic receptors, which leads to

systolic dysfunction (60). The effects of chronically activated RAS on the cardiovascular system after myocardial injury are driven by a) increased angiotensin II levels which lead to eccentric left ventricular (LV) hypertrophy, vasoconstriction and elevated plasma noradrenaline, and b) increased aldosterone levels, which result in multisystemic changes such as sodium reabsorption, potassium loss and arterial hypertension, vascular injury via inflammatory and endothelial dysfunction chains as well as ventricular hypertrophy and interstitial fibrosis (61–64).

Adverse post-infarction LV remodelling is associated with increased morbidity and mortality risk (65,66). Over the past few decades, several imaging markers to predict post-MI remodelling-related adverse outcomes have been established: among them, increased LV end-systolic volume, increased LV end-diastolic volume and decreased ejection fraction (67–69) as well as infarct size (70–73): these markers are discussed further.

1.5. Main concepts of cardioprotection

Limiting infarct size and subsequent adverse remodelling have become primary goals to improve prognosis regarding mortality, morbidity and development of heart failure (51). Since the 1980s, widely applied revascularisation therapy techniques have resulted in a hospitalisation mortality decrease from 30% to 5.5% in developed countries (74). However, this number has been on a plateau since 2008 (75), suggesting that new co-adjuvant treatment strategies are needed. Accordingly, various therapeutic strategies, labelled by the umbrella term of cardioprotection, have been developed, and several are further investigated. There are two types of cardioprotection: non-pharmacological (including mechanical) and pharmacological.

1.5.1. Non-pharmacological cardioprotection: Ischaemic and non-ischaemic conditioning

Ischaemic myocardial conditioning is now divided into four main types (pre-conditioning, post-conditioning, peri-conditioning and remote conditioning), whereas non-ischaemic conditioning includes methods such as intermittent hypoxic conditioning and physical exercise training as detailed in **Table 2**.

Ischaemic and non-ischaemic conditioning	
Pre-conditioning	Myocardial ischemic pre-conditioning refers to the protection conferred to ischemic myocardium by preceding brief periods of sublethal ischaemia separated by periods of reperfusion. Despite being an effective method in experimental models (76–78), it has an inherent limited value in AMI (unpredictable event), although it has shown to be protective in in elective PCI (79).
Post-conditioning	Ischaemic post-conditioning refers to the ability of a series of brief occlusions of the coronary artery, after a severe ischaemic insult, to protect against ischemic reperfusion injury of the myocardium during revascularisation (80). This phenomenon has been confirmed in early clinical studies (81,82) yet, its benefits have not been confirmed in large clinical trials (83–85).

Ischaemic and non-ischaemic conditioning	
Remote conditioning	Remote conditioning refers to the ability of protect the heart by performing repeated and temporary cessations of blood flow in distal organs such as the limb to create ischaemia in the tissue which results in the activation of physiological protective pathways. While the results were promising in the first clinical studies where a different vascular territory (such as a limb) was used for techniques including remote peri-conditioning (86,87), later clinical trials resulted in mixed findings, but the RIC-STEMI trial showed promising results (88–91). Yet, a fairly recent clinical study of anterior STEMI patients used CMR-derived MI size as an endpoint showed neutral 6-month follow-up results of remote peri-conditioning in the context of P2Y12 inhibitor administration prior to PCI (92).
Intermittent hypoxic conditioning	This phenomenon has been attributed to the exposure to high altitude hypoxia which limits ischaemia-induced myocardial necrosis and prevents life-threatening arrhythmias in conditions that simulate high altitude, whether combined with physical exercise or not (93,94).
Physical exercise training	A multifactorial process, where various types of exercise, such as endurance, resistance and interval training induce cardioprotection through an array of mechanisms (95). Exercise as a pre-conditioning method has been proven effective in small animals (96,97). Direct surrogate-based clinical evidence is lacking due to the limitation of applying physical exercise training in controlled conditions before acute myocardial injury, but indirect data suggests a protective effect both before and after the event (98,99).

Table 2. Types of myocardial conditioning

In all four types of ischaemic conditioning, the implementation of short ischaemia and reperfusion cycles are performed, "switching on" the paracrine, intracellular and neurohumoral mechanisms to release protective molecules and compounds. While these mechanisms are complex and not fully understood yet, it is known that both myocardial membrane receptor (predominantly protein G-based) and intracellular processes are involved and are, essentially, the same pathways that become activated during the reperfusion injury (**Figure 7**). Some of the major mediating factors are opioids, bradykinin, sphyngosine, adenosine and TNFα (tumour necrosis factor alpha) (100).
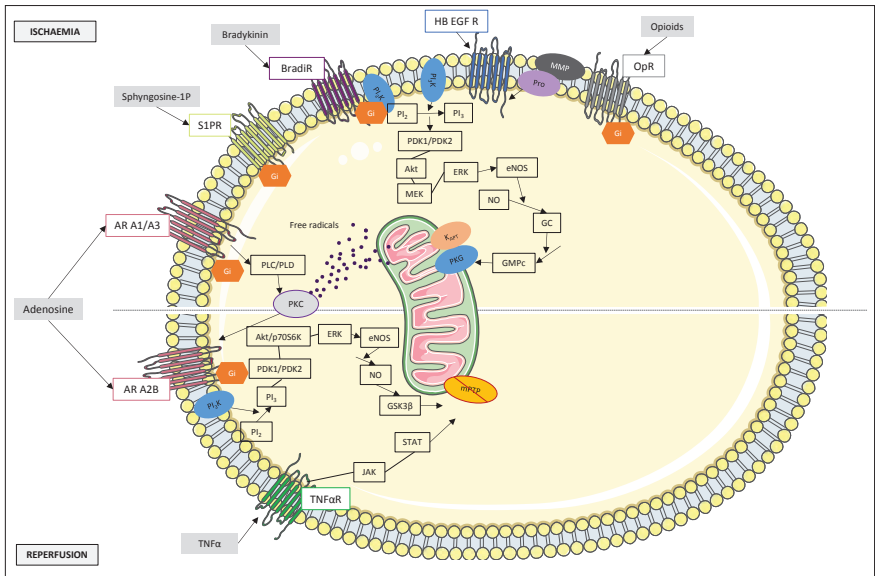
Figure 7. Major membrane-signalling pathways in pre- and post-conditioning. OpR: Opioid receptor. MMP: matrix metalproteinase. EGF: epidermal growth factor. HB-EGF-R: heparin-binding EGF-like growth factor receptor. Pro: pro- HB-EGF-R. PI2/PI3: phosphatidyl-inositol-di/triphosphate. PI3K: PI3 kinase. PDK1/2: phosphoinositide-dependent kinase-1/2. Akt: protein kinase-B. MEK: MAP kinase. ERK: extracellular signal-regulated kinase. eNOS: endothelial nitric oxide (NO) synthase. GC: guanilyl-cyclase. PKG: cGMP-dependent protein kinase. KATP: ATP-dependent potassium channel. BradiR: bradykinin receptor. S1PR: sphyngosine-1-phosphate receptor. AR A1/3/A2b: adenosine receptors. PLC/PLD: phospholipase C and D. PKC: protein kinase C. p70S6K: p70S6 kinase. KSK3β: beta-glycogen-synthetase kinase. TNFαR: tumour necrosis factor alpha receptor. JAK: Janus kinase. STAT: signal transducer and activator of transcription. mPTP: mitochondrial permeability transition pore. Modified from (30,101). Parts of the figure were drawn by using pictures from Servier Medical Art. Servier Medical Art by Servier is licensed under a Creative Commons Attribution 3.0 Unported License (https://creativecommons.org/licenses/by/3.0/).

1.5.2. Pharmacological conditioning

The need of a pharmacological intervention to reduce infarct size is clear but attempts have been controversial so far despite multiple clinical trials over the course of the past decades (**Table 3**). For the purpose of this work, the main introductory points will focus on cardioprotection – in particular, the one exerted by P2Y12 receptor inhibitors and adenosine.

Pharmacological conditioning: clinical trials			
Year	**Therapeutic Agent**	**Trial Design**	**Outcome**
2006	**Caldaret** Intracellular Ca2+ handling modulator	CASTEMI 387 patients randomised	**No difference** in infarct size measured by SPECT. No difference in LVEF on day 7 or 30.
2007	**Nicorandil** K+ channel opener/vasodilator	J-WIND-KATP 545 patients randomised	**No difference** in infarct size measured by CK-MB release.
2011	**Delcasertib** δ-protein kinase C inhibitor	PROTEC-TION-AMI 1,010 patients randomised	**No difference** in infarct size measured by CK-MB release or ST-segment resolution in either cohort. **No differences** in clinical outcomes.
2011	Erythropoietin	REVEAL 222 patients randomised	**No difference** in infarct size as measured by cardiac MRI.
2013	Metoprolol β-blocker	METO-CARD CNIC 270 patients randomised	**Controversial** differences in myocardial salvage

Pharmacological conditioning: clinical trials			
Year	**Therapeutic Agent**	**Trial Design**	**Outcome**
1999-2014	**Adenosine** G-protein activator	13 RCTs 4,273 patients	**No difference** in clinical outcomes, apart from heart failure.
2015	**Ciclosporine A** MPTP inhibitor	CIRCUS 970 patients randomised	**No differences** in clinical outcomes.
2017	**Danegaptide** Connexin-43 activator	585 patients randomised	**No difference** in myocardial salvage.
2004-2018	**Clopidogrel, prasugrel, ticagrelor** P2Y12 inhibitors	12 RCTs 52816 patients randomised	Prasugrel and ticagrelor more effective than clopidogrel in reducing the risk of MI and ST. Greater mortality reduction with ticagrelor than with clopidogrel. **No difference** between prasugrel and ticagrelor in the explored outcomes.

Table 3. Pharmacological conditioning: clinical trials (102–114)

1.5.3. The power of P2Y12 receptor inhibitors as antiplatelet and potential cardioprotective agents

P2Y12 receptor inhibitors, particularly in combination with the Cox inhibitor aspirin, have become a cornerstone in the management of STEMI revascularisation because of their antiplatelet properties. P2Y12 is the platelet membrane receptor for ADP, playing a key role in platelet activation that subsequently thrombus formation (**Figure 8).**
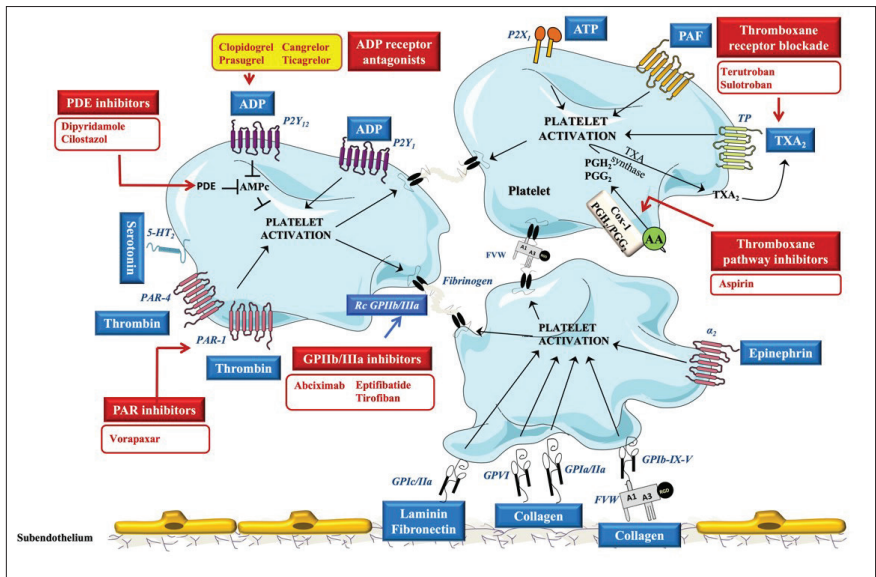
Figure 8. Role of P2Y12 receptor inhibitors in platelet activation. Based on (115) with permission (licence number 5367650862545).

P2Y12 receptor inhibitors are classified into thienopyridines and non-thienopyridine derivatives (**Table 4, Figure 9**). Thienopyridines are indirect inhibitors, with their active metabolites bind to the P2Y12 receptor irreversibly. Direct inhibitors are newer; they act on the P2Y12 receptor by changing its shape and inhibit it reversibly (116). When used in combination with aspirin, ticlopidine, first generation thienopyridine, has shown a reduction of cardiovascular events (death, MI, new coronary artery bypass graft surgery, new angioplasty) by 75% to the combination of aspirin and anticoagulants (117). However, as ticlopidine showed adverse effects such as neutropenia and thrombotic thrombocytopenic purpura, newly developed clopidogrel found its place in clinical practice (118,119).

Although the second generation thienopyridine clopidogrel is rapidly absorbed, it is metabolised in the liver via the cytochrome P (CYP) system, particularly the P450 component. Therefore, maximum plasma concentrations of the active metabolite increase in a dose-dependent way, meaning that it may take at least 60 minutes

to the maximum plasma concentrations, and the peak level may be delayed further at higher doses. In practice, before stenting a coronary artery, it takes four hours of a high (600mg) dose of clopidogrel to achieve the desired reduction of cardiovascular events (120,121). Additionally, likely due to individual genetic differences in absorption and/or hepatic metabolism and high platelet activity during ACS, up to 46% and 15% of patients do not optimally respond to 300mg and 600mg doses, respectively (112,122).

To overcome these limitations, newer agents have been developed. Prasugrel is a third generation thienopyridine that acts faster as it is less CYP dependent. Prasugrel does not require prior metabolism and reversibly change the P2Y12 receptor upon binding (116). Along with its more potent action, prasugrel is associated with a higher risk of severe haemorrhagic complications such as intracerebral bleeding (111,123). Ticagrelor, a triazolopirimidine, also acts faster than clopidogrel and showed a therapeutic advantage in lower overall mortality (124,125). While there have been discrepant results regarding the intracerebral risk of ticagrelor compared to clopidogrel, the PEGASUS study did not reveal significant differences (126). The therapeutic advantages of ticagrelor have raised interest in the cardioprotective effect of the drug, in addition to the more antiaggregant properties.

Cangrelor is a reversible and so far, the only approved P2Y12 receptor inhibitor available in intravenous form. Following an intravenous bolus and continuous infusion, maximum serum concentration (Cmax) is achieved within 2 minutes; its half-life is 3-6 minutes, and after stopping the infusion, platelets reverse to their normal function within an hour (127). Cangrelor's clinical efficacy has been shown in the context of ACS complications without significant increase in post-procedural bleeding compared to clopidogrel (128,129). However, primary results of FABOLUS-FASTER trial suggest that cangrelor, while more effective than prasugrel, results in lower platelet inhibition compared to tirofiban, a reversible antagonist of fibrinogen (130). As recently reviewed by

de Luca et al., there are several on-going clinical trials assessing its real-world use (131).

P2Y12 receptor inhibitors					
Thienopyridines (prodrugs)	Ad-minis-tration	Onset of action	Reversi-bility	CYP-depend-ent	Cardio-protec-tion
Ticlodipine	Oral	6h	-	+	?
Clopidogrel	Oral	2-8h	-	+	+
Prasugrel	Oral	30min-4h	-	-+	+
Non-thienopyridine derivatives (direct acting)			.		
Ticagrelor	Oral	30min-4h	+	-	+
Cangrelor	Intra-ve-nous	2min	+	-	+

Table 4. Summary of P2Y12 receptor inhibitors.
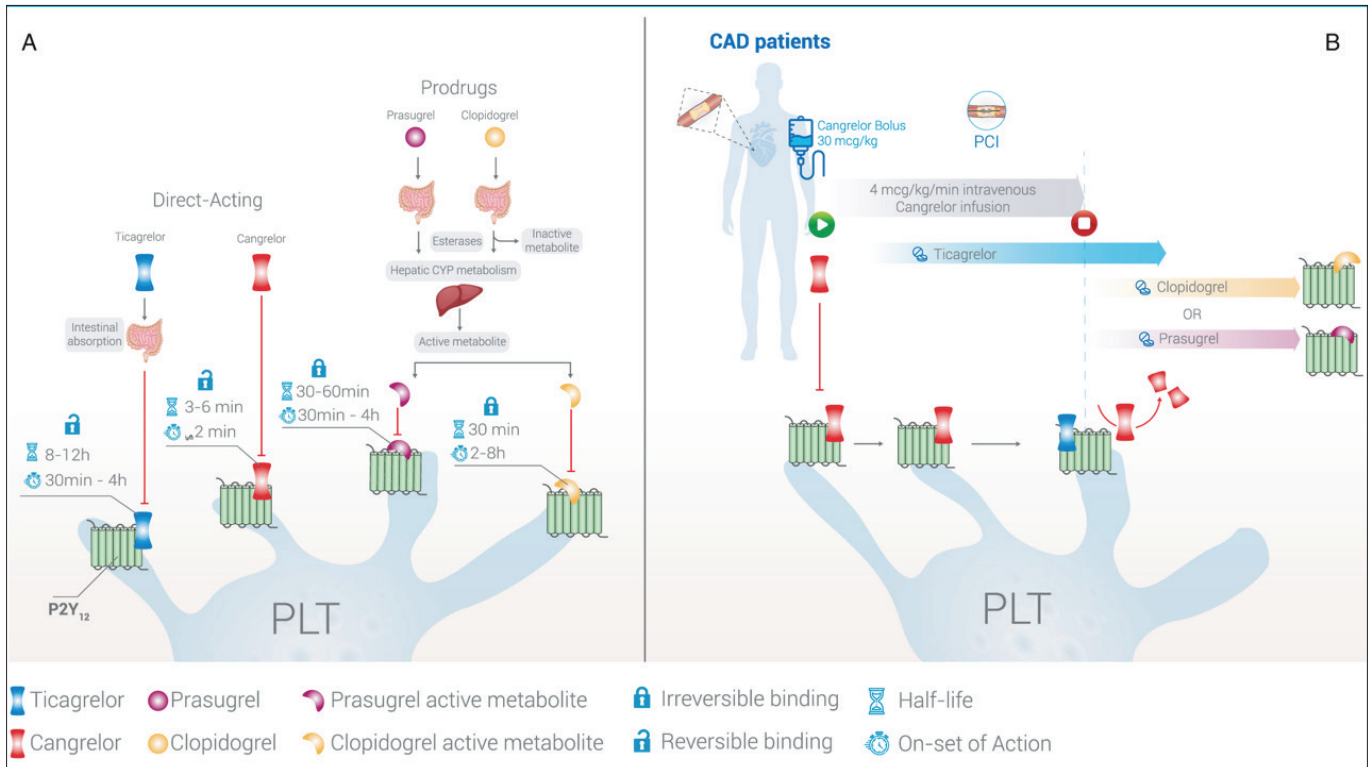
Figure 9. Overview of P2Y12 inhibitor pharmacokinetics with a focus on their metabolism, onset of action and half-life. Reused from (131) as per Creative Commons Attribution-NonCommercial-NoDerivs License.

Lately, evidence has shown that P2Y12 receptor inhibitors exert *cardioprotective* properties in the context of ischaemia-reperfusion injury. Cangrelor appears to be cardioprotective via the sphingosine kinase pathway (132). In an animal model and by use of the CMR, it has been demonstrated that, in contrast with clopidogrel, ticagrelor treatment showed association with acute (133) and long-term (134) cardiac structural and functional protective effects, when both P2Y12 receptor inhibitors were administered at doses that achieved comparable platelet inhibitory effect. Within these two studies ticagrelor-related acute and chronic protective effects were shown to be associated with the activation of myocardial adenosine monophosphate-activated protein kinase (AMPK) at a molecular level. AMPK, upon adenosine activation, exerts multiple cardioprotective effects, such as reduced oedema formation and infarct size, stimulation of wound healing post-MI, and protection against sepsis-induced organ damage and inflammation (135–139). Platelet-independent cardioprotective effects of ticagrelor occur most likely due to its ability to block cellular uptake of adenosine. This feature appears to be unique to ticagrelor compared to other agents in the group, and raises further questions to be studied in the field of ticagrelor and adenosine (or adenosine's antagonists such as caffeine) interactions in cardioprotective therapy (140).

1.5.4. Adenosine and apyrase

Adenosine is a potent endogenous protective molecule, concentrations of which rise in the extracellular space as a response to ischaemia. Essentially, regarding cardioprotection, adenosine helps the cells to adjust to a situation of reduced oxygen supply by:

1) swiftly reducing cell activities that require high energy,

2) allowing more nutrients and oxygen supply by inducing vasodilation, and

3) reducing the concentration of cytotoxic levels of extracellular adenosine triphosphate (ATP).

The metabolic pathway by which the increase of extracellular adenosine concentration occurs is via the breakdown of extracellular ATP by one of the membrane ectonucleotidase enzymes, endothelial apyrase (ADPase, or CD39), into adenosine diphosphate (ADP) first and then adenosine monophosphate (AMP). AMP is subsequently converted to adenosine by the enzyme ecto-5'-nucleotidase, CD73 (141) (**Figure 10**).
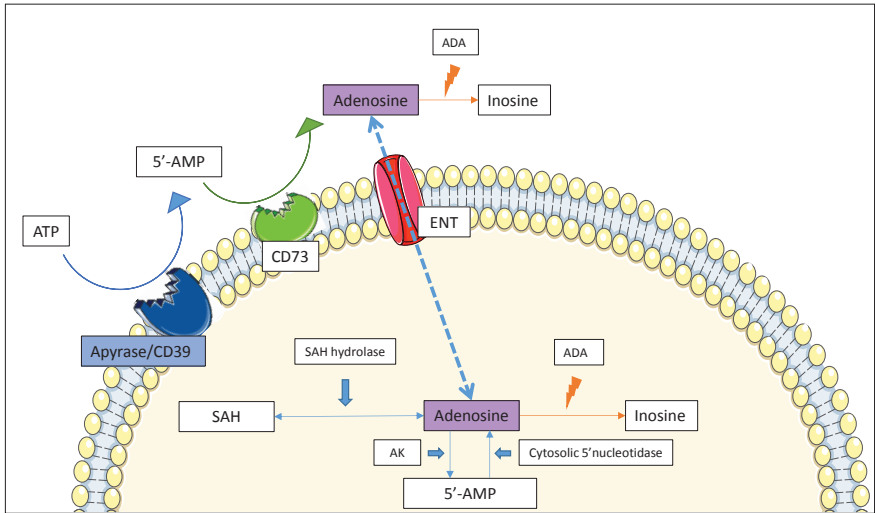
Figure 10. Extracellular and intracellular adenosine metabolism. Adapted from (142) with use permission granted (licence no. 5323210842777). AK: adenosine kinase; ENT: equilibrative nucleoside transpoter; SAH: S-adenosylhomocysteine. Parts of the figure were drawn by using pictures from Servier Medical Art. Servier Medical Art by Servier is licensed under a Creative Commons Attribution 3.0 Unported License (https://creativecommons.org/licenses/by/3.0/).

Generated through the ATP/ADP–AMP–adenosine pathway, adenosine then binds to adenosine receptors (AR), of which there are four subtypes (A_1, A_{2a}, A_{2b} and A_3). These receptors are widespread throughout the body and have a plethora of functions, including cardiac, metabolic, neuronal and renal domains (142). In the cardiovascular system, AR have a variety of biological effects (**Table 5**). In the context of myocardial ischaemia, cardiomyocyte A_1 and A_3 receptors are involved in ischaemic preconditioning,

while the other two are more involved in inflammatory response and in angiogenesis via immune and vascular endothelial cells, respectively (**Figure 11**) (142). Although ATP has been found to have cardiotoxic effects (143), adenosine, when binding to AR, has been shown to preserve microvascular flow, reduce ROS synthesis, inhibit platelets, reduce cell death, restore calcium homeostasis and attenuate the inflammatory process, among others (144–147). Additionally, Feliu et al. have recently shown that in human endothelial cell cultures exposed to hypoxia, ticagrelor's effect in preventing apoptosis involves the adenosine signalling pathway (148). Direct intracoronary administration of adenosine prior to reperfusion has been recently analysed with a suggestion of reduced heart failure after acute myocardial infarction (AMI) (107).

Effect of adenosine on the cardiovascular system	
Negative inotropic	A_1
Negative chronotropic	A_1
Negative dromotropic	A_1
Ischemic preconditioning	A_1 / A_3
Vasodilation	A_{2A} / A_{2B}
Platelet aggregation inhibition	A_{2A}

Table 5. Effect of adenosine on the cardiovascular system per receptor subtype. Adapted from (142) with use permission granted (licence no. 5323210842777).
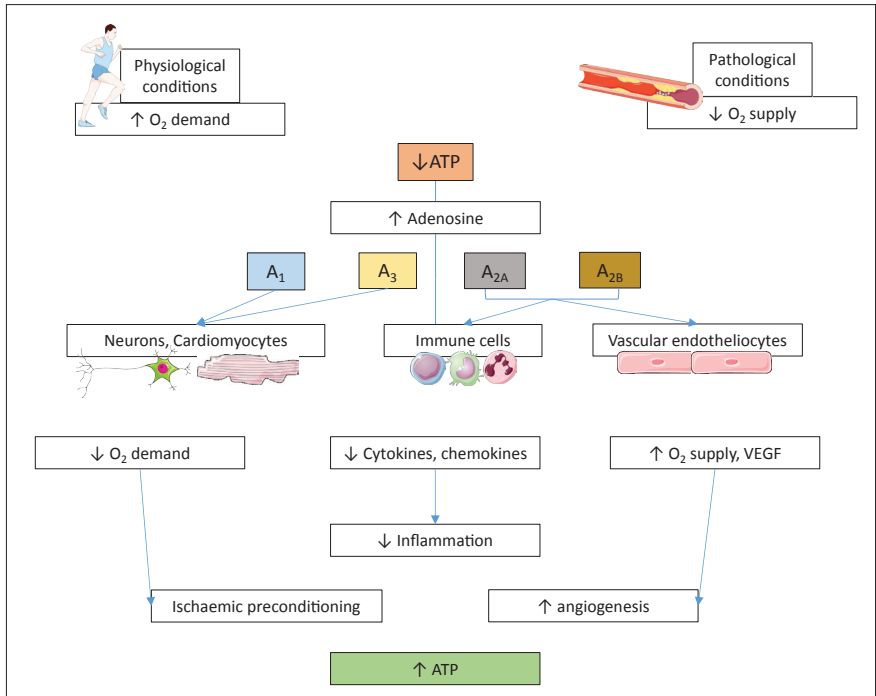
Figure 11. Overview of AR role in physiological and pathological conditions. VEGF: vascular endothelial growth factor. Adapted from (142) with use permission granted (licence no. 5323210842777). Parts of the figure were drawn by using pictures from Servier Medical Art. Servier Medical Art by Servier is licensed under a Creative Commons Attribution 3.0 Unported License (https://creativecommons.org/licenses/by/3.0/).

Importantly, adenosine's interaction with adenosine receptors is considered to be one of the pathways in ischemic conditioning. Blockade of apyrase (CD39) or ecto-5'-nucleotidase (CD73) has been found to eliminate preconditioning-related cardioprotective effects (100,149,150), and conversely, intravenous administration of apyrase reduced myocardial infarct size by 43% when administered 30min before ischemia induction in rats (150). Importantly, a recombinant soluble form of apyrase CD39, named AZD3366 (also known as APT-102) was developed in 2004: it has significantly more potency than the natural enzyme, with a fast onset and prolonged duration of action yet without significant bleeding time prolongation (151). AZD3366 has been shown to have more inhibitory effects on

arterial thrombus formation in mouse and dog models compared to clopidogrel (152). In addition, administration of AZD3366 (APT-102) has shown to inhibit venous thrombosis and intimal hyperplasia in humans (153).

1.6. Cardiovascular magnetic resonance imaging as a tool to monitor cardioprotection

Cardiovascular magnetic resonance (CMR) imaging, also sometimes abbreviated as cMRI, is an advanced cross-sectional non-ionising imaging technique, now considered the gold standard for quantifying cardiac chamber size and function and for non-invasive tissue characterisation (154,155). In addition, CMR markers are increasingly used in translational research and clinical trials regarding cardioprotective therapies (156).

1.6.1. Basic principles of cardiovascular MRI

Due to its high temporal and spatial resolution, CMR allows for detailed anatomical and functional assessment of the heart and vessels. Magnetic resonance imaging (MRI) is based on how tissue hydrogen atoms respond to high static magnetic field strength, generated magnetic field gradients and radiofrequency waves. The physics basis of this technique has been recently comprehensively reviewed by Vassiliou et al. (157). Depending on their parameters, the obtained images are grouped into sequences, of which the main are further described in **Table 6**. In cardiovascular applications, MRI sequences are electrocardiogram (ECG)-gated, and most are acquired during brief breath-holds.

In cardiovascular applications, intravenous gadolinium-based contrast agents are used for some of the sequences. Gadolinium, a metal that significantly alters T1 relaxation, is used for imaging in a chelate form and distributes evenly in the extracellular space of tissues; kidneys fully excrete it within 24 hours. In healthy

myocardium, gadolinium is washed out within 5-20 minutes. One of the fundamental techniques is the assessment of late gadolinium enhancement (LGE), based on gadolinium chelate kinetics: when cellular membranes are damaged (e.g. in AMI) or when extracellular space is increased (e.g. if a collagen scar is formed), gadolinium chelate is retained and can be detected by dedicated CMR sequences 10-15 minutes after injection.

Commonly used CMR sequences and their practical applications are outlined in **Table 6**.

Commonly used CMR sequences and their practical applications		
Sequence group	**Type**	**Applications**
Spin-echo	Morphological	"Static" images are acquired in a single phase of the cardiac cycle. Used for anatomical information, dark blood imaging and tissue characterisation, these sequences have T1 (longitudinal relaxation of hydrogen atoms) and T2 (transverse relaxation of hydrogen atoms) weighting properties.
Cine imaging	Functional	Gradient echo imaging throughout the cardiac cycles; the most commonly used are the gradient echo pulse sequence and the steady-state-free-precession (SSFP) sequence. These sequences are used for the dynamic assessment of sizes and function of chambers or vessels.

Commonly used CMR sequences and their practical applications		
Sequence group	**Type**	**Applications**
T2-weighted imaging	Morphological	T2-weighted spin-echo sequences, often acquired with additional fat suppression techniques, are frequently used to assess for tissue oedema or inflammation.
T2* imaging	Morphological	Based on atom interactions due to the magnetic field inhomogeneities. These sequences are applied to assess for tissular iron: for example, to detect haemorrhage after haemoglobin breakdown.
Phase contrast	Functional	Velocity-encoded pulse cine sequences that can be acquired in a two- or, as of more recently, in four-dimensional approach. These sequences are used to evaluate vessel or chamber blood flow volume, velocity and direction.
Perfusion imaging	Functional and morphological	T1-weighted sequence with multiple static acquired over time at a single phase of cardiac cycle. Immediately upon injection of intravenous contrast, allows for assessment of contrast distribution in chambers and then soft tissue. This sequence can be applied at different vascular phases. In ischaemic heart disease, it is commonly used to identify perfusion defects in different coronary artery territories.

Commonly used CMR sequences and their practical applications		
Sequence group	**Type**	**Applications**
Early and late gadolinium imaging	Morphological	T1-weighted gradient echo (inversion recovery) sequences acquired after intravenous gadolinium-based contrast administration. Early phase, acquired within a minute, allows for detection and quantification of intracavitary thrombus or, in the case of MI, microvascular obstruction. Late phase, acquired usually 10-15min after contrast administration: abnormal myocardium, after the inversion recovery null time is set to show normal myocardium as black, is enhanced. These sequences are used for assessment of infarct size and non-ischaemic myocardial fibrosis or infiltration.
Myocardial T1, T2, T2* mapping	Morphological	More recent, advanced sequences that have been developed to quantify tissular changes as opposed to the qualitative approach of the earlier mentioned respective counterparts without mapping. Among several other established or investigated uses of these techniques, measurement of myocardial extracellular volume (ECV) can be derived from T1 mapping.

Table 6. Commonly used CMR sequences and their practical applications

1.6.2. Clinical use of CMR in the context of myocardial infarction

In clinical medicine, CMR is widely indicated in cardiovascular diseases (154,158). Regarding MI, the technique has an important prognostic value (159,160). Based on the current practice, it can be summarised into four main cornerstones:

- *Volumetric assessment of cardiac chamber sizes and function.* Parameters such as end-diastolic, end-systolic and stroke volumes, ejection fraction, regional wall motion and ventricular mass can be obtained. Due to its accuracy and reproducibility, the technique is considered to be gold standard among all currently used modalities (161).

- *Myocardial oedema and myocardium at risk.* In acute (and to a lesser extent, in subacute) myocardial injury, tissular oedema results in increased signal intensity on T2-weighted imaging techniques (162). This alteration can be assessed qualitatively and quantitavely to derive parameters such as myocardial oedema and area at risk (i.e. which could later turn to necrosis): the latter is the difference between the oedema on T2-weighted sequences and LGE, and is a prognostic marker (163).

- *Microvascular obstruction (MVO) and intramyocardial haemorrhage (IMH).* Both phenomena result from ischaemia and reperfusion injuries and are associated with poor prognosis. Intramyocardial haemorrhage occurs when erythrocites extravasate from the vascular lumina into the tissue due to injury: that is, MVO can occur with or without haemorrhage. These entities can be assessed by CMR, using several techniques, first pass perfusion and early gadolinium phase being the most commonly used for MVO, and T2 and, more specifically, T2* imaging for IMH.

- *Necrosis/fibrosis.* Based on LGE imaging, infarct can be detected and quantified at virtually any timepoint of the disease, and the scan is most commonly performed at the phases of

acute infarction, early remodelling and late remodelling. In acute phase, while infarct size can be overestimated due to oedema, combining data acquired from T2-weighted imaging, additional information on myocardium at risk can be obtained. LGE in acute MI has an established prognostic value in chronic ventricular dysfunction (72). In chronic MI, LGE-based evaluation of myocardial viability has been an established tool for decision making due to its prognostic value on reversible myocardial dysfunction (164). Among multiple markers that are increasingly gaining researchers' attention, infarct size remains considered to be the most important adverse prognostic factor for long-term outcomes.

CMR markers are increasingly used as surrogate endpoints in translational research testing cardioprotective therapies. CMR imaging societies provide standardized protocols for image acquisition, interpretation, and reporting (165). In addition, regarding research studies, the JACC Scientific Expert Panel for Experimental and Clinical Trials provides a consensus of recommendations and standardization of imaging techniques (156).

1.7. Translational value of porcine model of myocardial infarction

Preclinical animal models have been widely used in basic science not only to investigate and to understand the pathophysiological and metabolic basis of coronary artery disease, but also to evaluate potential therapeutic strategies, as recommended by the European Society of Cardiology (ESC) Working Group (WG) Cellular Biology of the Heart (166). These tests allow the research teams to assess pharmacokinetics, dose efficacy as well as toxicity on other mammals before the potential product enters clinical testing.

Animal models vary: while small animals such as rodents are associated with lower costs, allow for quicker breeding and, thus, for example, are more readily available for transgenic studies, the similarity to human cardiovascular system is inferior compared to large animal models (167,168). For instance, rodents have a much higher resting heart rate and their collateral circulation can differ significantly from humans, which limits the use of coronary artery occlusion models for drug testing and imaging (169). Interestingly, other primates such as cynomolgus monkeys are more resistent to myocardial infarction following coronary artery occlusion, and are therefore rarely chosen for experimental studies of IHD (170). Thus, mammals with comparable anatomy and physiology to humans are preferred, and a large animal model is recommended in novel cardioprotective therapy studies by the ESC WG Cellular Biology of the Heart (166). For experimentally induced closed-chest MI, pig models are considered to have the best translatability due to the similarity of their cardiac anatomy and physiology to humans, including cardiac conductive system and sparse collateral coronary artery network, and this is also true regarding future perspectives of therapeutic strategies such as post-genomic technologies (168). Additionally, regarding imaging, clinical CMR protocols can be applied to pigs in a straightforward manner, allowing to use the same prognostic markers as in clinical trials: this adds to the translational value. However, this application requires methodological caution, as the translational axis of clinical CMR use in preclinical porcine model studies, including post-processing, has not been widely assessed in the literature. That is, there may be a scissor-like mismatch between the bench-to-bedside non-imaging biomarkers (widely studied and validated on animal models) and the modern bedside-to-bench CMR imaging biomarkers (widely studied and validated on clinical studies). This mismatch includes the lack of available evidence in large animal models on the impact of coronary ischaemia duration using CMR and on interchangeability of CMR post-processing software tools.

2. Hypothesis

Atherothrombosis, characterised by atherosclerotic lesion disruption with superimposed thrombus formation, is the major cause of AMI. The improved management of AMI patients has reduced morbidity and mortality in the acute phase; however, this success has resulted in an increased incidence of HF due to adverse post-MI LV remodeling. At present, treatment efforts are focused on limiting the damage in the setting of acute MI as well as on stimulating post-MI LV repair. Despite intensive experimental research that has been conducted within the last decades aiming to identify therapeutic strategies able to reduce cardiac damage in the setting of acute MI, none is currently implemented in the clinical setting. Therefore, a growing need to develop effective cardioprotective strategies remains. As previously demonstrated in a preclinical animal model, ticagrelor can limit infarct size and improve cardiac function by preventing adenosine uptake leading to an overall higher cardioprotection than that afforded by clopidogrel. Adenosine, besides being a key mediator in ischaemic conditioning, has shown to exert numerous cardiovascular beneficial effects that may counteract ischaemia/reperfusion damage providing overall cardioprotection.

Our main hypothesis is that increasing local adenosine availability by both preventing its uptake (ticagrelor) and inducing its synthesis (human recombinant apyrase) in the acute setting of MI will lead to a higher cardioprotection as compared to ticagrelor alone.

3. Objectives

Primary objective:

To examine, whether intravenous administration of a recombinant soluble form of human apyrase (AZD3366) prior to reperfusion limits cardiac damage and improves cardiac function to a larger extent than ticagrelor alone.

Two Secondary objectives:
- **Secondary objective 1.**

To demonstrate, in this preclinical animal model, how long myocardial ischaemia should be maintained to render significant structural and functional alterations amenable for therapeutic intervention.

- **Secondary objective 2.**

To validate, in this preclinical animal model, the clinically available post-processing softwares for CMR analyses.

4. Compendium of Publications

4.1. Article 1

Radike, M, Sutelman, P, Ben-Aicha, S, et al. A comprehensive and longitudinal cardiac magnetic resonance imaging study of the impact of coronary ischemia duration on myocardial damage in a highly translatable animal model. Eur J Clin Invest. 2023; 53:e13860. doi: 10.1111/eci.13860

This article is related to the **Secondary objective 1.**

Material reused with permission from (171), licence number 5386981243161.

WILEY

A comprehensive and longitudinal cardiac magnetic resonance imaging study of the impact of coronary ischemia duration on myocardial damage in a highly translatable animal model

Monika Radike[1,2] [iD] | Pablo Sutelman[1] | Soumaya Ben-Aicha[1] [iD] |
Manuel Gutiérrez[1,2] [iD] | Guiomar Mendieta[1] | Sebastià Alcover[1] | Laura Casaní[1] |
Gemma Arderiu[1] | María Borrell-Pages[1] [iD] | Teresa Padró[1,3] [iD] | Lina Badimon[1,3,4] [iD] |
Gemma Vilahur[1,3] [iD]

[1]Cardiovascular Program-ICCC, Research Institute Hospital de la Santa Creu i Sant Pau, Barcelona, Spain

[2]Radiology Department, Liverpool Heart and Chest Hospital NHS Foundation Trust, Liverpool, UK

[3]CiberCV, Institute Carlos III, Madrid, Spain

[4]Cardiovascular Research Chair UAB, Barcelona, Spain

Correspondence
Gemma Vilahur, Cardiovascular Program-ICCC, Research Institute Hospital de la Santa Creu i Sant Pau, c/ Sant Antoni Mª Claret 167, Barcelona 08025, Spain.
Email: gvilahur@santpau.cat

Abstract

Objectives: We performed a comprehensive assessment of the effect of myocardial ischemia duration on cardiac structural and functional parameters by serial cardiac magnetic resonance (CMR) and characterized the evolving scar.

Background: CMR follow-up on the cardiac impact of time of ischemia in a closed-chest animal model of myocardial infarction with human resemblance is missing.

Methods: Pigs underwent MI induction by occlusion of the left anterior descending (LAD) coronary artery for 30, 60, 90 or 120 min and then revascularized. Serial CMR was performed on day 3 and day 42 post-MI. CMR measurements were also run in a sham-operated group. Cellular and molecular changes were investigated.

Results: On day 3, cardiac damage and function were similar in sham and pigs subjected to 30 min of ischemia. Cardiac damage (oedema and necrosis) significantly increased from 60 min onwards. Microvascular obstruction was extensively seen in animals with ≥90 min of ischemia and correlated with cardiac damage. A drop in global systolic function and wall motion of the jeopardized segments was seen in pigs subjected to ≥60 min of ischemia. On day 42, scar size and cardiac dysfunction followed the same pattern in the animals subjected to ≥60 min of ischemia. Adverse left ventricular remodelling (worsening of both LV volumes) was only present in animals subjected to 120 min of ischemia. Cardiac fibrosis,

Lina Badimon and Gemma Vilahur contributed equally to this work.

myocyte hypertrophy and vessel rarefaction were similar in the infarcted myocardium of pigs subjected to ≥60 min of ischemia. No changes were observed in the remote myocardium.

Conclusion: Sixty-minute LAD coronary occlusion already induces cardiac structural and functional alterations with longer ischemic time (120 min) causing adverse LV remodelling.

KEYWORDS

adverse remodelling, CMR, ischemia duration, myocardial infarction, pig

1 | INTRODUCTION

In patients with ST-segment-elevation myocardial infarction (STEMI), prompt revascularization by primary percutaneous intervention has improved the prognostic outcome.[1] Yet, the extent of infarct size, a major determinant of mortality and heart failure development post-STEMI, remains too high.[2] Efforts in the last decades have focussed on discovering therapeutic strategies able to reduce cardiomyocyte death and regenerate the damaged heart. In this regard, multiple studies have assessed the cardioprotective efficacy of approaches either directed to endogenous mechanisms of cardioprotection (i.e. ischemic conditioning),[3–5] to novel therapeutic strategies,[6–10] or to the use of stem cell-derived therapies to trigger cardiac regeneration.[11,12] In this setting, preclinical studies in pig models of closed-chest complete left anterior descending coronary artery (LAD) occlusion (i.e. a STEMI-like situation) with subsequent reperfusion have become vital on the discovery and development of such therapeutic approaches and mandatory to determine their safety and efficacy before moving into clinical trials.[13–15] Indeed, pig hearts are very similar in size, anatomy and function to human hearts.[16] Yet, there is a need to understand the genesis and evolution of the myocardial ischemic damage produced by the occlusion of a coronary artery. An in-depth characterization of the impact of coronary ischemia time on myocardial tissue and function has yet to be performed to determine the time window of opportunity to salvage the ischemic heart with accurate techniques. So far, studies in pigs have implemented postmortem fluoroscopy and histology staining approaches to determine the impact of ischemia time on the area at risk and infarct size acutely post-MI (24 h postreperfusion)[17–20] Yet, none has assessed the impact of coronary ischemia time by implementing cardiac magnetic resonance (CMR), the gold standard noninvasive imaging technique for evaluating cardiac anatomy, volumes and function as well as myocardial tissue characterization in the setting

of MI. This is of paramount importance since multiple dynamic tissue changes occur in MI (oedema, microvascular obstruction, haemorrhage, cardiomyocyte necrosis and ultimately replacement by fibrosis) that contribute to long-term prognosis.[21] Furthermore, left ventricular ejection fraction (LVEF), infarct size and microvascular obstruction (MVO) have shown potential as imaging biomarkers to predict major long-term events and accordingly have been recommended to be included in preclinical trials.[22–26]

With all this information and needs as background, we hypothesized that there must be escalating ischemic times associated with an impairment of heart function, with the graded affectation of the different mechanisms that trigger early and/or delayed myocardial damage, and that the preclinical pig model could serve to dissect those different grades of ischemia-induced heart damage. Accordingly, here we have performed an in-depth mechanistic study on the impact of the duration of ischemic time, by coronary occlusion, on myocardial anatomical and functional parameters in pigs by serial CMR (clinical read-outs) complemented by molecular and histological insights into the damaged heart.

2 | METHODS

The experimental animal procedures were reviewed and approved by the Institutional Animal Care and Use Committees (CEEA-IR) and authorized by the Animal Experimental Committee of the local government (#5601) under the Spanish law (RD 53/2013) and European Directive 2010/63/EU. Besides, the investigation conforms to the Guide for the Care and Use of Laboratory Animals published by the US National Institutes of Health (NIH Publication No. 85–23, revised 1985) and follows the ARRIVE 2.0 guidelines.[27] All animals were allowed to acclimate 7 days before any intervention and housed in individual cages under light-controlled conditions and room temperature.

2.1 | Experimental design

A total of 41 female pigs (Specipig SL, Barcelona; Landrace; weight 40.5 ± 6.5 kg) were included in the study. Thirty-three pigs were randomly (Excel randomized function) distributed to undergo anterior STEMI induction by closed-chest coronary balloon occlusion of the left anterior descending coronary artery for 30 ($n = 8$), 60 ($n = 8$), 90 ($n = 9$) and 120 min ($n = 8$). After the ischemia period, the blood flow was restored by balloon deflation, and animals were allowed to recover. On day 3 and day 42 post-MI, animals were anaesthetized and brought to the 3 T-CMR facility for blinded assessment of global and regional parameters. Animals were euthanized after the last CMR acquisition (day 42) and cardiac tissue samples were collected for molecular and histological analyses.

A sham-operated group subjected to the same experimental procedure but without balloon inflation (no ischemia induction) was performed for baseline (physiological) CMR measurements for comparative purposes ($n = 8$).

2.2 | Closed-chest pig model of STEMI

On the day of MI-induction animals received buprenorphine (0.03 mg/kg) and cefazoline (25 mg/kg) as prophylaxis for pain and wound infection, respectively, and then anaesthetised by administering an intramuscular injection of ketamine (30 mg/kg), xylazine (2.2 mg/kg) and atropine (0.05 mg/kg). Once tranquillised, animals were endotracheally intubated and anaesthesia was maintained by isoflurane inhalation (2%). STEMI was experimentally induced by fluoroscopy-guided percutaneous coronary intervention, as we have previously described.[6,9] Coronary occlusion of the mid-left anterior descending (LAD) coronary artery was induced by balloon inflation, verifying a Thrombolysis In Myocardial Infarction (TIMI) 0 flow downwards. Ischemia was induced for 30, 60, 90 or 120 min, and then blood flow was restored (verification of TIMI 3 flow).

2.3 | 3T-CMR acquisition

CMR studies were conducted serially in all animals on day 3 (early remodelling phase) and day 42 (late remodelling phase) post-STEMI. The studies were performed on a 3.0 T-CMR system (Achieva®, Philips, Amsterdam, the Netherlands). Animals were anaesthetized with an intramuscular injection of a cocktail composed of ketamine, xylazine and atropine and maintained by a continuous intravenous propofol infusion to ensure mechanical ventilation. The following dedicated CMR sequences were acquired in all cases: 'cine' balanced steady-state free precession (bSSFP) imaging sequence to assess wall motion (WM) and cardiac function; T2-weighted short-tau inversion recovery (T2w-STIR) sequence to assess myocardial oedema; early gadolinium enhancement to study MVO (representing no-reflow phenomenon); and late gadolinium enhancement (LGE) to assess the amount and extent of myocardial necrosis. All the CMR studies followed the same scanning protocol. First, scout images [T1-turbo field echo (TFE) sequence] were obtained to localize the true axes of the heart and define a field of view involving the whole heart. Afterwards, the bSSFP cine imaging was performed in horizontal and vertical long axes (four-chamber and two-chamber views) and multiple contiguous short-axis images covering the whole LV. In the short-axis cine sequence, we acquired 24 cardiac phases of every slice to guarantee a correct WM and heart function evaluation. Once the cine sequences were acquired, a T2w-STIR sequence was obtained to assess myocardial oedema, correcting field inhomogeneities with shimming as necessary. After that, a gadolinium-based contrast agent was injected intravenously (Gd-GTPA, Gadovist®, Berlex Laboratories Inc., Wayne, NJ, USA) at a dose of 0.1 mmol/kg. The early gadolinium enhancement inversion recovery sequence was acquired 1 min after administering the contrast. The LGE sequences were obtained 10 min after the administration of contrast. Ten-minute LGE timing was chosen specifically following the results of our previous studies, where quality and reproducibility were deemed appropriate. Details of the technical parameters for CMR sequences have been previously published.[6,28]

2.4 | 3T-CMR data analysis

2.4.1 | Global functional and anatomical parameters

CMR data were independently and blindly analysed using dedicated software (QMASS MR version 7.6, Medis, Leiden, the Netherlands). The protocol of analysis for global functional/anatomical parameters was performed as previously reported.[6,29] Briefly, LV epicardial and endocardial borders were traced in each image of the cardiac phases representing the end-diastole and end-systole to obtain the left ventricular end-diastolic volume (LVEDV), left ventricular end-systolic volume (LVESV) and left ventricular ejection fraction (LVEF). Due to animals' cardiac orientation in a more cone-shaped chest, semi-automated and fully-automated segmentation of ventricular contours was deemed to be of insufficient quality, thus in both products, manual contouring was chosen.

LGE scar size was assessed by using manual planimetric segmentation on each slice, following the methods of our previous studies for reproducibility. The same method was used for the assessment of myocardial oedema and microvascular obstruction. The area of myocardial oedema was defined as the extent of the LV demonstrating high signal intensity on T2w-STIR images. The field and coil inhomogeneities were always corrected in the T2 signal using shimming, for which we had volumetric, manual or automatic modes and applied those as needed to achieve reliable results. Area at risk (AAR) was calculated as oedema (gr)/LV mass (gr). The size of infarction (day 3) or scar (day 42) was quantified from the extent of myocardial enhancement in the LGE CMR sequence.

2.4.2 | Cardiac remodelling parameters: WM and myocardial viability

LV regional analysis for each of the 16 American Heart Association myocardial segments was performed.[30] The endocardial and epicardial borders of the LV were defined in all slices representing the end-diastolic and -systolic phases. Thereafter, the WM [WM = the end-systolic wall thickness (EST) − end-diastolic wall thickness (EDT)] was automatically calculated as previously reported.[28] We also determined the number of dysfunctional segments and myocardial viability as previously reported.[6,28] Briefly, dysfunctional segments were considered those segments with a WM < 2 mm, whereas myocardial recovery was assessed as the percentage of segments with a WM on day 3 <2 mm (dysfunctional segments) that presented a WM on day 42 ≥2 mm (recovered segments). These measurements and analyses were performed only including the jeopardized segments (mid and apical antero/septal segments; target segments 7, 8, 13 and 14).[31]

2.5 | Cardiac sample collection and morphometric determination of scar size

After the last CMR, animals were euthanized with an intravenous administration of 10 ml KCl 2 M. Sham-operated animals were euthanized following the same approach. All hearts were carefully excised and segmented in six transverse divisions (1 cm width) to alternatively collect slices for 2,3,5-triphenyl tetrazolium (TTC) staining (scar area) or molecular/histological analyses. We obtained myocardial samples from the ischemic (infarcted) myocardium and nonischemic (remote) cardiac regions of ischemia animals and, accordingly, the LV septum and the LV lateral wall of sham-operated pigs.

All tissue samples were obtained, frozen, pulverized in liquid nitrogen and homogenically minced in Tripure® or lysis buffer for RNA and protein isolation, respectively. An independent blinded observer determined scar size through planimetry assessment employing IMAGEJ® software analysis (NIH).

2.6 | Molecular and histological approaches

2.6.1 | Myocardial characterization of fibrosis and cardiomyocyte dimensions

We blindly examined, in the ischemic and nonischemic regions of all pigs: (1) mRNA levels for collagen 1A1, collagen 1A2, collagen 3A1, smad2 and vimentin (Table S1); (2) protein expression of transforming growth factor (TGF)-β type II receptor (Abcam, Cambridge, United Kingdom), Smad2/3 and phosphorylated-Smad2/3 (Ser423/425, Santa Cruz, Dallas, Texas); and, (3) immunohistochemistry for collagen I (Rabbit polyclonal Abcam, ab34710) and collagen III (Rabbit polyclonal Merck-Millipore-Chemicon AB747) by using the avidin-biotin immunoperoxidase technique. RT-PCR and Western Blot analyses were carried out as previously performed.[32] For histological analyses, images were captured with a Nikon eclipse 80i microscope (Nikon, Tokyo, Japan) and digitalized by a Retiga-1300i (Teledyne QImaging, Surrey, British Columbia, Canada). Staining was calculated by a blinded observer from an average of 5-fields/sample and expressed as (%) = (positively stained area/[total tissue area − vascular luminal areas]) × 100 using IMAGEJ.

We also blindly determined by conventional light microscopy and hematoxilin/eosin staining cardiomyocyte dimensions including the surface and volume (model of a myocyte as an elliptic cylinder; $\pi ABL/4 = \pi r^2 L$).

2.6.2 | Microvascular rarefaction

Capillary density was determined by blindly assessing transcript levels of the endothelial marker von Willebrand factor [vWF] and lectin staining as previously reported.[11]

2.7 | Haematological and biochemical follow-up

Blood samples were collected at baseline, before STEMI, post-STEMI and 3- and 42-days post-MI and we assessed haematological (System 9000, Serono-Baker Diagnostics) and biochemical (lipid and glucose levels,

T A B L E 1 Impact of ischemia on cardiac structural and functional parameters assessed by serial CMR

CMR: Structural parameters

	Time of Ischemia	3 days post-AMI	42 days post-AMI	Δ 42 days vs 3 days
LV Mass (gr)	*sham*	60.8 [56.9–62.5]		
	30 min	64.2 [55.6–70.3]	89.3 [78.7–97.3]	21.9 [14.8–32.3][e]
	60 min	68.7 [63.7–71.0]	90.4 [84.0–95.1]	22.2 [16.3–29.8][e]
	90 min	63.4 [60.7–67.4]	92.7 [87.6–97.0]	28.5 [20.8–31.3][e]
	120 min	66.5 [56.8–75.7]	95.2 [82.9–100.9]	29.3 [17.4–37.0][e]
Oedema (gr LV)	*sham*	0.0 [0.0–0.0]	-	-
	30 min	0.0 [0.0–0.0]	-	-
	60 min	12.8 [12.0–14.1][a]	-	-
	90 min	13.3 [10.3–17.2][a]	-	-
	120 min	13.3 [12.2–16.5][a]	-	-
Necrosis (gr LV)	*sham*	0.0 [0.0–0.0]		
	30 min	0.0 [0.0–0.0]	0.0 [0.0–0.0][b]	0.0 [0.0–0.0]
	60 min	11.0 [10.5–11.8][a]	9.3 [8.1–10.1][b]	−1.4 [−3.0––0.8]
	90 min	13.3 [9.0–15.0][a]	8.7 [6.0–10.4][b]	−4.5 [−5.6––2.2][e]
	120 min	12.8 [10.2–14.6][a]	9.0 [6.9–11.7][b]	−3.8 [−5.4––1.7][e]
Necrosis (% LV)	*sham*	0.0 [0.0–0.0]		
	30 min	0.0 [0.0–0.0]	0.0 [0.0–0.0][b]	0.0 [0.0–0.0]
	60 min	15.8 [15.0–18.0][a]	10.4 [9.3–10.9][b]	−5 [−8.2––3.7][e]
	90 min	20.2 [14.7–23.8][a]	9.6 [6.2–12.2][b]	−11.5 [−12.3––6.9][e]
	120 min	17.2 [15.3–25.7][a]	11.16 [7.4–11.8][b]	−9.0 [−13.9––7.3][e]
MVO % LV)	*sham*	0.0 [0.0–0.0]		
	30 min	0.0 [0.0–0.0]	-	-
	60 min	0.1 [0.0–0.2]	-	-
	90 min	1.7 [0.7–2.2][ac]	-	-
	120 min	1.2 [0.5–2.5][ec]	-	-
AAR (gr LV)	*sham*	0.0 [0.0–0.0]		
	30 min	0.0 [0.0–0.0]	-	-
	60 min	19.7 [17.4–21.7][a]	-	-
	90 min	21.2 [16.7–26.3][a]	-	-
	120 min	21.7 [16.2–29.0][a]	-	-

Infarct size / AAR

	Time of ischemia	3 days post-AMI		
Infarct size/AAR (gr)	*sham*	0.0 [0.0–0.0]	-	-
	30 min	0.0 [0.0–0.0]	-	-
	60 min	55.2 [49.5–67.0][a]	-	-
	90 min	57.9 [56.3–60.3][a]	-	-
	120 min	55.8 [50.7–66.7][a]	-	-

CMR: Functional parameters

	Time of ischemia	3 days post-AMI	42 days post-AMI	Δ 42 days vs 3 days
LVEF (%)	*sham*	54.3 [52.9–55.9]		
	30 min	54.2 [51.9–59.8]	58.8 [52.5–62.2]	−0.2 [−3.3–6.4]
	60 min	43.9 [42.6–51.5][a]	40.6 [39,1–49.8][b]	−3.5 [−4.7–2.1]
	90 min	44.9 [40.9–48.8][a]	44.2 [37.0–60.3][b]	3.9 [−5.6–12.6]
	120 min	46.7 [41.1–49.2][a]	45.9 [43.9–47.8][b]	1.2 [−4.4–2.4]

(Continues)

TABLE 1 (Continued)

LVEDV (ml)	sham	90.2 [87.4–93.1]		
	30 min	86.9 [75.5–99.6]	95.4 [90.5–104.5]	7.3 [−3.8–21.3]
	60 min	83.3 [80.0–96.2]	111.9 [99.1–116.9]	21.7 [9.1–32.0][e]
	90 min	93.1 [81.1–112.1]	120.5 [112.6–128.7][b]	31.2 [16.6–38.7][e]
	120 min	89.5 [83.9–106.6]	144.3 [121.2–164.8][bcd]	28.9 [29.2–58.0][e]
LVESV (ml)	sham	41.6 [40.5–42.2]		
	30 min	37.3 [31.3–48.3]	42.8 [36.2–48.7]	6.0 [0.8–13.4]
	60 min	47.7 [43.3–51.8][a]	68.1 [47.3–70.8][b]	16.9 [6.7–22.3][e]
	90 min	55.3 [42.2–62.9][a]	65.8 [50.6–68.9][b]	5.4 [0.1–21.7]$^{p = 0.08}$
	120 min	55.8 [45.1–64.4][a]	78.0 [60.5–94.3][bc]	28.9 [14.6–31.7][e]

Abbreviations: AAR—area at risk; LV—left ventricle; LVEDV—left ventricular end-diastolic volume; LVEF—left ventricular ejection fraction; LVESV—left ventricular end-systolic volume; MVO—microvascular obstruction; Δ—change.

Note: Data are expressed as median [IQR]. $N = 8$ animals per group except for 120 min of ischemia ($n = 7$).

[a] $p < 0.05$ vs sham and 30 min of ischemia.

[b] $p < 0.05$ vs 30 min of ischemia.

[c] $p < 0.05$ vs 60 min of ischemia.

[d] $p < 0.05$ vs 90 min of ischemia.

[e] $p < 0.05$ vs day 3.

and markers of liver and renal function; CLIMA MC15 from RAL) parameters.

2.8 | Statistical analysis

We performed tests for normality (Shapiro–Wilk) and homoscedasticity (Bartlett test) and thereafter performed nonparametric statistical analyses Kruskal–Wallis and Mann–Whitney. Results are reported as medians and interquartile range [IQR]. Spearman's correlation was also performed. A cut-off value of $p < 0.05$ was used to consider the statistical significance. Statistical analyses were performed with the GRAPHPAD PRISM 8.0.2 software package.

3 | RESULTS

3.1 | Impact of ischemia on cardiac damage and function

Two pigs, one during the 90 min of ischemia and another during the 120 min of ischemia, died from fatal ventricular arrhythmias and were not included in the study. Hence, data are reported on a total of $n = 39$ animals (sham: $n = 8$; 30 min: $n = 8$; 60 min: $n = 8$; 90 min: $n = 8$; 120 min: $n = 7$).

Cardiac parameters were evaluated after MI or sham operation by CMR (Table 1; Figure 1). Oedema, myocardial infarction and microvascular obstruction (MVO) were almost undetectable on day 3 post-STEMI in animals subjected to 30 min of ischemia. By contrast, animals subjected

to ischemic times of 60 min and above showed significant oedema formation and necrotic damage on day 3 post-MI. MVO was observed in 64% of the animals (20 out of 31 pigs) subjected to coronary ischemia and was mostly present in those animals subjected to 90 min of ischemia or more (Table 1; Figure 1B). Of note, the presence of MVO was associated with significantly larger infarcts (Figure 1B) and a positive correlation was observed between the degree of MVO and infarct size (Figure 1C). The cardiac damage, expressed as both grams and percentage of left ventricular tissue with oedema and LGE, was comparable among the three groups with ischemic times of 60, 90 and 120 min. The same accounted for the AAR. Scar tissue analyses on day 42 revealed a similar pattern of myocardial injury, although as expected, the LGE quantity decreased by around 4%–5% over time in pigs subjected to ≥60 min of ischemia.

Histopathological analyses substantiated the CMR findings on structural heart damage, demonstrating myocardial scar in those animals subjected to ≥60 min of ischemia (Figure 2A,B). Accordingly, we observed a significant correlation between infarct size assessed by TTC staining and CMR (Figure 2C).

The impact on myocardial functional parameters was also dependent on the duration of coronary occlusion (Table 1 and Video S1). No significant differences were observed in left ventricular contraction and volumes between sham-operated animals and animals subjected to 30 min of ischemia, supporting the minimal structural cardiac damage. By contrast, 60 min of ischemia already impaired LVEF at the expense of LVESV increase without modifying LVEDV. The LVEF had a trend towards a decline with an increased duration of ischemia, but there
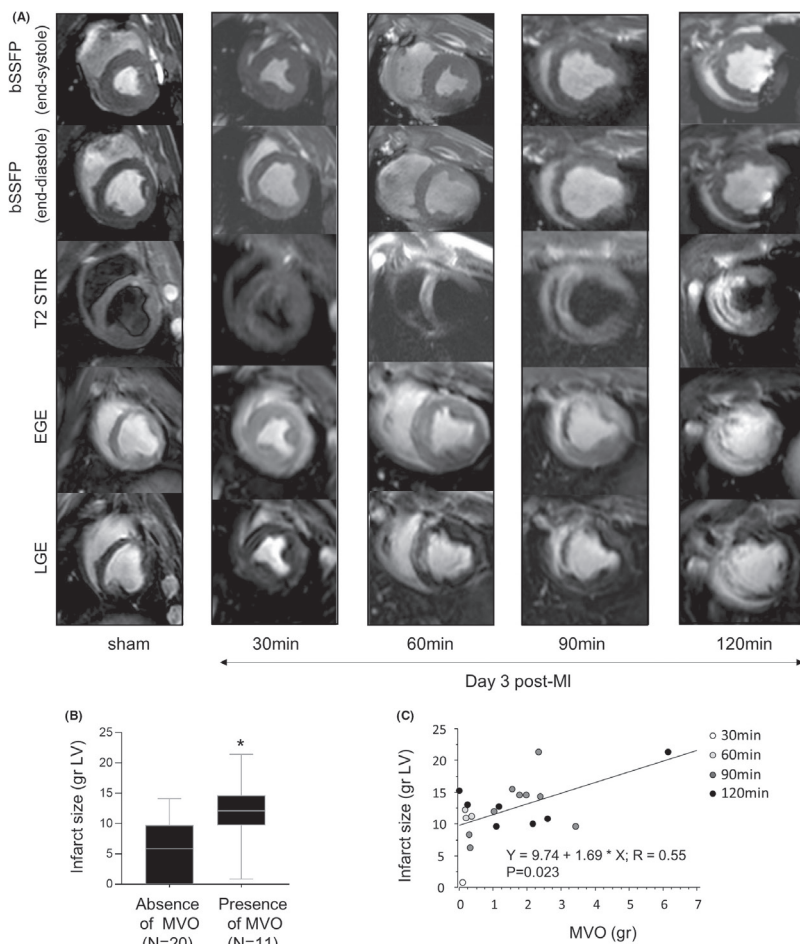
FIGURE 1 CMR analyses. (A). CMR representative images of mid short-axis plane in sham-operated animals and on day 3 after myocardial infarction in animals subjected to 30, 60, 90 and 120 min of coronary ischemia. (B). Infarct size in the presence or absence of MVO. (C). Correlation (Spearman's correlation) between MVO and infarct size. EGE—early gadolinium enhancement; LGE—late gadolinium enhancement; MVO—microvascular obstruction; bSSFP—balanced steady-state free precession; t2W-STIR—T2-weighted short-tau inversion recovery; MI—myocardial infarction. *$p < 0.05$ vs absence of no-reflow. Data are presented as median [IQR]. Number of animals included in the analyses: sham $n = 8$; 30 min = 8; 60 min = 8; 90 min = 8; 120 min = 7.
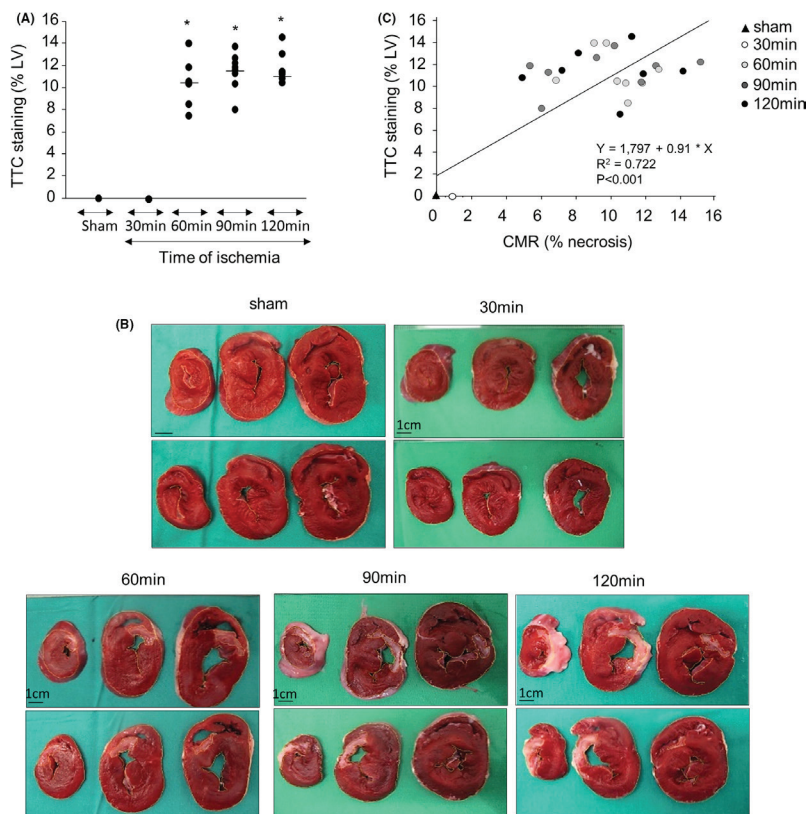
FIGURE 2 Impact of time of coronary ischemia on infarct size assessed by histopathology. (A). Individual data (and median) of the percentage of TTC staining according to the time of ischemia. (B). Representative images; (C). Correlation (Spearman's correlation) between TTC staining and CMR on day 42 post-AMI. *$p < 0.05$ vs 30 min and sham. Number of animals included in the analyses: 0 min $n = 8$; 30 min = 8; 60 min = 8; 90 min = 8; 120 min = 7.

was no statistically significant difference among the three groups. LVEF decrease on day 42 was comparable to that observed on day 3 post-STEMI in pigs subjected to ≥60 min of ischemia. Yet, LV volumes differed. As such, LVEDV increased in a time of ischemia-dependent fashion reaching statistical significance in the group subjected to 120 min of ischemia. LVESV was significantly increased in all animals subjected to ≥60 min; yet, changes were significantly greater in the 120 min of ischemia group.

3.2 | Impact of ischemia on left ventricle remodelling parameters

We evaluated WM abnormalities in the jeopardized myocardial segments (Figure 3A). On day 3, no WM abnormalities were detected in either sham-operated or animals subjected to 30 min of ischemia (Figure 3B). By contrast, segmental WM was significantly impaired in pigs subjected to 60, 90 and 120 min of ischemia (WM = 1.15, 1.22

and 1.38 mm, respectively), an effect that persisted up to day 42. In line with these observations, the proportion of dysfunctional segments (WM < 2.0 mm) was higher in those animals that underwent ≥60 min of persistent ischemia (≈60% of the segments vs ≈10% in animals subjected to 30 min of ischemia).

On day 42, pigs subjected to ≥60 min remained with WM below 2 mm and showed a comparable number of dysfunctional (Figure 3C) and percentage of recovered (Figure 3D) segments.

3.3 | Impact of ischemia time on cardiac fibrosis in the evolving scar

We evaluated transcript levels and protein expression of several markers of fibrous tissue deposition after 42 days of MI. As shown in Figure 4, no changes were detected as to Smad2 transcript levels throughout the different cardiac regions and among the different animal groups. Gene levels el Col1A1, Col1A2, Col3A1 and vimentin were significantly and similarly upregulated in the scar region of

animals subjected to ≥60 min of ischemia as compared to sham and 30 min of ischemia animals and to the remote cardiac regions' expression levels. In line with this transcriptomic data, animals subjected to ≥60 min of ischemia showed higher activation of Smad2/3 protein, a higher activation of Smad2/3 (p-Smad2/3) and a higher content of TGFβRII protein in the scar region compared with all animals ($p < 0.05$ vs sham and 30 min of ischemia; Figure 5). Similarly, significantly higher levels of collagen 1 and 3 protein were detected in the infarct zone of animals subjected to ≥60 min of ischemia (Figure 6).

3.4 | Impact of ischemia time on cardiomyocyte hypertrophy

The cross-sectional areas and the volume of cardiomyocytes (Figure 7) in the LV septal region were significantly larger than those in the remote distal myocardium in all pigs (sham and STEMI) at 42 days post-MI. Both area and volume were significantly enhanced in the infarcted region of animals subjected to ≥60 min of ischemia.
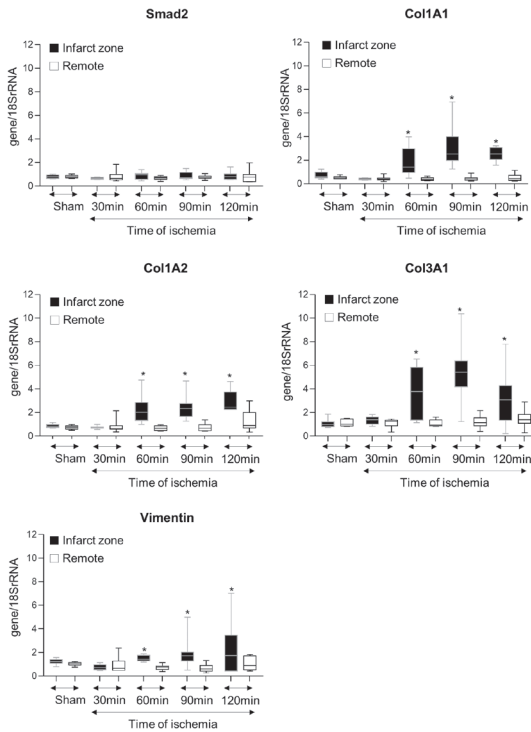
FIGURE 4 Impact of time of coronary ischemia on transcript levels of fibrosis-related markers in the myocardium of all pigs on day 42 post-MI; *$p < 0.05$ vs 30 min and sham. We performed a nonparametric statistical analysis (Kruskal–Wallis and Mann–Whitney analyses), and the results are reported as medians and interquartile range [IQR]. Number of animals included in the analyses: sham $n = 8$; 30 min = 8; 60 min = 8; 90 min = 8; 120 min = 7.
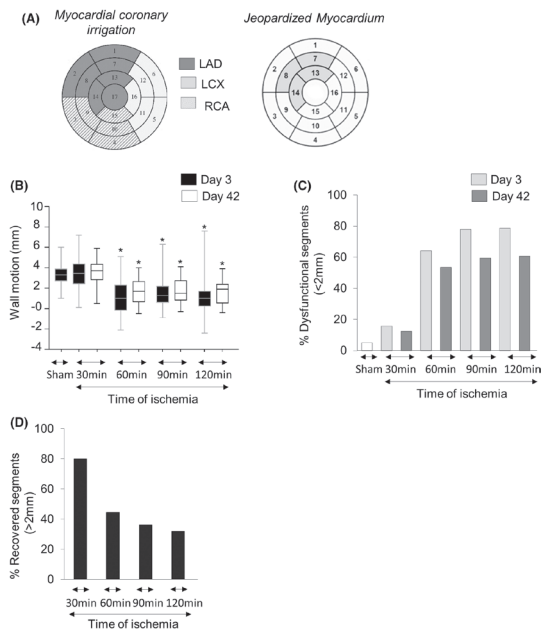
3.5 | Impact of ischemia time on microvascular rarefaction

No changes were detected in transcript levels of vWF (Figure 8A) and lectin staining (Figure 8B) in the entire myocardium of sham-operated animals and those subjected to 30 min of ischemia. Yet, lower VWF gene expression and lower vessel density by lectin staining were observed in the scar region of animals subjected to ≥60 min of ischemia.

3.6 | Animals' follow-up

Haematological, biochemical parameters (liver, kidney, lipids and glucose levels), body temperature and body weight progression were similar among all animals included in the study (Table S1).

4 | DISCUSSION

In this study we have performed, in a clinically relevant closed-chest pig model of experimental MI, a comprehensive CMR analysis of the influence of the duration of myocardial ischemia (30, 60, 90 and 120 min) on cardiac structural and functional outcomes over time (early and late remodelling phase post-MI). Furthermore, we also provide an in-depth characterization at a molecular and cellular level of the evolving scar. We report that the occlusion of the LAD coronary artery for 60 min induces cardiac structural and functional alterations that persist

over 42 days. No signs of cardiac damage are detected after 30 min of closed-chest balloon coronary ischemia compared with sham-operated animals. By contrast, longer ischemic periods (up to 120 min) favour the development of adverse cardiac remodelling as evidenced by an increase in both LV systolic and diastolic volumes. The evolving scar of animals subjected to ≥60 min of ischemia shows significant signs of microvascular rarefaction, myocyte hypertrophy and the activation of the TGFβ/smad2/3/collagen axis and consequent local collagen fibril formation and deposition at 42 days post-MI.

Within the last 40 years, multiple therapeutic strategies aimed to limit the size of infarction have been tested in several animal models, yet, none has translated into the clinical scenario.[33] The reasons for this failure to translate cardioprotection into the clinical setting have been attributed to several factors, including the use of inappropriate animal models of MI and the lack of their in-depth characterization.[34,35] Small animal models (mice, rats) are useful for specific mechanistic evaluations but do not recapitulate human pathophysiology and it is not recommended to translate their results into humans directly.[36,37] Primates are closer to humans, yet, they exhibit a surprising resistance against myocardial infarction[38]; and dogs exhibit collateral circulation, which is a protective mechanism to counteract coronary ischemia.[39] Because of their human cardiovascular resemblance (comparable hemodynamics, anatomy and metabolic requirements and lack of collateral circulation), closed-chest pig models of LAD ischemia/reperfusion have become mandatory for final proof-of-concept studies before moving into clinical trials aimed to test cardioprotective/regenerative strategies. Yet, although the time course of infarct evolution in the setting of ischemia/reperfusion has been studied in several animal models of STEMI, including pigs[17–20,40–42] and in a few clinical studies,[43,44] it is still unclear which is the impact of the duration of ischemia on modern and clinically available CMR imaging techniques in translational studies.[45] As such, no preclinical study has determined the influence of ischemia time on critical structural parameters, including cardiac necrosis, oedema and MVO, and on global and regional parameters of LV performance and remodelling.

Previously published studies in open-chest pig models have shown transmural infarctions after 60 min of ischemia.[18] Fujiwara et al.[18] performed LAD occlusion in open-chest pigs using a Vesseloops rubber band for 20, 30, 60
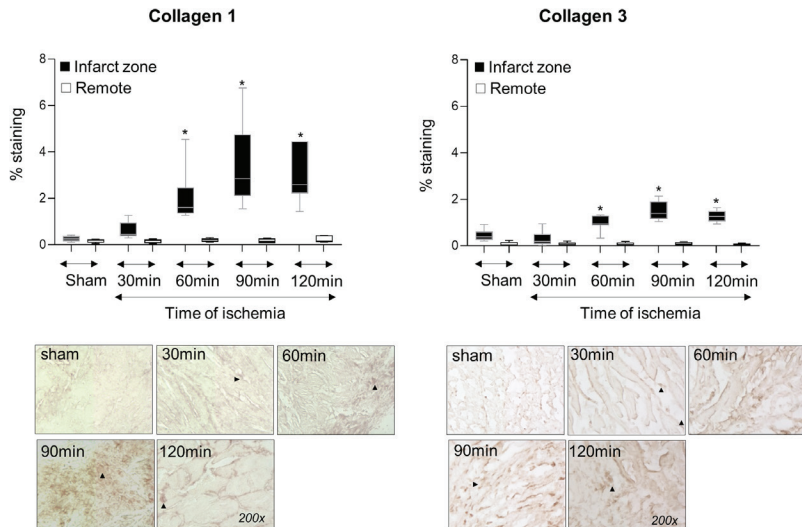
FIGURE 6 Impact of time of coronary ischemia on myocardial collagen content on day 42 post-MI. Collagen staining on the entire heart and representative images for the infarcted myocardium. *$p < 0.05$ vs 30 min and sham. We performed a nonparametric statistical analysis (Kruskal–Wallis and Mann–Whitney analyses), and the results are reported as medians and interquartile range [IQR]. Number of animals included in the analyses: sham $n = 8$; 30 min = 8; 60 min = 8; 90 min = 8; 120 min = 7

and 120 min and then reperfused for 8 h or remained with a permanent occlusion. Infarct size was determined by Masson's trichrome staining and the risk area by postmortem angiography. They reported no significant differences in infarct size expressed as the risk area between animals banded for 60 min or above, supporting the need to reperfuse within 1 h after occlusion. In a study in a closed-chest model of balloon-induced MI, Silvis et al.[20] evaluated the impact of 60, 75 and 90 min of ischemia followed by 24 h reperfusion in thiopental anaesthetised pigs. No differences were observed in the AAR as % LV between the different occlusion groups. Infarct size/AAR increase was significantly higher at 75 min than 60, and no differences were observed between 75 and 90 min. Likewise, Naslund et al.[17] also evaluated infarct size (expressed as AAR and TTC staining) in closed-chest balloon-induced MI pigs (30, 60 and 90 min and then left for 24 h postreperfusion) also anaesthetised with barbiturics (sodium pentopharbibtal). Although no significant difference between data from animals subjected to 60 min occlusion versus longer ischemic periods was observed, they detected an infarct size of 46% AAR in those animals subjected to 30 min of

ischemia. The use of injectable anaesthetic agents instead of volatile anaesthesia may account for such discrepancies. In this regard, the use of isoflurane has been demonstrated to provide a certain degree of cardioprotection.[46]

The ratio of IS and the AAR, measured with TTC/Evans' blue double staining, is considered the gold standard outcome measurement to investigate IS and the potential of cardioprotective strategies, yet, it does not provide in vivo accurate data for tissue characterization and MVO (an estimate of no-reflow). With high accuracy, CMR provides imaging features and dynamic changes of the infarcted myocardium (oedema, necrosis and MVO) over time. Within the last years, CMR has evolved into a gold standard tool for noninvasive characterization and evaluation of myocardial structural and functional abnormalities post-MI and for identifying potential benefits associated with new cardioprotective strategies in experimental and clinical trials.[21] In this regard, a scientific expert panel consensus document has recently recommended, at a preclinical and clinical level, the assessment of LGE extent as the CMR primary endpoint and LVEF and MVO as main secondary endpoints for diagnosis and risk stratification for future cardiovascular events.[21,47]
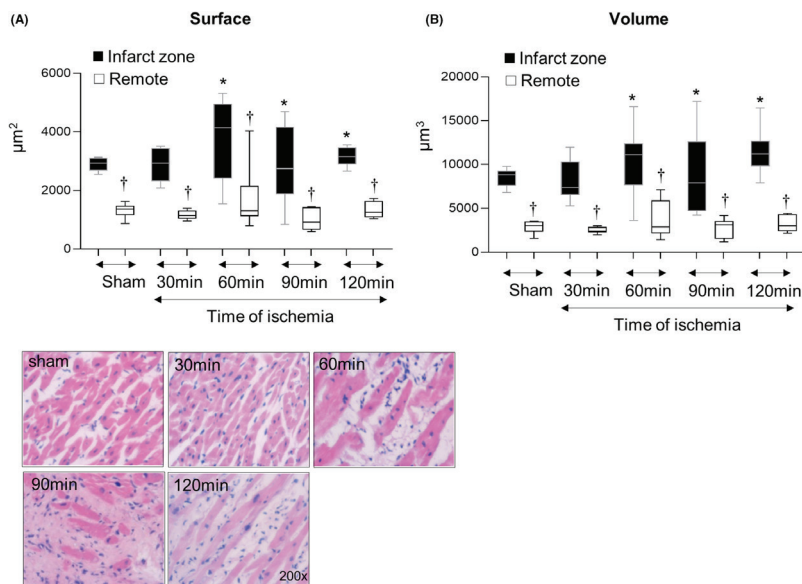
FIGURE 7 Impact of time of coronary ischemia on cardiomyocyte dimensions. (A). Cardiomyocyte surface. (B). Cardiomyocyte volume. $p < 0.05$ vs sham and 30 min of ischemia; †$p < 0.05$ vs infarct zone. We performed a nonparametric statistical analysis (Kruskal–Wallis and Mann–Whitney analyses), and the results are reported as medians and interquartile range [IQR]. Number of animals included in the analyses: sham $n = 8$; 30 min = 8; 60 min = 8; 90 min = 8; 120 min = 7.

The ideal post-MI timing for evaluating CMR endpoints in acute injury appears to be between days 3 and 7 since LGE and MVO show relative stability and proven prognostic value in this time window.[48,49] Our CMR data show a comparable degree of myocardial damage, expressed as LGE-infarct size and oedema formation on day 3 post-STEMI in animals subjected to 60 min of ischemia that is not further aggravated in animals exposed to longer occlusion times. Yet, although infarct size and oedema did not expand beyond 60 min of ischemia in our model of MI, MVO showed a time-dependent increase supporting the concept that the longer the coronary ischemia the worse myocardial injury.

Regarding oedema, Fernández-Jiménez et al.[50] reported a bimodal pattern of oedema formation following 40 min of MI in ketamine-anaesthetised pigs in which oedema firstly peaked at 24 h and a plateau for the second oedema wave was observed on day 4. Since oedema formation is highly dependent on the size of infarction,[51] whether smaller infarcts or different AAR display the same time-dependent oedema pattern remains to be assessed in

order to standardize the best timing for CMR analyses.[14] Interestingly, we have developed a model with infarctions within the order of magnitude of those obtained in the era of modern revascularization procedures (around 16% LV) ensuring an enhanced translatability to the clinical arena of the obtained results.[52,53] Yet, it is important to consider that large infarcts may overestimate cardioprotective interventions, likely contributing to the failure to translate successful and novel experimental strategies to the clinical setting. However, despite a comparable degree of myocardial damage, MVO is mildly present after 60 min of ischemia and markedly increased from 90 min of ischemia onwards. Importantly, the extent of MVO on CMR, reflecting the extent of no-reflow, has been found associated with 1-year all-cause mortality, even after adjustment for infarct size, thus providing additional prognostic information.[25,54]

We report on the longitudinal structural changes that affect the infarcted myocardium and show that at 42 days post-STEMI, scar size is comparable among pigs subjected to 60 min or longer and smaller than that observed
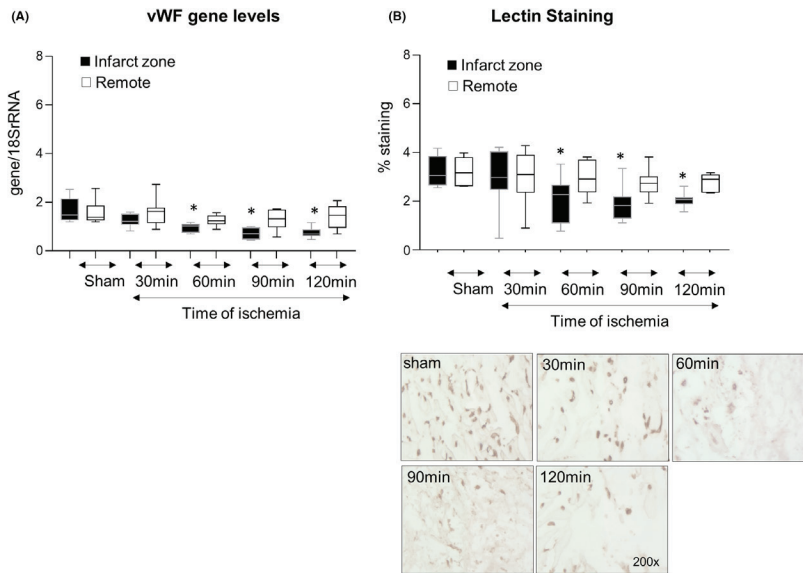
FIGURE 8 Impact of time of coronary ischemia on microvascular rarefaction in the entire myocardium. (A). Transcript levels of von Willebrand Factor (vWF). (B). Lectin staining $*p < 0.05$ vs sham and 30 min of ischemia. We performed a nonparametric statistical analysis (Kruskal–Wallis and Mann–Whitney analyses), and the results are reported as medians and interquartile range [IQR]. Number of animals included in the analyses: sham $n = 8$; 30 min = 8; 60 min = 8; 90 min = 8; 120 min = 7.

on day 3. Previous studies in closed-chest pig LAD ischemia/reperfusion have also shown that increasing occlusion times result in an increased infarct size (expressed per AAR) reaching a plateau, and ischemia times longer than 2 h have not shown to lead to larger infarcts as compared to persistent coronary occlusion.[18,20] Notably, CMR was not available in these studies. Likely, the smaller scar sizes detected on day 42, are possibly due to the inherent shrinkage related to cardiac healing, as the infarcted myocardium (assessed by LGE) evolves from necrosed, inflamed and oedematous tissue (on day 3) to a scar (on day 42) over time.

We also provide evidence of the impact of ischemia time on functional data at global (percentage of LV contraction and volumes) and segmental levels. As such, LVEF and LVESV are significantly and similarly impaired, on day 3 only in those animals subjected to 60 min of ischemia or longer, an effect that persists up to day 42. Segmental analyses of the jeopardized myocardium also evidenced wall motion abnormalities in those animals subjected to 60 min whereas no evidence of dyskinesia was observed in animals subjected

to 30 min of ischemia. Interestingly, however, LVEDV, a marker of adverse ventricular remodelling was only found to be markedly impaired (by more than 37%) in animals subjected to 120 min at 42 days post-MI. In this regard, a relative ≥20% increase in LVEDV between measurements has been historically associated with the development of ventricular remodelling of the entire left ventricle and, most importantly, with an increased risk of symptomatic heart failure and mortality.[55,56] Nonetheless, these data remain controversial since these studies were mostly assessed by echocardiography without validation in CMR studies. More recent evidence has pointed to lower thresholds of % changes in LV volumes and function (12 to 20%).[57,58]

Finally, the pathophysiological mechanisms behind the detected worsening of cardiac contractility observed in pigs subjected to ≥60 min coronary occlusion include the activation of the TGFβR/Smad/collagen axis and consequent collagen fibril deposition, cardiomyocyte hypertrophy and microvessel rarefaction, a hallmark of fibrotic disease. Of note, we report regional differences in cardiac

myocyte dimensions in noninfarcted pigs being larger in the septal wall than the lateral wall. A previous study has demonstrated a transmural gradient of cellular dimensions in the LV of the rat but not of the hamster or the guinea pig.[59] Our pig data are relevant for properly evaluating LV response to AMI. Besides, although no further changes were detected in those animals that display diastolic dysfunction (as increased LVEDV), this pathological condition might also be related to neurohormonal and hemodynamic alterations.[60–62]

This study has several shortcomings worth discussing. As this study assessed juvenile Landrace pigs, the relative damage inflicted by balloon inflation in healthy coronary arteries of young pigs may differ from that on the diseased atherothrombotic arteries observed in humans. Secondly, due to the lack of reliable internal quality control specifically regarding the sequence parameters and reproducibility of measurement at the time of the study, we could not assess intramyocardial haemorrhage, which could have provided another important biomarker. Besides, the addition of T1 mapping studies would have provided a valuable determination to better depict the impact of time of ischemia on cardiac remodelling. Finally, we have investigated the effect of the duration of ischemia in normolipidemic conditions. Still, the presence of co-morbidities may increase cardiac damage and dysfunctional heart performance upon the acute coronary artery occlusion, as we have previously observed.[63–67]

5 | CONCLUSION

By using clinical CMR acquisition and postprocessing protocols and modern imaging markers that are widely adopted in clinical trials and diagnostic imaging, this study provides further insight into the natural history of myocardial infarction depending on ischemia duration. We provide a comprehensive longitudinal CMR analysis of the impact of ischemia time on clinically relevant cardiac structural and functional outcomes in a highly translatable animal model. As such, closed-chest mid-LAD coronary occlusion for 60 min suffices to induce myocardial damage and systolic alterations in pigs whereas longer ischemic periods (120 min) result in further adverse remodelling in the late phase. Our findings can help to refine and standardize animal model studies by optimizing the resources, ensuring ethical considerations to eventually achieve feasible and reproducible results in clinical trials of cardioprotection.

ORCID

Monika Radike https://orcid.org/0000-0002-4004-4150
Soumaya Ben-Aicha https://orcid.org/0000-0001-5572-5883
Manuel Gutiérrez https://orcid.org/0000-0001-7362-4330
María Borrell-Pages https://orcid.org/0000-0002-1759-9756
Teresa Padró https://orcid.org/0000-0003-1921-954X
Lina Badimon https://orcid.org/0000-0002-9162-2459
Gemma Vilahur https://orcid.org/0000-0002-2828-8873

REFERENCES

1. Simes RJ, Topol EJ, Holmes DR Jr, et al. Link between the angiographic substudy and mortality outcomes in a large randomized trial of myocardial reperfusion. Importance of early and complete infarct artery reperfusion. GUSTO-I investigators. *Circulation*. 1995;91(7):1923-1928.
2. De Luca G, Suryapranata H, Ottervanger JP, Antman EM. Time delay to treatment and mortality in primary angioplasty for acute myocardial infarction: every minute of delay counts. *Circulation*. 2004;109(10):1223-1225.
3. Hausenloy DJ, Barrabes JA, Bøtker HE, et al. Ischaemic conditioning and targeting reperfusion injury: a 30 year voyage of discovery. *Basic Res Cardiol*. 2016;111(6):70.
4. Heusch G. 25 years of remote ischemic conditioning: from laboratory curiosity to clinical outcome. *Basic Res Cardiol*. 2018;113(3):15.

5. Kleinbongard P, Skyschally A, Gent S, Pesch M, Heusch G. STAT3 as a common signal of ischemic conditioning: a lesson on "rigor and reproducibility" in preclinical studies on cardioprotection. *Basic Res Cardiol*. 2018;113(1):3.

6. Mendieta G, Ben-Aicha S, Gutiérrez M, et al. Intravenous statin administration during myocardial infarction compared with oral post-infarct administration. *J Am Coll Cardiol*. 2020;75(12):1386-1402.

7. Mendieta G, Ben-Aicha S, Casani L, Badimon L, Sabate M, Vilahur G. Molecular pathways involved in the cardioprotective effects of intravenous statin administration during ischemia. *Basic Res Cardiol*. 2019;115(1):2.

8. Díaz-Munoz R, Valle-Caballero MJ, Sanchez-Gonzalez J, et al. Intravenous metoprolol during ongoing STEMI ameliorates markers of ischemic injury: a METOCARD-CNIC trial electrocardiographic study. *Basic Res Cardiol*. 2021;116(1):45.

9. Ibanez B, Prat-González S, Speidl WS, et al. Early metoprolol administration before coronary reperfusion results in increased myocardial salvage: analysis of ischemic myocardium at risk using cardiac magnetic resonance. *Circulation*. 2007;115(23):2909-2916.

10. Davidson SM, Ferdinandy P, Andreadou I, et al. Multitarget strategies to reduce myocardial ischemia/reperfusion injury: JACC review topic of the week. *J Am Coll Cardiol*. 2019;73(1):89-99.

11. Vilahur G, Oñate B, Cubedo J, et al. Allogenic adipose-derived stem cell therapy overcomes ischemia-induced microvessel rarefaction in the myocardium: systems biology study. *Stem Cell Res Ther*. 2017;8(1):52.

12. Gao L, Gregorich ZR, Zhu W, et al. Large cardiac muscle patches engineered from human induced-pluripotent stem cell-derived cardiac cells improve recovery from myocardial infarction in swine. *Circulation*. 2018;137(16):1712-1730.

13. van der Velden J, Asselbergs FW, Bakkers J, et al. Animal models and animal-free innovations for cardiovascular research: current status and routes to be explored. Consensus document of the ESC working group on myocardial function and the ESC Working Group on Cellular Biology of the Heart. *Cardiovasc Res*. 2022:1-36. doi:10.1093/cvr/cvab370

14. Lecour S, Andreadou I, Bøtker HE, et al. IMproving Preclinical Assessment of Cardioprotective Therapies (IMPACT) criteria: guidelines of the EU-CARDIOPROTECTION COST action. *Basic Res Cardiol*. 2021;116(1):52.

15. Bolli R, Ghafghazi S. Cell therapy needs rigorous translational studies in large animal models. *J Am Coll Cardiol*. 2015;66(18):2000-2004.

16. Lelovas PP, Kostomitsopoulos NG, Xanthos TT. A comparative anatomic and physiologic overview of the porcine heart. *J Am Assoc Lab Anim Sci*. 2014;53(5):432-438.

17. Naslund U, Haggmark S, Johansson G, Pennert K, Reiz S, Marklund SL. Effects of reperfusion and superoxide dismutase on myocardial infarct size in a closed chest pig model. *Cardiovasc Res*. 1992;26(2):170-178.

18. Fujiwara H, Matsuda M, Fujiwara Y, et al. Infarct size and the protection of ischemic myocardium in pig, dog and human. *Jpn Circ J*. 1989;53(9):1092-1097.

19. Reimer KA, Vander Heide RS, Richard VJ. Reperfusion in acute myocardial infarction: effect of timing and modulating factors in experimental models. *Am J Cardiol*. 1993;72(19):13G-21G.

20. Silvis MJM, van Hout GPJ, Fiolet ATL, et al. Experimental parameters and infarct size in closed chest pig LAD ischemia reperfusion models; lessons learned. *BMC Cardiovasc Disord*. 2021;21(1):171.

21. Ibanez B, Aletras AH, Arai AE, et al. Cardiac MRI endpoints in myocardial infarction experimental and clinical trials: JACC scientific expert panel. *J Am Coll Cardiol*. 2019;74(2):238-256.

22. Stiermaier T, Jobs A, de Waha S, et al. Optimized prognosis assessment in ST-segment-elevation myocardial infarction using a cardiac magnetic resonance imaging risk score. *Circ Cardiovasc Imaging*. 2017;10(11):e006774.

23. Stone GW, Selker HP, Thiele H, et al. Relationship between infarct size and outcomes following primary PCI: patient-level analysis from 10 randomized trials. *J Am Coll Cardiol*. 2016;67(14):1674-1683.

24. Selker HP, Udelson JE, Ruthazer R, et al. Relationship between therapeutic effects on infarct size in acute myocardial infarction and therapeutic effects on 1-year outcomes: a patient-level analysis of randomized clinical trials. *Am Heart J*. 2017;188:18-25.

25. de Waha S, Patel MR, Granger CB, et al. Relationship between microvascular obstruction and adverse events following primary percutaneous coronary intervention for ST-segment elevation myocardial infarction: an individual patient data pooled analysis from seven randomized trials. *Eur Heart J*. 2017;38(47):3502-3510.

26. Bonanad C, Monmeneu JV, Lopez-Lereu MP, et al. Prediction of long-term major events soon after a first ST-segment elevation myocardial infarction by cardiovascular magnetic resonance. *Eur J Radiol*. 2016;85(3):585-592.

27. Percie du Sert N, Ahluwalia A, Alam S, et al. Reporting animal research: explanation and elaboration for the ARRIVE guidelines 2.0. *PLoS Biol*. 2020;18(7):e3000411.

28. Vilahur G, Gutiérrez M, Casani L, et al. P2Y12 antagonists and cardiac repair post-myocardial infarction: global and regional heart function analysis and molecular assessments in pigs. *Cardiovasc Res*. 2018;114(14):1860-1870.

29. Mendieta G, Ben-Aicha S, Casani L, Badimon L, Sabate M, Vilahur G. Intravenous statin administration during ischemia exerts cardioprotective effects. *J Am Coll Cardiol*. 2019;74(3):475-477.

30. Ortiz-Perez JT, Rodriguez J, Meyers SN, Lee DC, Davidson C, Wu E. Correspondence between the 17-segment model and coronary arterial anatomy using contrast-enhanced cardiac magnetic resonance imaging. *JACC Cardiovasc Imaging*. 2008;1(3):282-293.

31. López Lereu MP, Bodi V, Sanchis J, et al. Reliability of cardiac magnetic resonance imaging indicators of myocardial viability for predicting the recovery of systolic function with a first acute myocardial infarction with a patent culprit artery. *Rev Esp Cardiol*. 2004;57(9):826-833.

32. Vilahur G, Juan-Babot O, Pena E, Onate B, Casani L, Badimon L. Molecular and cellular mechanisms involved in cardiac remodeling after acute myocardial infarction. *J Mol Cell Cardiol*. 2011;50(3):522-533.

33. Heusch G, Skyschally A, Kleinbongard P. Translation, translation, translation: the need for large animal studies in cardioprotection research. *Circ Res*. 2018;123(8):931-933.

34. Heusch G. Myocardial ischaemia-reperfusion injury and cardioprotection in perspective. *Nat Rev Cardiol*. 2020;17(12):773-789.

35. Heusch G, Gersh BJ. Is cardioprotection salvageable? *Circulation*. 2020;141(6):415-417.

36. Bøtker HE, Hausenloy D, Andreadou I, et al. Practical guidelines for rigor and reproducibility in preclinical and clinical studies on cardioprotection. *Basic Res Cardiol*. 2018;113(5):39.

37. Heusch G. Cardioprotection research must leave its comfort zone. *Eur Heart J*. 2018;39(36):3393-3395.

38. Shen YT, Fallon JT, Iwase M, Vatner SF. Innate protection of baboon myocardium: effects of coronary artery occlusion and reperfusion. *Am J Phys*. 1996;270(5 Pt 2):H1812-H1818.

39. Sasayama S. Effect of coronary collateral circulation on myocardial ischemia and ventricular dysfunction. *Cardiovasc Drugs Ther*. 1994;8(Suppl 2):327-334.

40. Kloner RA, Ellis SG, Lange R, Braunwald E. Studies of experimental coronary artery reperfusion. Effects on infarct size, myocardial function, biochemistry, ultrastructure and microvascular damage. *Circulation*. 1983;68(2 Pt 2):I8-I15.

41. Hale SL, Kloner RA. Effect of early coronary artery reperfusion on infarct development in a model of low collateral flow. *Cardiovasc Res*. 1987;21(9):668-673.

42. Naslund U, Haggmark S, Johansson G, Marklund SL, Reiz S. A closed-chest myocardial occlusion-reperfusion model in the pig: techniques, morbidity and mortality. *Eur Heart J*. 1992;13(9):1282-1289.

43. Hedstrom E, Engblom H, Frogner F, et al. Infarct evolution in man studied in patients with first-time coronary occlusion in comparison to different species–implications for assessment of myocardial salvage. *J Cardiovasc Magn Reson*. 2009;11:38.

44. Bouisset F, Gerbaud E, Bataille V, et al. Percutaneous myocardial revascularization in late-presenting patients with STEMI. *J Am Coll Cardiol*. 2021;78(13):1291-1305.

45. Heusch G. Critical issues for the translation of cardioprotection. *Circ Res*. 2017;120(9):1477-1486.

46. Van Allen NR, Krafft PR, Leitzke AS, Applegate RL 2nd, Tang J, Zhang JH. The role of volatile anesthetics in cardioprotection: a systematic review. *Med Gas Res*. 2012;2(1):22.

47. Niccoli G, Montone RA, Ibanez B, et al. Optimized treatment of ST-elevation myocardial infarction. *Circ Res*. 2019;125(2):245-258.

48. Bulluck H, Hammond-Haley M, Weinmann S, Martinez-Macias R, Hausenloy DJ. Myocardial infarct size by CMR in clinical cardioprotection studies: insights from randomized controlled trials. *JACC Cardiovasc Imaging*. 2017;10(3):230-240.

49. Fernández-Jiménez R, Barreiro-Pérez M, Martin-García A, et al. Dynamic edematous response of the human heart to myocardial infarction: implications for assessing myocardial area at risk and salvage. *Circulation*. 2017;136(14):1288-1300.

50. Fernández-Jiménez R, Sánchez-González J, Agüero J, et al. Myocardial edema after ischemia/reperfusion is not stable and follows a bimodal pattern: imaging and histological tissue characterization. *J Am Coll Cardiol*. 2015;65(4):315-323.

51. Horneffer PJ, Healy B, Gott VL, Gardner TJ. The rapid evolution of a myocardial infarction in an end-artery coronary preparation. *Circulation*. 1987;76(5 Pt 2):V39-V42.

52. Hjortbak MV, Olesen KKW, Seefeldt JM, et al. Translation of experimental cardioprotective capability of P2Y12 inhibitors into clinical outcome in patients with ST-elevation myocardial infarction. *Basic Res Cardiol*. 2021;116(1):36.

53. Francis R, Chong J, Ramlall M, et al. Effect of remote ischaemic conditioning on infarct size and remodelling in ST-segment elevation myocardial infarction patients: the CONDI-2/ERIC-PPCI CMR substudy. *Basic Res Cardiol*. 2021;116(1):59.

54. Heusch G. Coronary microvascular obstruction: the new frontier in cardioprotection. *Basic Res Cardiol*. 2019;114(6):45.

55. McKay RG, Pfeffer MA, Pasternak RC, et al. Left ventricular remodeling after myocardial infarction: a corollary to infarct expansion. *Circulation*. 1986;74(4):693-702.

56. Redfield MM, Jacobsen SJ, Burnett JC Jr, Mahoney DW, Bailey KR, Rodeheffer RJ. Burden of systolic and diastolic ventricular dysfunction in the community: appreciating the scope of the heart failure epidemic. *JAMA*. 2003;289(2):194-202.

57. Reindl M, Reinstadler SJ, Tiller C, et al. Prognosis-based definition of left ventricular remodeling after ST-elevation myocardial infarction. *Eur Radiol*. 2019;29(5):2330-2339.

58. Legallois D, Hodzic A, Alexandre J, et al. Definition of left ventricular remodelling following ST-elevation myocardial infarction: a systematic review of cardiac magnetic resonance studies in the past decade. *Heart Fail Rev*. 2022;27(1):37-48.

59. Campbell SE, Gerdes AM, Smith TD. Comparison of regional differences in cardiac myocyte dimensions in rats, hamsters, and Guinea pigs. *Anat Rec*. 1987;219(1):53-59.

60. Mishra S, Kass DA. Cellular and molecular pathobiology of heart failure with preserved ejection fraction. *Nat Rev Cardiol*. 2021;18(6):400-423.

61. Lam CSP, Voors AA, de Boer RA, Solomon SD, van Veldhuisen DJ. Heart failure with preserved ejection fraction: from mechanisms to therapies. *Eur Heart J*. 2018;39(30):2780-2792.

62. Jeong EM, Dudley SC Jr. Diastolic dysfunction. *Circ J*. 2015;79(3):470-477.

63. Kleinbongard P, Botker HE, Ovize M, Hausenloy DJ, Heusch G. Co-morbidities and co-medications as confounders of cardioprotection-Does it matter in the clinical setting? *Br J Pharmacol*. 2020;177(23):5252-5269.

64. Andreadou I, Schulz R, Badimon L, et al. Hyperlipidaemia and cardioprotection: animal models for translational studies. *Br J Pharmacol*. 2020;177(23):5287-5311.

65. Vilahur G, Gutiérrez M, Casaní L, et al. Hypercholesterolemia abolishes high-density lipoprotein-related cardioprotective effects in the setting of myocardial infarction. *J Am Coll Cardiol*. 2015;66(21):2469-2470.

66. Lazou A, Ikonomidis I, Bartekova M, et al. Chronic inflammatory diseases, myocardial function and cardioprotection. *Br J Pharmacol*. 2020;177(23):5357-5374.

67. Andreadou I, Tsoumani M, Vilahur G, et al. PCSK9 in myocardial infarction and cardioprotection: importance of lipid metabolism and inflammation. *Front Physiol*. 2020;11:602497.

SUPPORTING INFORMATION

Additional supporting information can be found online in the Supporting Information section at the end of this article.

4.2. Article 2.

Radike M, Ben-Aicha S, Gutiérrez M, et al. Comparison of two cardiac magnetic resonance imaging postprocessing software tools in a pig model of myocardial infarction. Revista Espanola de Cardiologia (English ed.). 2022 Jul:S1885-5857(22)00180-3. DOI: 10.1016/j.rec.2022.06.009. PMID: 35809893.

This article is related to the **Secondary objective 2.**

Material reused with editorial permission from (172).

Scientific letter

Comparison of two cardiac magnetic resonance imaging postprocessing software tools in a pig model of myocardial infarction

Comparación de dos programas de posprocesamiento de imágenes de cardiorresonancia magnética en un modelo porcino de infarto de miocardio

To the Editor,

Cardiovascular magnetic resonance (CMR) imaging has been increasingly used for testing of translational and clinical trial surrogate endpoints in cardioprotective therapies. While the JACC Scientific Expert Panel provides imaging technique recommendations and standardization[1], postprocessing and analysis methods vary institutionally. Moreover, most previous CMR postprocessing comparison and software testing data stem from human hearts. Pig hearts largely resemble their human counterparts. However, pigs have cone-shaped chests and higher resting heart rates than humans. Medis Suite (QMass MR v.3.2.60.4, The Netherlands) and CVI42 (v.5.11, Circle Cardiovascular Imaging, Canada) are among the most widely used scanner-independent CMR postprocessing software programs. However, their interchangeability to assess anatomical and functional parameters in preclinical models has not been tested. We aimed to compare Medis Suite and CVI42 readouts in a pig model of experimentally induced closed-chest acute myocardial infarction (MI). All procedures were authorized by the Animal Experimental Committee (#5601) of the local government.[2] We assessed anatomical and functional parameters in randomly selected 28 LandracexLarge white female pig datasets, which included baseline (before MI), early- (3 days post-MI), and late- (42 days post-MI) remodeling phase scans.[2] In addition, 25 of

28 scans included a dobutamine stress study (5-10-20-30 µg/kg/min of i.v. dobutamine at 3-minute intervals to elevate heart rate by 30-50%) using the volumetric module. To exclude interobserver- and experience-related variabilities, all images were blindly assessed by a Level 3 accredited operator. Due to animals' cardiac orientation, the quality of semi- and fully-automated ventricular contour segmentation was suboptimal in both products; thus, manual contouring was chosen.

The following were recorded: left ventricular (LV) end-diastolic volume, LV end-systolic volume, LV stroke volume, LV ejection fraction (LVEF), LV mass, right ventricular (RV) end-diastolic volume, RV end-systolic volume, RV stroke volume, and RV ejection fraction. Edema, microvascular obstruction (MVO), and necrosis mass were assessed on T_2 short-tau inversion recovery and T_1 inversion recovery sequences at early (1 minute) and late (10 minutes) gadolinium phases, respectively. On Medis Suite, we used visual assessment-defined manual planimetry on the volumetry module to draw the region(s) of interest (the late gadolinium enhancement [LGE] volume was multiplied by the myocardial density of 1.055 g/mL), and the full-width half-max (FWHM) technique, using the tissue characterization module with semiautomatic pixel value segmentation. Of note, MVO measurement on Medis Suite FWHM is planimetry-based, as the region of interest is user-defined without semiautomatic segmentation. On CVI42, as planimetry was unavailable for tissue characterization, we used FWHM. The day 42 LGE data were correlated with infarct size assessed by triphenyl tetrazolium chloride (TTC) staining.[2]

To detect low and strong correlation variables, accepting an alpha risk of 0.05 and a beta risk of 0.2 in 2-sided tests, 28 datasets were needed to detect a correlation coefficient of 0.51. A dropout rate of 0% was anticipated. After normal distribution testing (Shapiro-Wilk), data were analyzed for correlation by the Pearson
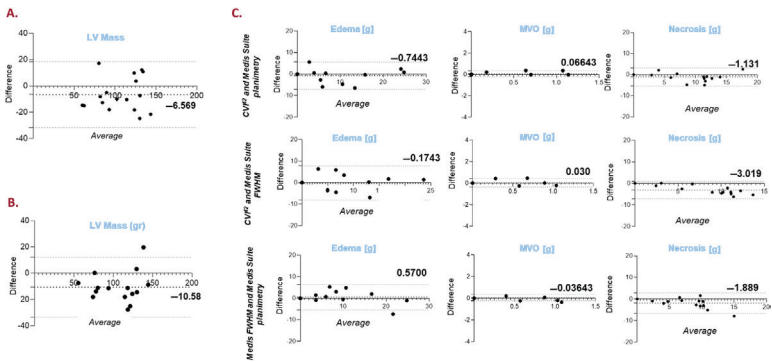
Figure 1. Bland-Altman graphs (Medis Suite-CVI42) vs average to analyze systematic differences at rest (A) and stress (B) of the left ventricular mass. C: Bland-Altman graphs to analyze systematic differences in the tissue characterization parameters between different methods. Dotted black lines indicate mean difference (bias; see also value in bold) and dashed grey lines indicate limits of agreement 95%. FWHM, full-width half maximum; LV, left ventricle; MVO, microvascular obstruction.

Scientific letter / Rev Esp Cardiol. 2022;xx(x):xxx–xxx
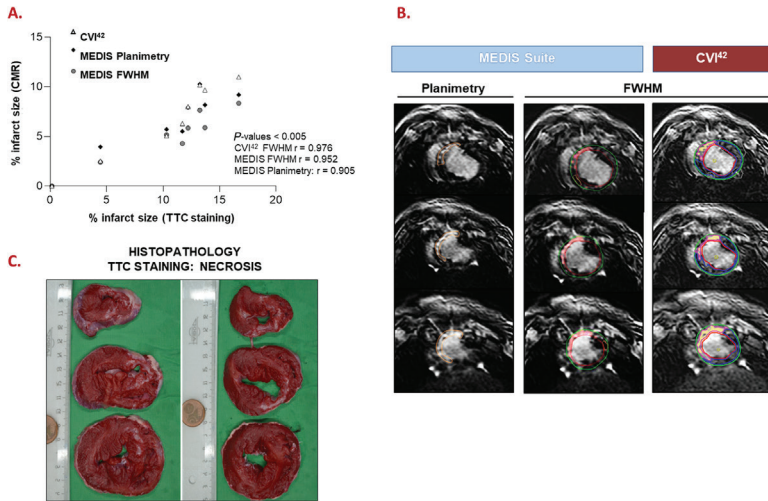
Figure 2. Correlation between the CMR-derived necrosis percentage (Medis Suite and CVI[42]) and histopathology (TTC staining) on the 8 datasets (A). Representative same-day CMR (B) and histopathology (C) images from the same animal. CMR, cardiovascular magnetic resonance; FWHM, full-width half maximum.

or Spearman tests, when appropriate. The Wilcoxon matched-pairs signed-rank test and the paired t-test were used to compare groups, matched as pair measurements of the same subject. For groups not following a normal distribution, equivalent nonparametric tests were performed.

The 28 datasets consisted of 3 baseline, 15 early remodeling, and 10 late remodeling phases; among the latter, 8 had histopathological analysis. Dobutamine stress was available in 25 datasets (89%). The 2 products provided similar data for biventricular volumes and LVEF, with significantly related correlation curves between measurements and Bland-Altman plots, showing only a minor systematic measurement error at rest and stress (P = nonsignificant). Only LV mass showed a mean difference of 10.58 g at stress (figure 1). The data were very similar in all structural parameters; as such, using planimetry and FMWH, we detected a high correlation between software in the necrosis, edema, and MVO quantification (P = non-significant), and Bland-Altman plots showed near-zero systematic differences for the 3 tested parameters (figure 1). LGE quantification agreed better on planimetry on Medis Suite and CVI[42] compared with FWHM on Medis Suite vs CVI[42], and planimetry vs FWHM on Medis Suite alone. FWHM on both showed a better correlation with histopathology (TTC staining) than planimetry. However, CVI[42] FWHM performed better than Medis Suite FWHM (figure 2).

Our results of volumetry comparison align with previous human data.[3] Likewise, the LV mass variability agrees with human studies,[4,5] supporting the contouring bias and suggesting that LV mass and its derivates (eg, fibrosis percentage) may be less reliable in tachycardia with hyperdynamic ventricles. While LV mass is rarely calculated under stress, the contouring variability in a hyperdynamic LV may be reduced by using the same software. As tissue characterization techniques have evolved, most CMR infarct

validation studies in animal models (mainly dogs) are from the 1980s-1990s.[6] Despite different available techniques, we report good reproducibility in all 3 tissue parameters in pigs. LGE correlated best between planimetry on Medis Suite and FWHM on CVI[42]. However, direct comparison between CMR scar size and TTC staining (both performed on day 42) revealed better FWHM performance in histopathological correlation vs planimetry, particularly on CVI[42]. Small software-specific differences in semiautomatic segmentation may have contributed to this finding, indicating the need for further histopathology-validated studies for technique standardization.

In conclusion, both software tools can be used interchangeably for biventricular volumes, edema, and MVO. A single product should be considered for LV mass and necrosis follow-up. Because CMR use in experimental disease models has been increasing along with ever-evolving markers and postprocessing techniques, researchers should evaluate their postprocessing methods carefully to deliver reproducible results for a truly reliable bench-to-bedside translation.

AUTHORS' CONTRIBUTIONS

M. Radiké: conception and design, data analysis and interpretation, manuscript drafting. S. Ben-Aicha: data analysis and interpretation; M. Gutiérrez: manuscript drafting and data interpretation. A. Hidalgo: conception and design; final manuscript approval. L. Badimon and G. Vilahur: conception and design; critical revision for important intellectual content; final manuscript approval; both authors are corresponding authors.

CONFLICTS OF INTEREST

None to declare.

Acknowledgements

Monika Radike,[a,b] Soumaya Ben-Aicha,[c] Manuel Gutiérrez,[b] Alberto Hidalgo,[d] Lina Badimón,[a,e,f] and Gemma Vilahur[a,f,*]

[a]*Institut de Recerca, Hospital de la Santa Creu i Sant Pau, Institut de Investigacions Biomèdiques (IIB)-Sant Pau, Barcelona, Spain*
[b]*Radiology Department, Liverpool Heart and Chest Hospital, Liverpool, United Kingdom*
[c]*Imperial College London, National Heart and Lung Institute, London, United Kingdom*
[d]*Departamento de Radiología, Hospital de la Santa Creu i Sant Pau, IIB-Sant Pau, Barcelona, Spain*
[e]*Centro de Investigación en Red de Enfermedades Cardiovasculares (CIBERCV), Spain*
[f]*Cardiovascular Research Chair, Universitat Autònoma de Barcelona, Barcelona, Spain*

* Corresponding authors:
E-mail addresses: gvilahur@santpau.cat (G. Vilahur);
lbadimon@santpau.cat (L. Badimón).

REFERENCES

1. Ibanez B, Aletras AH, Arai AE, et al. Cardiac MRI. Endpoints in Myocardial Infarction Experimental and Clinical Trials: JACC Scientific Expert Panel. *J Am Coll Cardiology.* 2019;74:238–256.
2. Vilahur G, Gutiérrez M, Casani L, et al. Protective Effects of Ticagrelor on Myocardial Injury After Infarction. *Circulation.* 2016;134:1708–1719.
3. Zange L, Muehlberg F, Blaszczyk E, et al. Quantification in cardiovascular magnetic resonance: agreement of software from three different vendors on assessment of left ventricular function, 2D flow and parametric mapping. *J Cardiovasc Magnet Reson.* 2019;21:12.
4. Clay S, Alfakih K, Messroghli DR, Jones T, Ridgway JP, Sivananthan MU. The reproducibility of left ventricular volume and mass measurements: a comparison between dual-inversion-recovery black-blood sequence and SSFP. *Eur Radiol.* 2006;16:32–37.
5. Suinesiaputra A, Bluemke DA, Cowan BR, et al. Quantification of LV function and mass by cardiovascular magnetic resonance: multi-center variability and consensus contours. *J Cardiovasc Magnet Reson.* 2015;17:63.
6. Kim RJ, Fieno DS, Parrish TB, et al. Relationship of MRI Delayed Contrast Enhancement to Irreversible Injury, Infarct Age, and Contractile Function. *Circulation.* 1999;100:1992–2002.

4.3. Additional materials and methods

This study is related to the **Primary Objective.**

Administration of a soluble apyrase, AZD3366, on top of ticagrelor confers additional cardioprotective benefits to that of ticagrelor alone: study in a preclinical animal model by CMR analyses

- *Ethical approval*

All experimental animal studies conducted the study were approved by the Institutional Animal Care and Use Committees and authorized by the Animal Experimental Committee of the local government and following the Guide for the Care and Use of Laboratory Animals of the U.S. National Institutes of Health (NIH Publication No. 85-23, revised 1985), the relevant legislature according to the Spanish Law (RD 53/2013) and the European Directive 2010/63/EU, and the ARRIVE 2.0 (Animal Research: Reporting of In Vivo Experiments) guidelines (173).

4.3.1. Dose-finding sub-study

- *Experimental design*

Regular chow-fed Landrace pigs (females; n=9; weight ≈40kg) were tranquilized with tiletamine, zolazepam and medetomidine and randomly distributed to intravenously receive escalating doses of AZD3366 (Astra Zeneca; 0.3mg/kg; 1mg/kg and 3 mg/kg).

- *LTA-induced platelet aggregation*

Based on the reported antithrombotic properties of AZD3366 (174), we assessed the degree of platelet inhibition exerted by the different doses of AZD3366 by light transmittance aggregometry (LTA) as a readout of its effectiveness. For this purpose, blood (5mL) was collected in citrate at baseline (prior treatment) and 5min,

30 min, 1 h, 2 h, 3 h, 9 h, 1 day, 2 days, 7 days and 14 days post AZD3366 intravenous administration and centrifuged for platelet-rich plasma (PRP) obtention. LTA triggered by ADP (5, 10 and 20 µM) was determined as maximal percentage of platelet inhibition [% of platelet inhibition = (100%) – (%maximal aggregation).

- *Ear Bleeding Time (BT)*

Saline ear BT was measured in all animals at baseline, 5min after APT-102 administration and at 48 hours, as previously performed (175). Briefly, the marginal edge of the ear was quickly transfixed (standardised incision of 3 mm length through the entire thickness of the ear) with a surgical blade (No.11) and immediately placed into a beaker containing citrated saline solution at 37°C. The time between incision and cessation of bleeding was recorded as BT. Time was recorded as 45 min if bleeding has not spontaneously stopped by this time.

- *Heart rate and blood pressure*

Heart rate and blood pressure were monitored at different time periods (Baseline, 5min, 30min, 9h, 1d, 2d, 7d and 14 days post-treatment).

- *Assessment of AZD3366 plasma levels*

Blood was collected at baseline (before treatment; time 0min) and at 5min, 30min, 1h, 2h, 3h, 12h, 24h, and 48h post- AZD3366 administration to determine AZD3366 plasma concentration. This analysis was conducted by Astra Zeneca.

4.3.2. Main study: experimental design

The experimental design is depicted in **Figure 12**. Regular chow-fed Landrace pigs (females; n=32; weight≈ 40 kg) were administered an oral loading dose of ticagrelor (180mg) and 2h later subjected to MI induction (1.5h closed-chest LAD coronary balloon occlusion) (176). Prior to reperfusion, pigs were randomized

to intravenously receive 1) vehicle (n=8); 2) 1mg/kg AZD3366 (n=8); or 3) 3mg/kg AZD3366 (n=8). After reperfusion all pigs were administered maintenance dose of ticagrelor (90mg/bid) for 42 days. A non-treated placebo-MI group was run for comparative purposes (n=8). Serial-CMR imaging was performed at baseline (prior-MI induction), at day 3 (early remodelling phase) and at day 42 (late remodelling phase) post-MI. Sample size (n=8 animals per group) was selected based on our previous work in the same animal model testing ticagrelor cardioprotective effects at comparable time points (133,177).
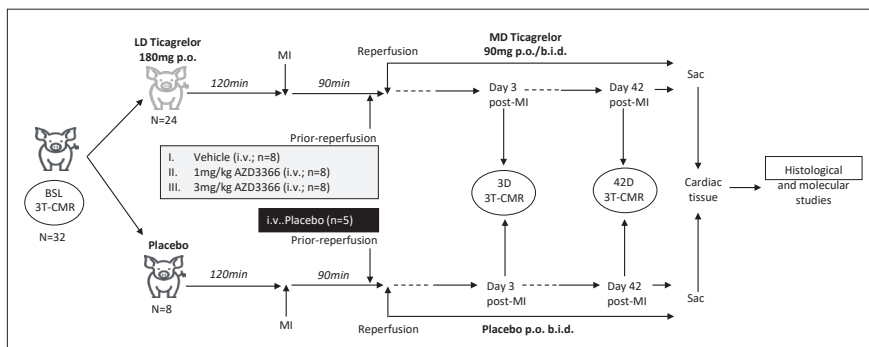
Figure 12. Study scheme. Animal distribution based on placebo-only, ticagrelor and vehicle and ticagrelor and 1mg/kg or 3mg/kg ATP-102 (AZD3366) treatment. b.i.d. (bis in die): twice daily; BSL: baseline; CMR: cardiac magnetic resonance; i.v.: intravenous LD: loading dose; MD: maintenance dose; MI: myocardial infarction induction; po: per os; Sac: sacrifice.

- *Closed-chest animal model of STEMI*

MI was experimentally induced by fluoroscopy-guided percutaneous coronary intervention as previously described (176,178). Briefly, prior to the procedure, pigs were anesthetized with a combination of intramuscular tiletamine+zolazepam (7mg/kg) + medetomidine (0.07 mg/kg). Animals received a continuous and stable flow of oxygen (inspired fraction of 0.5%) during all the intervention with permanent control of arterial saturation. Anaesthesia was maintained with inhalatory isoflurane (2%) throughout the entire procedure (both during MI-induction as well as in the reperfusion period). Continuous electrocardiographic

monitoring with hemodynamic parameters was performed. Coronary occlusion of the mid left anterior descending artery posterior to the emergence of the second diagonal branch was induced for 90min by balloon inflation, verifying a Thrombolysis In Myocardial Infarction (TIMI) 0 flow downwards.

After the 90min of ischaemia, reperfusion was installed by balloon deflation confirming TIMI 3 flow restoration, and animals were allowed to recover.

- *3T-CMR acquisition and analysis: global and regional structural and functional analyses*

CMR studies were conducted serially in all animals at baseline, day 3 and day 42 post-MI as previously reported (133,176). The following dedicated CMR sequences were acquired in all cases:
- anatomical localisers for study planning
- "cine" (gradient echo pulse) imaging sequence to assess wall motion and cardiac function at rest;
- T2w-STIR sequence to assess myocardial oedema;
- inversion recovery at early gadolinium phase to study microvascular obstruction (no-reflow phenomenon);
- inversion recovery at late gadolinium phase to assess the amount and extent of myocardial necrosis/fibrosis;
- the rest "cine" (gradient echo pulse) imaging sequence volumetric model was replicated to assess wall motion and cardiac function at dobutamine stress (intravenous infusion of 5 µg/kg/min of dobutamine, the dose was increased at 3-minute intervals to 10-20-30 µg/kg/min to elevate the heart rate by 30-50%).

Details of the technical parameters for CMR sequences have been outlined in the Introduction section and have been previously published (133,176). The protocol of analysis for global and regional functional/anatomical parameters was also performed as previously reported (133,177,176).

- *Light transmittance aggregometry*

Blood samples (15mL) were collected at baseline, prior MI-induction (after ticagrelor administration) and just after reperfusion for the assessment of ADP-induced LTA.

- *TTC staining*

After the last (day 42) CMR analysis, animals; hearts was arrested with potassium chloride, rapidly excised, sliced and stained with TTC in order to determine the size of the scar by planimetry using the National Institute of Health software Image J.

- *Molecular and histological characterization of the evolving scar*

To assess the potential effect of the different treatment regimes (ticagrelor ± AZD3366) on new vessel formation and fibrosis within the evolving scar, myocardial samples were processed for: 1) histological analyses of lectin (angiogenesis) and Sirius red (collagen fibrils); and 2) Western Blot analysis of Smad2/3 and phosphorylated-Smad2/3 (Ser423/425; Santa Cruz)]. The effects of ticagrelor and AZD3366 treatment on AMPK activation and Cox2 were assessed based on previous findings (179,180), accordingly, the expression of AMPK, AMPK phosphorylated at Thr172 (P-AMPK), and Cox2 were determined in the scar and remote myocardium.

- *Statistics*

Continuous variables are expressed as mean ± standard deviation (SD). After testing for normal distribution (Shapiro-Wilk test), data that followed a normal distribution were evaluated by repeated ANOVA measures followed by paired t-test to analyse variables within each group whereas unpaired t-test was used for all single time-point measurements. Data that not followed a normal distribution were evaluated by Kruskal Wallis. Data were accordingly expressed as mean ± SD or as median [interquartile range]. A cut-off value of $p < 0.05$ was used to consider statistical significance. Statistical analyses were performed with the GraphPad Prism software package.

5. Overall Summary of Results

The results of this thesis cover two preparatory studies, related to the Secondary Objectives 1 and 2 (Articles 1 and 2, respectively) and the study, related to the Primary objective.

Regarding the first article (section 4.1), the results are detailed in the listed publication. Briefly, we performed a comprehensive assessment of the effect of myocardial ischaemia duration on cardiac structural and functional parameters by serial cardiac magnetic resonance (CMR) and characterised the evolving scar. CMR follow-up on the cardiac impact of time of ischaemia in a closed-chest animal model of myocardial infarction with human resemblance is missing. Pigs underwent MI induction by occlusion of the left anterior descending (LAD) coronary artery for 30, 60, 90 or 120 min and then revascularised. Serial CMR was performed on day 3 and day 42 post-MI. CMR measurements were also run in a sham-operated group. Cellular and molecular changes were investigated. On day 3, cardiac damage and function were similar in sham and pigs subjected to 30 min of ischaemia. Cardiac damage (oedema and necrosis) significantly increased from 60 min onwards. Microvascular obstruction was extensively seen in animals with ≥90 min of ischaemia and correlated with cardiac damage. A drop in global systolic function and wall motion of the jeopardized segments was seen in pigs subjected to ≥60min of ischaemia. On day 42, scar size and cardiac dysfunction followed the same pattern in the animals subjected to ≥60min of ischaemia. Adverse left ventricular remodelling (worsening of both LV volumes) was only present in animals subjected to 120 min of ischaemia. Cardiac fibrosis, myocyte hypertrophy and vessel rarefaction were similar in the infarcted myocardium of pigs subjected to ≥60 min of ischaemia. No changes were observed in the remote myocardium. To conclude, sixty-minute LAD coronary occlusion already induces cardiac structural and functional alterations with longer ischaemic time

(120 min) causing adverse LV remodelling. Based on this study, we selected the 90-minute ischaemia duration to include microvascular obstruction as a parameter.

Regarding the second article (section 4.2), the results are detailed in the listed publication. Briefly, both software tools, having provided similar data for biventricular volumes, LVEF, oedema, and MVO, can be used interchangeably for these parameters. As LV mass calculation showed differences particularly at dobutamine stress and at different methods LGE quantification, a single product should be considered for LV mass and necrosis follow-up. FWHM on both showed a better correlation with histopathology (TTC staining) than planimetry. However, CVI[42] FWHM performed better than Medis Suite FWHM. Because CMR use in experimental disease models has been increasing along with ever-evolving markers and postprocessing techniques, researchers should evaluate their postprocessing methods carefully to deliver reproducible results for a truly reliable bench-to- bedside translation.

Regarding the study related to the Primary Objective (section 4.3), the results can be divided into two parts:

1. A dose-finding substudy for AZD3366

- *Platelet aggregation*
The inhibitory effect of different doses of AZD3366 on LTA-induced platelet aggregation triggered by ADP (5, 10 and 20 µM) is shown in **Figure 13** and **Supplemental Figures 1-3**.
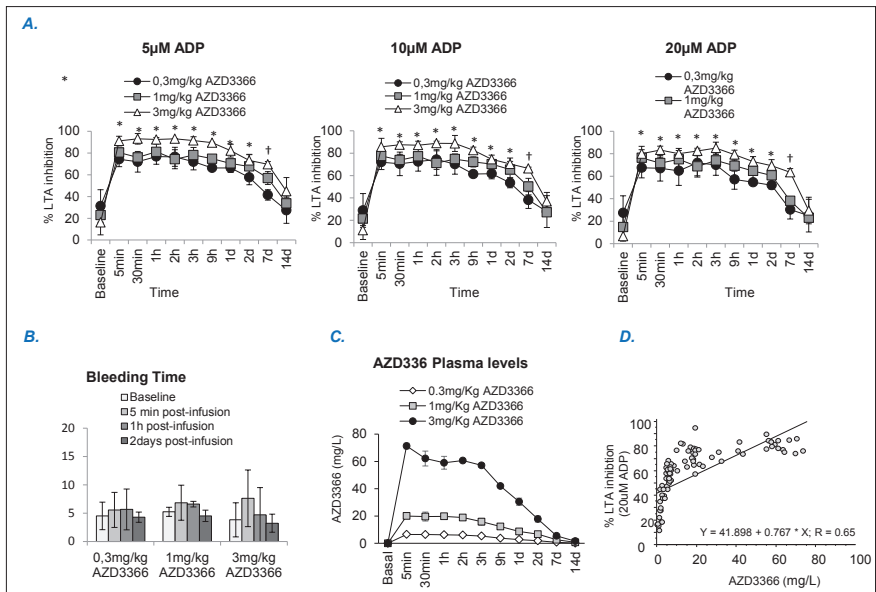
Figure 13. Dose finding study. A. Degree of platelet function inhibition assessed by ADP-induced LTA. B. Ear bleeding time. C. Plasma levels of ATP-102 (AZD3366). D. Correlation between plasma levels and the degree of platelet inhibition. Data are expressed as mean±SD; n=3 animals/group. *p<0.05 vs baseline for all ATP-102 doses; †p<0.05 vs baseline for 1 and 3 mg/kg ATP-102, over the course of 14 days.

All AZD3366 doses markedly and acutely inhibited ADP-induced platelet aggregation. This inhibitory effect was significantly higher in animals treated with AZD3366 3mg/kg as compared to the other two doses (particularly when platelets were challenged with 5µM and 10 µM ADP) and peaked as early as 5min post-infusion and remained in a maximal steady state up to day 1. Thereafter, platelet function progressively recovered over time although the platelet inhibitory effect of 3mg/kg AZD3366 remained significantly higher up to day 7 as compared to animals treated with 0.3 and 1 mg/kg AZD3366 (**Figure 13** and **Supplemental Figures 1-3**).

- *Ear Bleeding time*

No significant changes were detected in ear bleeding time at any tested time point and at any tested AZD3366 dose (**Figure 13B**).

- *AZD3366 plasma levels*

There was a dose-dependent raise in AZD3366 plasma levels that peaked at 5min post-dosing, remained high up to 3h and followed a monophasic decline with a terminal pharmacokinetic half-life of 7 days (**Figure 13C**). We detected a significant correlation between AZD3366 plasma levels and the degree of platelet inhibition challenged by ADP 20µM (**Figure 13D**).

Based on all these data, we decided to select the doses of 1 and 3 mg/kg AZD3366 to carry out the main study.

2. Main study

- *CMR serial analyses: effects of AZD3366 on cardiac damage*

The extent of myocardial oedema (area-at-risk) and MVO were significantly lower in all ticagrelor-treated pigs as compared to vehicle. Yet, administration of 3 mg/kg AZD3366 on top of ticagrelor further reduced oedema formation by 40% as compared to all other treated groups (**Figure 14**).

Tissue characterisation parameters

		Day 3 post-AMI	Day 42 post-AMI
LV mass (gr)	Vehicle	78.8 ± 19.1	104.2 ± 14.4 * **
	Ticagrelor	81.7 ± 14.8 *	109.1 ± 16.9 * **
	Ticagrelor+1mg/kg AZD3366	74.9 ± 6.7 *	109.1 ± 13.6 * **
	Ticagrelor+3 mg/kg AZD3366	76.8 ± 5.0 **	106.4 ± 25.3 * **
Area-at-risk (gr LV)	Vehicle	21.3 ± 6.7	
	Ticagrelor	11.3 ± 2.0 †	
	Ticagrelor+1mg/kg AZD3366	10.1 ± 6.8 †	
	Ticagrelor+3 mg/kg AZD3366	6.6 ± 1.7 † ‡	
Area-at-risk (% of LV)	Vehicle	27.3 ± 6.2	
	Ticagrelor	14.1 ± 2.6 †	
	Ticagrelor+1mg/kg AZD3366	13.5 ± 8.8 †	
	Ticagrelor+3 mg/kg AZD3366	8.4 ± 2.2 † ‡	
MVO (gr)	Vehicle	2.3 ± 0.9	
	Ticagrelor	0.6 ± 0.9 †	
	Ticagrelor+1mg/kg AZD3366	1.1 ± 1.2 †	
	Ticagrelor+3 mg/kg AZD3366	0.3 ± 0.3 †	
LGE (gr LV)	Vehicle	14.3 ± 6.2	10.9 ± 6.1
	Ticagrelor	7.4 ± 2.9 †	4.5 ± 2.2 †
	Ticagrelor+1mg/kg AZD3366	7.2 ± 3.9 †	5.1 ± 3.8
	Ticagrelor+3 mg/kg AZD3366	2.8 ± 2.9 † ‡ Ω	2.6 ± 1.9 †
LGE (% of LV)	Vehicle	17.9 ± 4.4	10.2 ± 5.3
	Ticagrelor	9.0 ± 3.3 † **	4.1 ± 1.6 †
	Ticagrelor+1mg/kg AZD3366	9.7 ± 5.2 †	4.8 ± 3.4 †
	Ticagrelor+3 mg/kg AZD3366	3.6 ± 2.6 † ‡ Ω	2.4 ± 1.5 †

Figure 14. CMR findings of tissue characterisation parameters. * p<0.05 vs baseline; ** p<0.05 vs day 3 ; † p<0.05 vs vehicle; ‡ p<0.05 vs ticagrelor; Ω p<0.05 vs ticagrelor+1mg/kg ATP-102 (AZD3366). Data are presented as mean ± SD. n= 8 animals/group. MVO: microvascular obstruction; LGE: late gadolinium enhancement.

Administration of ticagrelor also resulted in a significant and marked reduction on infarct size (either expressed as grams or % of LV) in comparison to vehicle administered animals, an effect that was found to be further enhanced by 45% in those animals administered intravenous infusion of 3mg/kg AZD3366. At day 42, all treated animals consistently showed a pronounced reduction in the size of the scar as compared to vehicle pigs although animals administered 3mg/kg AZD3366 showed a clear trend (p=0.05) towards a further significant reduction as compared to the other treated groups (**Figure 14**). Histopathological analyses by TTC staining correlated with CMR-assessed scar mass (r=0.843; p<0.005; **Figure 15**).
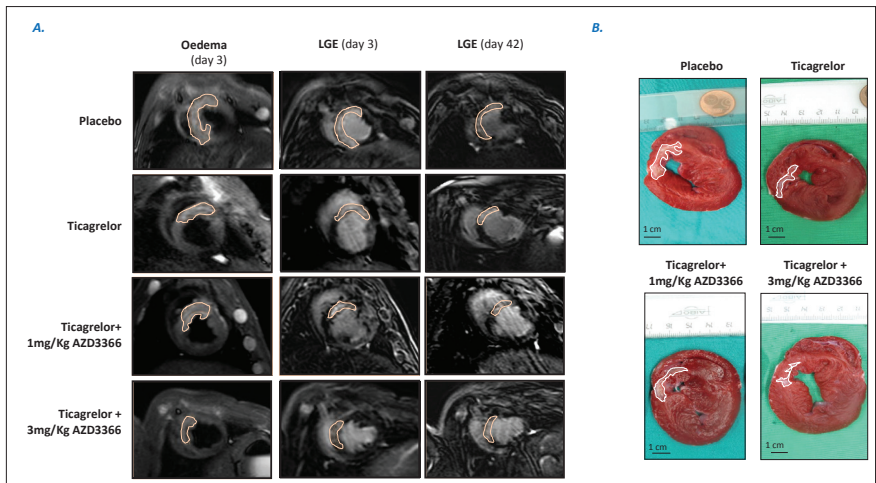
Figure 15. Cardiac damage. A. Assessed by CMR at days 3 and 42 post-MI induction. B. Gross pathology images. LGE=late gadolinium enhancement.

- *CMR serial analyses: effects of AZD3366 on cardiac function over time*

At rest

LVEDV, reflecting cavity size increase, was significantly elevated at day 3 in vehicle and ticagrelor alone treated groups as compared to baseline (**Figure 16A**). In contrast, LVEDV was found to be preserved in animals treated with ticagrelor+AZD3366 (1 and 3 mg/kg) compared to both baseline and vehicle administered pigs. At 42 days post-MI, all four groups of animals showed a significant deterioration in LVEDV as compared to baseline and day 3.

A. Functional parameters at rest

		Baseline	Day 3 post-AMI	Day 42 post-AMI
LVEDV (mL)	Vehicle	80.4 ± 10.7	107.9 ± 5,3 *	139.2 ± 20.4 * **
	Ticagrelor	71.8 ± 15.8	96.7 ± 20,8 *	131.2 ± 22.0 * **
	Ticagrelor+1mg/kg AZD3366	72.4 ± 9.3	89.8 ± 14.2 †	127.6 ± 17.9 * **
	Ticagrelor+3 mg/kg AZD3366	81.9 ± 13.9	89.3 ± 10.1 †	134.1 ± 44.1 * **
LVESV (mL)	Vehicle	34.2 ± 5.5	58.1 ± 8.1 *	76.7 ± 13.2 * **
	Ticagrelor	33.6 ± 6.9	47.9 ± 15.3	66.7 ± 17.4 *
	Ticagrelor+1mg/kg AZD3366	32.8 ± 4.9	47.4 ± 9.1	62.2 ± 19.7 *
	Ticagrelor+3 mg/kg AZD3366	38.6 ± 6.8	39.9 ± 11.8 †	64.1 ± 29.9 *
LVEF (%)	Vehicle	57.4 ± 5.2	46.1 ± 7.0 *	44.7 ± 6.5 * **
	Ticagrelor	53.3 ± 4.7	51.4 ± 5.7	49.7 ± 7.3
	Ticagrelor+1mg/kg AZD3366	54.7 ± 3.1	47.3 ± 4.7	51.3 ± 12.7
	Ticagrelor+3 mg/kg AZD3366	52.9 ± 2.2	55.3 ± 12.8	53.5 ± 8.7

B. Functional parameters at obutamine stress

		Baseline	Day 3 post-MI	Day 42 post-MI
LVEDV (mL)	Vehicle	51.5 ± 11.7	61.5 ± 9.7	104.2± 21.0 * **
	Ticagrelor	48.4 ± 8.6	65.5 ± 9.5	98.8 ± 23.5 * **
	Ticagrelor+1mg/kg AZD3366	53.1 ± 18.6	80.4 ± 20.4 *	102.7 ± 9.8 *
	Ticagrelor+3 mg/kg AZD3366	56.2 ± 13.1	64.4 ± 10.6	82.3 ± 22.3 *
LVESV (mL)	Vehicle	18.9 ± 2.6	32.4 ± 13.6 *	43.0 ± 10.7 *
	Ticagrelor	16.2 ± 5.9	28.5 ± 7.8 *	38.7 ± 12.3 *
	Ticagrelor+1mg/kg AZD3366	18.6 ± 7.8	34.1 ± 5.1 *	41.1 ± 2.2 *
	Ticagrelor+3 mg/kg AZD3366	19.1 ± 5.3	19.1 ± 2.5 †$	31.1 ± 12.4 * **
LVEF (%)	Vehicle	70.3 ± 6.7	48.6 ± 14.0 *	57.8 ± 11.5
	Ticagrelor	66.6 ± 10.7	56.2 ± 11.3	65.6 ± 10.5
	Ticagrelor+1mg/kg AZD3366	65.2 ± 9.8	55.7 ± 9.4	60.5 ± 2.9
	Ticagrelor+3 mg/kg AZD3366	65.7 ± 7.4	69.8 ± 5.6†	62.6 ± 7.4

C. Regional analyses of the infarcted segments
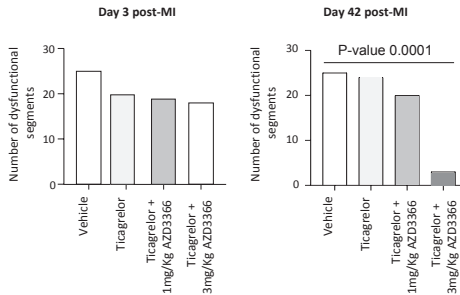
Figure 16. Follow-up CMR functional parameters. A. Cardiac function at rest. B. Cardiac function dobutamine stress. C. Regional analyses of the infarcted segments according to the 16-segment model (American Heart Association). Bar graphs indicate the number of dysfunctional segments at 3 days and 42 days post-MI). LVEDV: left ventricular end-diastolic volume; LVESV: left ventricle end-systolic volume; SV: stroke volume; LVEF: left ventricular ejection fraction; AMI: acute myocardial infarction. * *p<0.05 vs baseline*; ** *p<0.05 vs day 3*; † *p<0.05 vs vehicle*; $p<0.05 vs Ticagrelor+1 mg/Kg AZD3366 (ATP-102). Data are expressed as mean±SD. n= 8 animals/group.

As per LVESV, this was found to be significantly elevated in vehicle animals at 3 days post-MI and further increased at day 42 post-MI. No changes in LVESV were observed in animals administered ticagrelor ± AZD3366 at day 3 post-MI; the higher AZD3366 dose led to a significant reduction on LVESV as compared to vehicle pigs. LVESV was found deteriorated in all animals at day 42 as compared to baseline and vehicle animals also significantly worsened vs day 3.

Finally, LVEF was only found to be impaired in vehicle administered animals, an effect that persisted up to 42 days post-MI. In contrast, LVEF was preserved in animals administered ticagrelor ± AZD3366 at day 3 and day 42 post-MI.

Upon dobutamine stress

At day 3, there were no differences in LVEDV between the different animal groups and vs baseline. In contrast, LVESV and LVEF were found to be preserved in animals administered ticagrelor plus 3mg/kg AZD3366 (**Figure 16B**). At day 42, all animals displayed a comparable worsening in both LV volumes and no differences were observed as per LVEF as compared to baseline.

- *Left ventricular regional analyses*

We assessed the proportion of dysfunctional segments (wall motion <2.0mm) within the target segments (i.e., jeopardized myocardium; 28 segments/group) at early and late remodelling phases. The number of dysfunctional segments tend to be lower in ticagrelor (±AZD3366) treated animals at day 3 post-MI and markedly declined (more than 80%) at day 42 in animals administered 3mg/kg AZD3366 (**Figure 16C**).

- *Platelet function*

LTA at baseline was comparable among all animals. The degree of platelet inhibition induced by ticagrelor alone was around 50% upon challenge with ADP (**Figure 17**). In line with the sub-study findings, the addition of AZD3366 prior reperfusion almost abolished

ADP (5, 10 and 20 µM)-triggered platelet aggregation post-MI. This inhibitory effect persisted, although to a lesser extent, at 3 days post-MI (**Figure 17**).
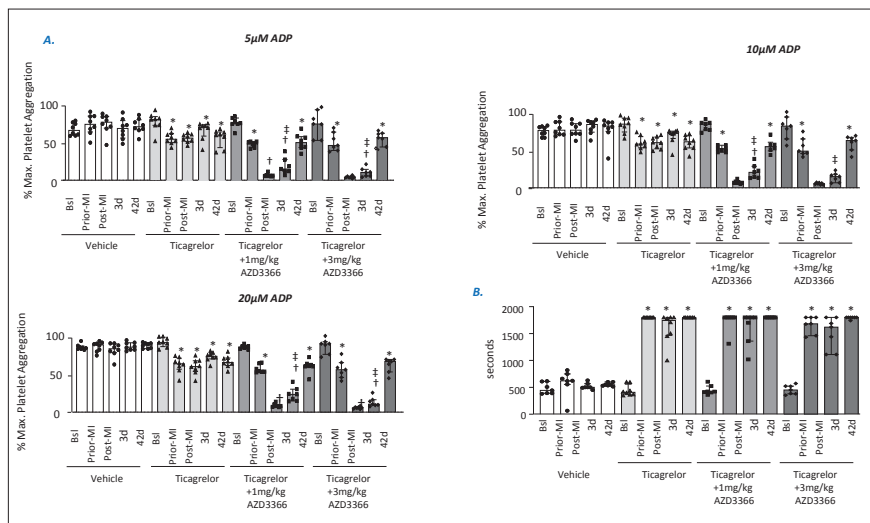
Figure 17. LTA and bleeding time monitoring. A. LTA induced by 5, 10 and 20 µM ADP at different time points and in all animal groups. B. Bleeding time. Bsl: baseline; MI: myocardial infarction; d: day. *p<0.05 vs Bsl or vehicle; †p<0.05 vs prior-MI, Bsl and vehicle; ‡ p<0.05 vs post-MI (Kruskal-Wallis test); n=8 animals/group. Data presented as median [IQR].Bsl: baseline.

- *Bleeding time*

Ticagrelor prolonged bleeding time in all treated animals as compared to baseline and vehicle animals regardless of AZD3366 administration (**Figure 17B**).

- *Myocardial characterization of vessel density and fibrosis: molecular and histological analyses.*

As shown in **Figure 18A**, no differences were observed in vessel density in the scar region of the different animal groups.
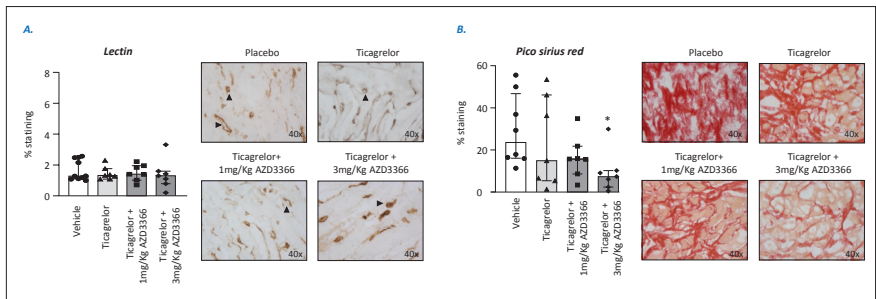
Figure 18. Neovessel formation and fibrosis in the evolving scar. A. Lectin staining to depict blood vessels (black arrows). B. Pico Sirius red staining to depict collagen fibrils. *p<0.05 vs all the other groups. Data presented as median [IQR]. N=8 animals/group.

As per collagen fibril deposition, Sirius red staining was found to be significantly diminished in the scar of ticagrelor + 3mg/kg AZD3366 treated animals as compared to all the rest (**Figure 18A**). Such decrease was not associated with changes in in smad2/3 expression nor activation (**Figure 19A and D**).
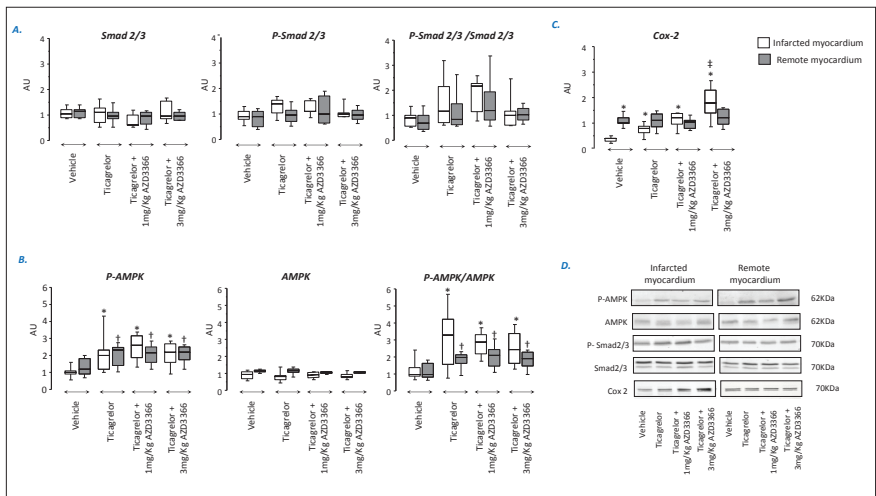
Figure 19. Molecular analyses in the myocardium. A. Smad2/3 expression and activation; B. AMPK expresssion and activation. C. Cox 2 expression. D. Representative Western Blot images. *p<0.05 vs vehicle ishemic myocardium; †p<0.05 vs vehicle remote myocardium; ‡p<0.05 vs all the other groups. n=8 animals/group. Data is expressed and median [IQR].

As shown in **Figure 19B and D**, AMPK protein expression was comparable among all animal groups and in both cardiac regions. In contrast, AMPK activation was found to be enhanced in the entire myocardium of all ticagrelor-treated pigs, an effect that was not further enhanced by the addition of AZD3366.

Cox2 protein levels were found to be lower in the scar zone of vehicle animals as compared to the other animal groups and to the non-infarcted cardiac zone (**Figure 19C and D**). Administration of ticagrelor preserved Cox2 expression in entire myocardium and infusion of 3mg/kg of AZD3366 resulted in higher Cox2 levels in the infarcted heart (**Figure 19C and D**).

- *Animal follow-up*

No differences were observed in haematological, lipid levels, and liver and hepatic parameters among all animals and throughout all the study (**Figures 20-21**).

Haematological parameters		RBC	HGB	HCT	MCV	PLT	MPV	WBC
Placebo	Baseline	6.0 ± 0.6	11.1 ± 0.8	27.5 ± 2.7	46.0 ± 1.6	427.6 ± 86.8	7.4 ± 0.4	16.4 ± 5.4
	Post-MI	5.2 ± 0.7	9.7 ± 1.0	23.7 ± 2.2	44.8 ± 2.0	292.8 ± 43.1	7.2 ± 0.3	18.0 ± 4.8
	3 days post-MI	5.7 ± 0.4	10.6 ± 0.9	26.0 ± 2.2	45.4 ± 2.4	426.8 ± 61.9	7.4 ± 0.3	18.0 ± 3.0
	42 days post-MI	5.5 ± 0.5	10.1 ± 0.6	26.3 ± 2.6	47.7 ± 3.6	324.0 ± 75.1	7.6 ± 1.0	19.1 ± 4.7
Ticagrelor	Baseline	6.1 ± 0.3	11.3 ± 0.4	29.0 ± 1.3	47.7 ± 2.3	533.4 ± 80.3	7.4 ± 0.4	18.6 ± 4.8
	Post-MI	5.2 ± 0.4	9.7 ± 0.9	23.7 ± 2.3	45.6 ± 2.5	387.3 ± 69.1	7.2 ± 0.5	20.4 ± 10.7
	3 days post-MI	5.4 ± 0.4	10.2 ± 0.7	25.1 ± 1.2	46.3 ± 2.5	513.6 ± 61.4	7.4 ± 0.6	21.0 ± 4.2
	42 days post-MI	5.4 ± 0.6	9.9 ± 1.0	24.7 ± 3.0	46.0 ± 2.7	396.0 ± 38.9	7.3 ± 0.3	19.8 ± 4.8
Ticagrelor+1mg/kg AZD3366	Baseline	6.0 ± 0.3	11.2 ± 0.6	28.8 ± 1.5	48.3 ± 2.7	504.3 ± 114.8	7.5 ± 0.6	19.3 ±7.4
	Post-MI	4.8 ± 0.3	8.9 ± 0.9	22.0 ± 1.8	46.1 ± 3.2	367.6 ± 79.7	7.5 ± 0.5	23.5 ± 9.4
	3 days post-MI	5.3 ± 0.6	10.2 ± 0.9	25.1 ± 2.5	47.1 ± 3.2	469.0 ± 105.7	7.2 ± 1.1	20.9 ± 7.3
	42 days post-MI	5.3 ± 0.6	9.9 ± 1.1	25.1 ± 3.2	47.5 ± 3.9	361.0 ± 55.8	7.5 ± 0.3	19.8 ± 3.9
Ticagrelor+3 mg/kg AZD3366	Baseline	6.0 ± 0.6	11.2 ± 1.0	28.4 ± 2.0	47.6 ± 1.8	583.8 ± 160.7	7.9 ± 0.4	21.4 ± 10.0
	Post-MI	4.8 ± 0.6	8.9 ± 1.1	21.8 ± 2.3	45.5 ± 2.1	411.6 ± 68.3	7.3 ± 0.4	18.1 ± 6.6
	3 days post-MI	5.0 ± 0.7	9.4 ± 1.1	23.2 ± 2.9	46.4 ± 2.6	493.0 ± 93.6	7.6 ± 0.5	18.2 ± 6.1
	42 days post-MI	5.3± 0.3	9.6 ± 0.8	24.5 ± 1.6	46.7 ± 2.3	437.9 ± 50.6	7.6 ± 0.4	21.4 ± 7.3

| *Lipid parameters*		Glucose	Glucose	Total-C	LDL-C	HDL-C	non-HDL-C
Placebo	Baseline	101.1 ± 30.2	51.9 ± 23.1	111.3 ± 34.5	76.3 ± 35.6	24.7 ± 4.6	86.6 ± 35.6
	Post-MI	125.6 ± 26.4	41.7 ± 7.9	89.6 ± 16.3	55.9 ± 16.0	25.4 ± 4.7	64.2 ± 16.4
	3 days post-MI	119.7 ± 31.0	39.7 ± 13.0	113.2 ± 9.8	72.2 ± 19.1	33.1 ± 11.8	80.1 ± 17.4
	42 days post-MI	102.0 ± 34.3	43.2 ± 22.5	89.6 ± 16.8	54.3 ± 19.7	26.7 ± 8.2	62.9 ± 20.2
Ticagrelor	Baseline	103.9 ± 12.2	37.5 ± 8.4	95.9 ± 17.4	57.3 ± 17.9	31.0 ± 4.3	64.8 ± 17.9
	Post-MI	128.0 ± 23.0	34.9 ± 15.9	84.8 ± 12.4	49.2 ± 9.9	28.6 ± 4.2	56.1 ± 11.7
	3 days post-MI	126.2 ± 22.0	47.9 ± 19.8	108.6 ± 13.6	61.6 ± 14.3	37.4 ± 11.3	71.2 ± 15.3
	42 days post-MI	106.6 ± 24.8	37.8 ± 23.8	88.5 ± 15.4	54.0 ± 15.8	26.9 ± 3.9	61.5 ± 12.0
Ticagrelor+1mg/kg AZD3366	Baseline	110.1 ± 12.2	39.1 ± 15.1	88.8 ± 16.9	52.3 ± 13.4	28.7 ± 6.8	60.1 ± 15.0
	Post-MI	110.8 ± 14.7	41.6 ± 17.2	83.3 ± 19.6	43.9 ± 13.5	31.6 ± 6.4	52.3 ± 15.0
	3 days post-MI	112.2 ± 12.3	39.3 ± 22.3	100.5 ± 21.6	54.3 ± 15.3	38.4 ± 11.5	62.1 ± 14.4
	42 days post-MI	93.4 ± 14.0	50.5 ± 42.3	81.3 ± 14.1	41.5 ± 10.9	29.6 ± 5.9	51.6 ± 13.4
Ticagrelor+3 mg/kg AZD3366	Baseline	107.9 ± 33.2	44.9 ± 27.4	94.5 ± 18.5	50.0 ± 12.9	35.5 ± 7.3	59.0 ± 14.8
	Post-MI	123.0 ± 24.7	41.4 ± 16.2	85.3 ± 17.2	44.4 ± 10.4	32.6 ± 8.2	52.7 ± 10.5
	3 days post-MI	111.7 ± 20.4	51.6 ± 23.9	113.4 ± 16.8	61.9 ± 12.3	41.2 ± 6.5	73.4 ± 13.3
	42 days post-MI	91.7 ± 19.7	66.1 ± 18.3	98.6 ± 18.2	54.2 ± 14.2	31.2 ± 7.7	67.4 ± 13.3

Figure 20. Follow-up hematological and lipid levels. RBC: red blood cells; HGB: hemoglobin; HCT: hematocrit; MCV; mean corpuscular volumen; PLT: platelet count; MPV: mean platelet volumen; WBC; White blood cells; LDL-C: low-density lipoprotein-cholesterol; HDL: high-density lipoprotein-cholesterol

Renal and liver parameters		Urea	Creatinine	GOT	GPT
Placebo	Baseline	23.3 ± 3.9	1.3 ± 0.3	27.3 ± 5.1	32.9 ± 6.2
	Post-MI	23.4 ± 5.1	1.6 ± 0.3	49.8 ± 46.7	32.4 ± 8.1
	3 days post-MI	22.2 ± 4.9	1.4 ± 0.2	32.6 ± 8.7	49.5 ± 16.5
	42 days post-MI	26.0 ± 9.8	1.7 ± 0.2	32.5 ± 16.5	36.6 ± 10.9
Ticagrelor	Baseline	14.2 ± 5.1	1.2 ± 0.2	32.6 ± 15.4	39.6 ± 11.0
	Post-MI	22.3 ± 6.0	1.4 ± 0.3	42.2 ± 20.3	35.6 ± 10.7
	3 days post-MI	20.6 ± 60.1	1.5 ± 0.3	25.0 ± 7.1	50.6 ± 10.5
	42 days post-MI	23.4 ± 6.5	1.7± 0.3	27.4 ± 13.4	41.9 ± 7.0
Ticagrelor+1mg/kg AZD3366	Baseline	15.5 ± 5.8	1.2 ± 0.2	30.3 ± 11.3	37.1 ± 7.9
	Post-MI	27.9 ± 10.2	1.4 ± 0.2	65.6 ± 43.1	35.5 ± 9.0
	3 days post-MI	17.5 ± 3.5	1.4 ± 0.2	31.3 ± 11.4	63.8 ± 18.2
	42 days post-MI	27.8 ± 10.0	1.9 ± 0.3	41.3 ± 46.3	38.4 ± 8.9
Ticagrelor+3 mg/kg AZD3366	Baseline	16.5 ± 7.2	1.3 ± 0.2	24.4 ± 8.6	34.4 ± 5.8
	Post-MI	23.1 ± 4.7	1.4 ± 0.3	55.8 ± 26.7	31.9 ± 9.2
	3 days post-MI	16.2 ± 4.7	1.3 ± 0.2	47.4 ± 46.6	56.6 ± 21.3
	42 days post-MI	25.4 ± 8.0	2.1 ± 0.5	29.3 ± 12.5	36.7 ± 7.3

Figure 21. Follow-up hematological and lipid levels. RBC: red blood cells; HGB: hemoglobin; HCT: hematocrit; MCV; mean corpuscular volumen; PLT: platelet count; MPV: mean platelet volumen; WBC; White blood cells; GOT: glutamic-oxaloacetic transaminase; GPT: Glutamic Pyruvic Transaminase
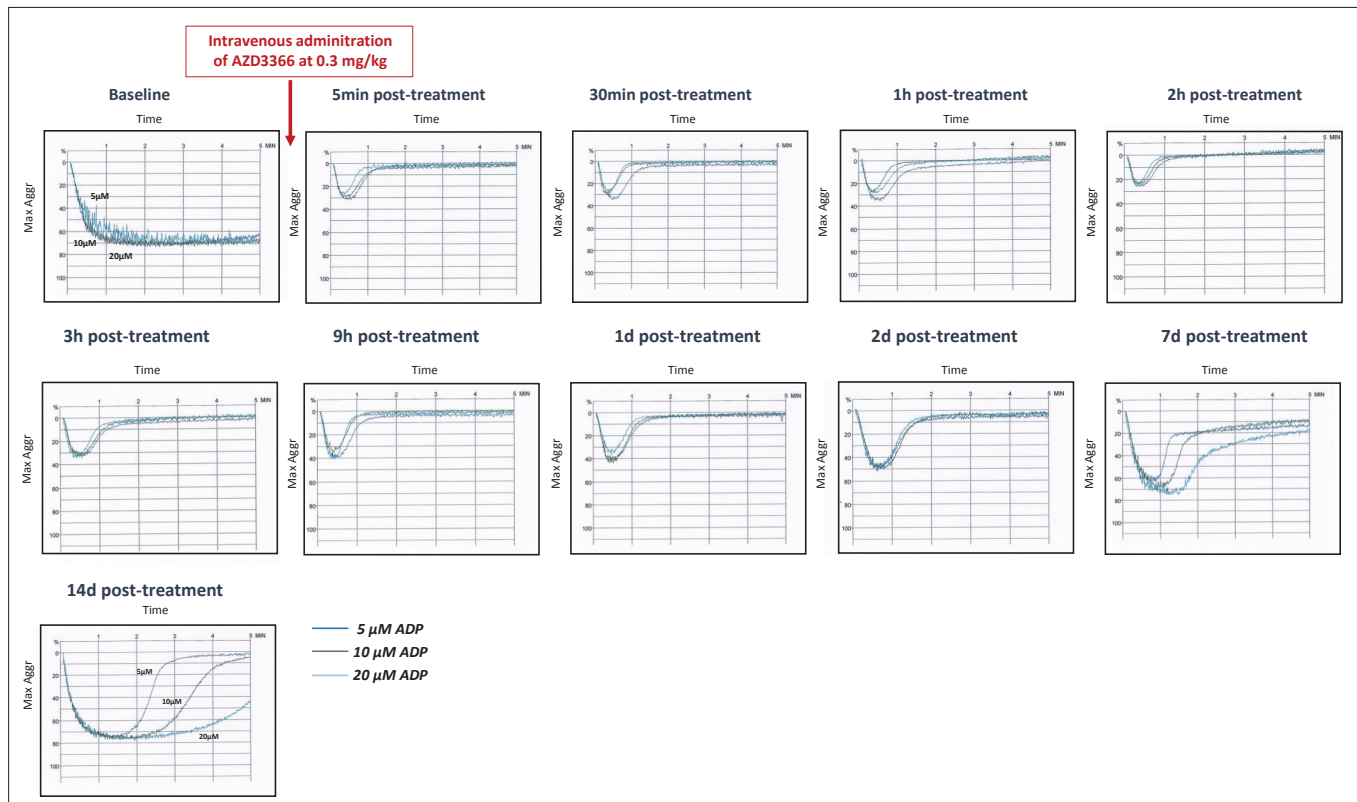
Supplemental Figure 1. Representative LTA response over time in one animal treated with i.v 0.3mg/kg ATP-102 (AZD3366). ADP was used at 5, 10 and 20 μM.
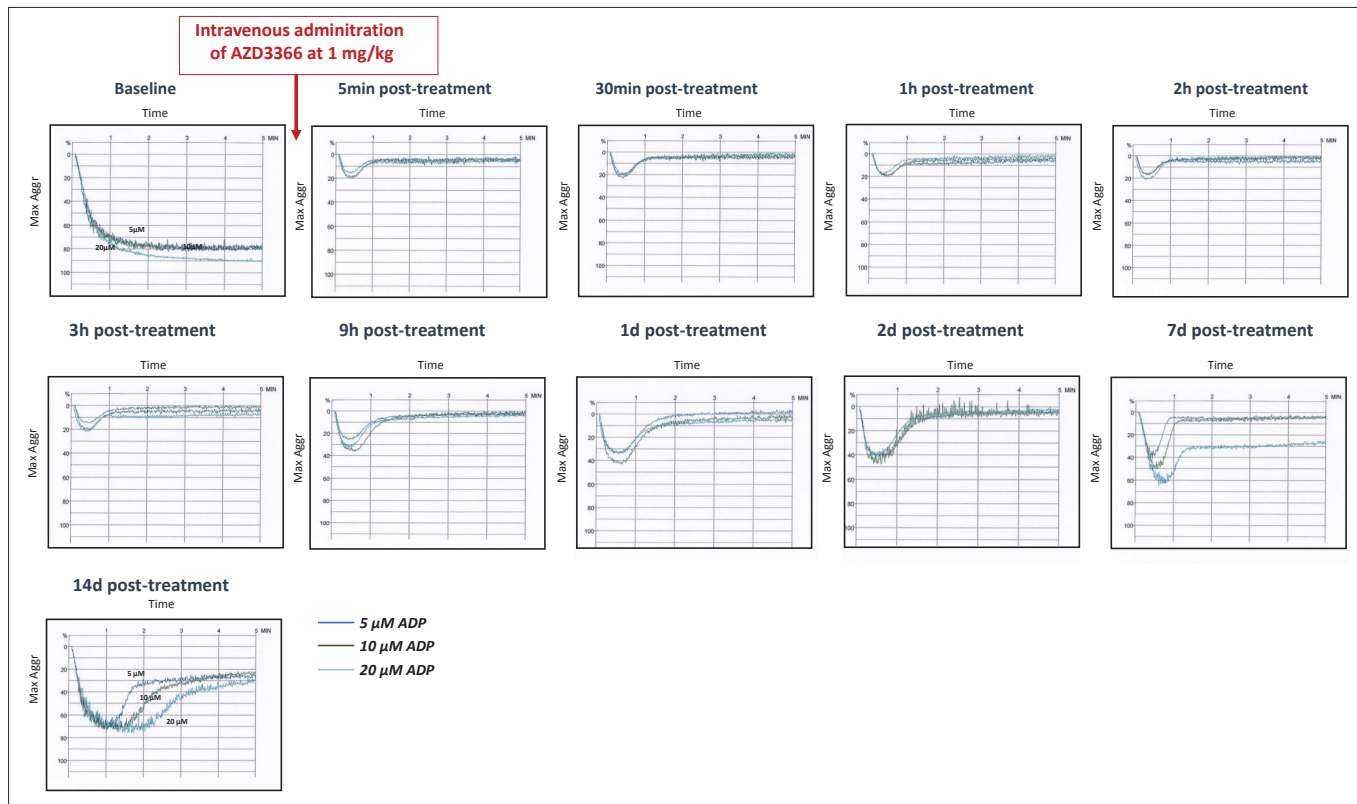
Supplemental Figure 2. Representative LTA response over time in one animal treated with i.v 1mg/kg ATP-102 (AZD3366). ADP was used at 5, 10 and 20 µM.
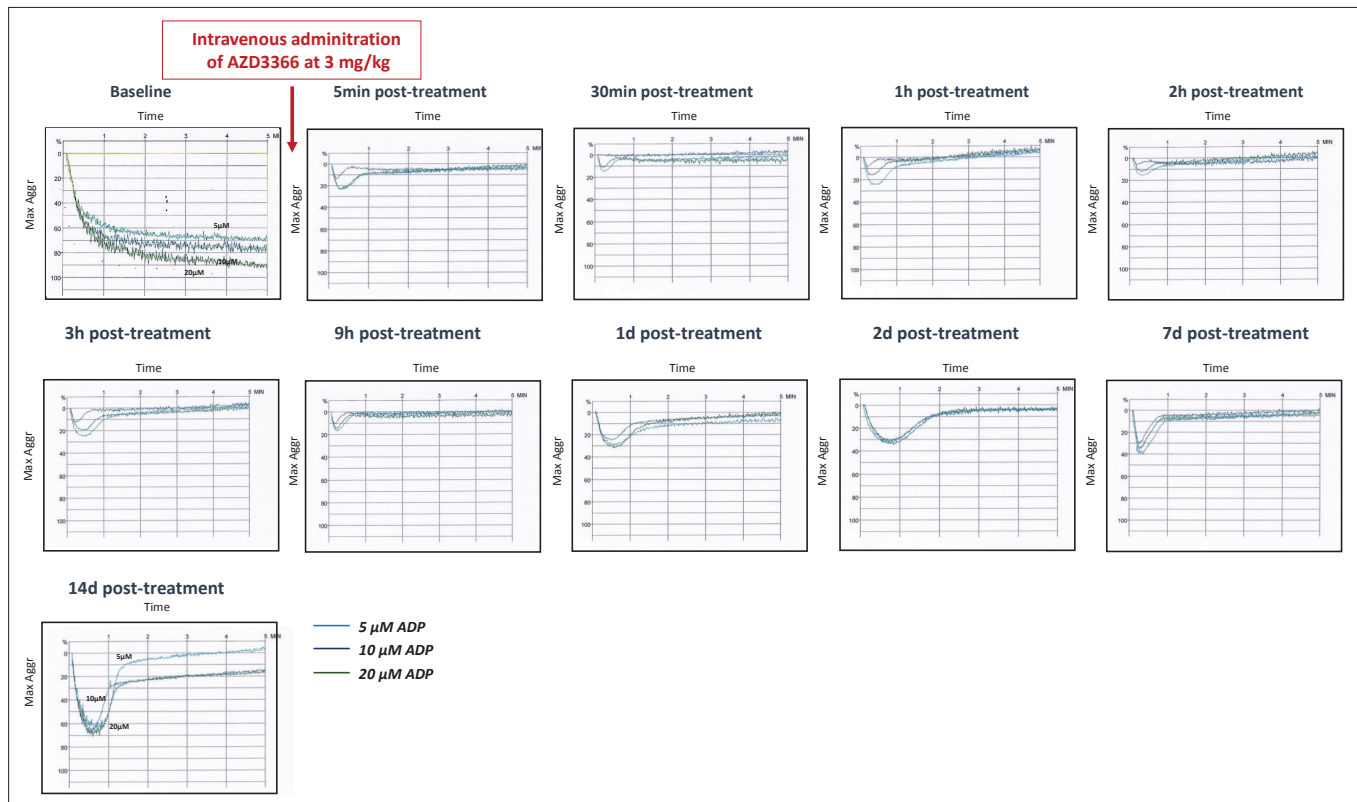
Supplemental Figure 3. Representative LTA response over time in one animal treated with i.v 3mg/kg ATP-102 (AZD3366). ADP was used at 5, 10 and 20 μM.

6. Overall Summary of Discussion

The discussion of this thesis covers the two preparatory studies, related to the Secondary Objectives 1 and 2 (Articles 1 and 2, respectively) and the study, related to the Primary objective.

Secondary objective 1. **To demonstrate, in this preclinical animal model, how long myocardial ischaemia should be maintained to render significant structural and functional alterations amenable for therapeutic intervention.**

Duration of coronary occlusion, along with collateral circulation and the size of the coronary artery territory affected, is widely known to be among the main factors determining the infarct size. This study was performed to identify the optimal ischaemia duration for induction of myocardial damage features, assessed by CMR parameters, and to compare the findings with molecular and cellular features of the scar.

While cardioprotective strategies have been promising in animal models, none has translated into the clinical scenario (181). Animal model differences and lack of transition / translation to human surrogate endpoints may be among the reasons (182–185). Closed-chest pig models are preferable in preclinical cardioprotection studies due to their cardiovascular features' similarity to humans to provide a transitionary step to clinical trials, thus, specifically, a closed-chest pig STEMI models has been designed to evaluate CMR structural and functional parameters of myocardial injury in the setting of different ischaemia duration. Previous ischaemia duration studies on pigs were performed using open or closed chest models and generally showed 60-minute ischaemia duration as the cut-off point for their findings; yet, none of these studies used CMR parameters (186–189). CMR, a clinical gold standard technique for cardiac function and structure, has been recommended CMR-derived

parameters as preclinical and clinical endpoints in cardiovascular studies (156).

Our AMI findings fall within the described optimal 3-7-day assessment window (190,191). Regarding ischaemia duration, the cut-off time for a significant acute injury formation was 60 minutes for most tissue parameters where, importantly, oedema and LGE did not expand significantly beyond this duration. However, MVO, a CMR marker for no-reflow phenomenon, assessed on EGE phase, showed a pattern of forming with longer ischaemia periods (90 minutes and longer), and increased with longer durations – this finding aligns with the prognostic value of MVO as an independent marker (192,193).

On late remodelling phase at day 42, the injury was smaller compared to day 3. This reduction of injury size follows the previously described pathophysiology of cardiac remodelling after reperfused AMI: inflamed and necrosed myocardium later undergoes a process of fibrosis. Regarding the duration, tissue parameters followed the 60-minute cut-off pattern among the duration groups. This result follows the previous studies where infarct size was assessed as AAR, without CMR parameters: infarct sizes remained the same after 2h or longer ischaemia (187,188).

Assessment of ventricular function showed a similar trend as the tissue parameters: 60-minute cut-off was sufficient to induce significant LVEF and regional wall function impairment, and this change persisted to day 42. Nevertheless, late remodelling phase ventricular dilatation with a significant LVEDV increase – reflecting adverse ventricular remodelling – had a clear cut-off point of 120-minute ischaemia at day 42 assessment. While LVEDV increase of ≥20 % has been widely used as a remodelling marker to predict heart failure and mortality in the literature, these studies were based on echocardiography, not CMR findings (194,195). More recently, following a systematic review of clinical studies, 12-20% LVEDV increase at three months on CMR has been proposed as the adverse remodelling marker (196). In this context, 90-minute

cut-off point, showing a statistically significant 15% LVEDV increase compared to 30-min, may be more applicable to future studies.

Molecular and cellular findings support the 60-min ischaemia cut-off in the assessment of TGFβR/Smad/collagen axis, collagen fibril deposition, cardiomyocyte hypertrophy and microvessel rarefaction. In addition, a regional gradient in myocyte dimensions was observed: in infarcted pigs, septal wall myocytes were smaller – contrary to the non-infarcted pig specimens, where the cells were larger in the septal segments compared to the lateral wall. This result provides a reference point when assessing pig model histopathology, as this pattern is not observed in all rodents, for example (197).

As per this study, the following limitation should be acknowledged. Regarding the use of CMR in future studies of ischaemia duration, it may be valuable to further characterise the myocardial injury with additional parameters such as T2* and myocardial mapping measurements: this would allow to study intramyocardial haemorrhage and diffuse interstitial oedema as a biomarker.

Secondary objective 2. **To validate, in this preclinical animal model, the clinically available post-processing software for CMR analyses.**

CMR, part of routine diagnostic practice in cardiovascular disease, is being increasingly used in preclinical pharmacological studies due to its high translatability into the clinical phase. CMR image postprocessing and analysis is one of the cornerstones for reproducible provision of CMR biomarkers. In the context of preclinical research, the use of CMR has a few cautionary aspects:

- While preclinical laboratories use different vendors for image postprocessing and analysis, the vast majority of previous CMR post-processing comparison work in the literature has been done using clinical datasets (human hearts).
- Software testing during design is typically performed on healthy volunteer hearts or on clinical study subjects.

Pig hearts, while in many aspects resembling human counterparts significantly, differ in a few aspects. First, the topography differs slightly: a pig's chest is rather cone-shaped, compared to the more rectangular human chest (**Figure 20**). Secondly, pig hearts have a higher resting heart rate compared to humans, which means that pig studies are acquired at a heart rate that would be labelled as tachycardia in humans. As the use of CMR in experimental disease models has been continuously increasing, methodology validation and comparison studies have been performed in a much lesser extent. That is, to date, CMR post-processing has been extended to experimental models without validation of the technique, which in itself may pose limitations to the methods and results in experimental studies using CMR.

	Axial	Coronal	Sagittal
Pig			
Human			
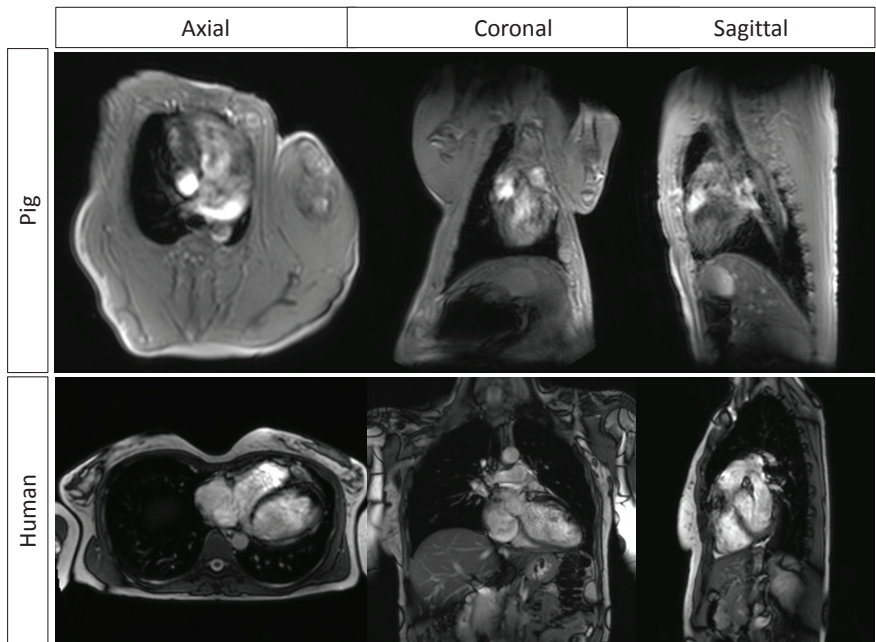
Figure 22. Three body axis localisers used for CMR scan planning of pig heart (top row, gradient echo) and representative images of volunteer human heart (bottom row, steady state free precession) scans. Both studies have been performed on scanners of the same field strength using standard clinically available sequences.

Quantitative CMR markers of ventricular size, function, and tissue characterization are widely used to plan, monitor treatment, and to provide prognostic information. Several CMR post-processing software products are available, either provided by scanner vendors or independently designed. Software packages may differ in image display settings and the approach used to contour anatomical structures and to assess tissue regions of interest. For example, a spectrum of ventricular functional modules exists, from operator-dependent manual planimetry to semi-or fully automated contouring; in recent years, machine learning has also been applied (198,199). In tissue analysis, the solutions range from a planimetry-based ROI assessment to multiple techniques of manual or semi-automated pixel value threshold-based quantification (200). So far, several clinical studies have compared different software products in a spectrum of clinical contexts – routine morphological and flow assessment, quantification of myocardial scar of different aetiologies, myocardial perfusion, etc (201,200,202–204). However, to the best of our knowledge, this was the first study to compare two products routinely used for CMR post-processing (Medis Suite and CVI[42]) in a highly translational animal model of experimentally induced MI and provide further histopathological validation. We reported that ventricular parameters, both at rest and after dobutamine infusion, are reproducible between both products, except for LV mass and LVEF that agreed less in dobutamine stress in isolated tests (Bland-Altman and CCC, respectively). As per tissue characterization, all measurements were reproducible among both products and necrosis and when assessed by FWHM, correlated better with the gold standard histopathology in terms of the infarct size, particularly on CVI[42].

There was a good correlation among ventricular volumes in line with human studies to compare different software products (202,204). In particular, right ventricular parameters correlated strongly, which may reflect the influence of the contouring technique of a skilled observer, as opposed to the variability of manual and automated

techniques, different level observers, and multi-observer approach (205). This emphasizes the need for training and standardization for good reproducibility. Some contradictory results regarding LV mass and LVEF were noted under dobutamine stress. Bland-Altman plots showed CVI[42] measured, on average, 10.5mg more LV mass than Medis Suite, but their CCC agreement was strong. On the other hand, LVEF showed virtually no bias on Bland-Altman plots, but the agreement between softwares was moderate. This is probably explained by the way discordant measurements are distributed. Despite a higher absolute agreement, CVI[42] repeatedly overestimated LV mass compared to Medis Suite. However, even when LVEF absolute agreement was lower, there was no definite pattern in discordant LVEF values.

Despite reports of low inter-observer, intra-observer, and inter-study variability (206–208), Suinesiaputra et al. have studied different operators measuring, among other ventricular parameters, the end-diastolic LV mass. The design included different software products with an emphasis to use manual contouring as well as the inclusion of trabeculae and papillary muscles into the blood pool. The authors reported an average variability of 10.9g in human left ventricular mass (201). Other studies showed lower reproducibility in LV mass on steady-state free precession sequences, particularly in inexperienced operators (209,210). Thus, our dobutamine stress findings support the contouring bias and suggest that comparison of LV mass and its derivates (e.g., fibrosis percentage) may be less reliable than that of the volumes in tachycardia with hyperdynamic ventricles (as seen with the effect of dobutamine infusion) performed on different products. Of note, LV mass is rarely calculated under stress compared to rest conditions, thus the clinical implications are likely limited. Similarly, variability in contouring in a hyperdynamic LV may have also accounted for the lower agreement in LVEF acquired during dobutamine stress, which suggests that using the same product may increase reproducibility.

T2-weighted sequences with fat saturation are used in almost every cardiovascular CMR department to assess for myocardial oedema in the myocardial injury of any aetiology. Besides, oedema imaging is widely used in combination with LGE assessment to define myocardium at risk (211). We observe a strong agreement in the quantification of oedema between both softwares. As previously reported by Ibañez et al. (156), it is essential to note all animals were scanned at precisely the same time points of MI and post-MI period, which eliminates potential discrepancies secondary to the dynamic process of post-ischaemic "healing" and its longitudinal changes in oedema formation and infarct size (212).

There have been several studies validating CMR infarct imaging to ex-vivo histopathology on animal models, the majority before 2010 (211,213–216). T1-based inversion recovery sequence is routine in the detection of MVO and necrosis in early and late phases after gadolinium administration, respectively. CMR-derived infarct size has been considered a prognostic marker for recovery, revascularization, mortality, and major adverse cardiovascular events (217–220). In our study, the two products differed in available techniques for tissue characterization techniques: manual planimetry and semi-automated methods were available on Medis Suite, while CVI[42] had a semi-automated thresh-hold based technique. Despite the above-mentioned different techniques, our results show good reproducibility with MVO quantification, and LGE showed the best correlation between planimetry on Medis Suite and FWHM on CVI[42]. Yet, direct comparison between scar size (assessed by CMR in the late remodelling phase) and TTC staining (performed on the same day of CMR analyses) revealed that FWHM, especially on CVI[42], performed better in histopathological validation compared to planimetry on Medis Suite. In this regard, small software-specific differences in semi-automatic segmentation may have contributed to this result, demonstrating the need for further histopathology-validated studies for standardization of the technique.

Regarding this study, there have been a few limitations. Homogeneous cohort included only one type of myocardial pathology, not allowing to exclude whether the presence of concomitant pathologies (e.g. myocarditis) would affect the outcome. Secondly, we conducted a single-operator study design and although we did not assess intra-observer variability, multiple previous CMR studies have shown low intra-observer variability, particularly in well-trained operators   as accounts in our study, and these results can be translated into experimental animal models. Considering that most translational research teams rely on very few (often only one) CMR readers and tend to have limited access to different software types, the study design, a validation tool for cardiovascular research in an animal model, likely reflects the daily practice in such settings. For differently setup laboratories, however, a design with multiple observers may be of value. Thirdly, our study had only three baseline cases out of the full dataset. This, however, means that 1) baseline vs post-intervention cases provide a real-life approach into assessing the parameters in normal and pathological scans, and 2) the remaining cases had had a coronary artery occlusion prior to the scans and thus additional myocardial tissue abnormalities to assess for. There may be a scope for further studies using larger datasets in pre-defined phases of the disease. Finally, out of several semi-automated tissue characterization methods, we have only used FWHM as it has been reported as the most accurate and reproducible technique both in clinical and pre-clinical studies (200,221,222). Despite these limitations, the results of this study help to fill a much-needed gap of software product use in translational cardiovascular research in the setting of growing popularity of CMR in this field.

Overall, this study has provided a validation of methods regarding different imaging parameters with new data on potential pitfalls and bias, helpful to ensure reproducibility. While achieving Secondary objective 2, these results contribute to the collective knowledge of the technique and to the need to report these tools in research studies.

Primary objective. To examine, whether the intravenous administration of a recombinant soluble form of human apyrase (AZD3366) prior to reperfusion limits cardiac damage and improves cardiac function to a larger extent than ticagrelor alone.

Within the last years, multiple studies have supported the ability of P2Y12 receptor antagonists to exert infarct-sparing effects beyond their antiplatelet properties (223). In this regard, ticagrelor has demonstrated a high cardioprotective potential through adenosine-mediated effects (133,177). In the present study, we demonstrate that intravenous administration prior reperfusion of a soluble recombinant apyrase (AZD3366) on top of ticagrelor exerts additive and synergistic cardioprotective effects to that observed by ticagrelor alone.

Recent data have demonstrated the ability of AZD3366 to attenuate ischaemia reperfusion injury leading to smaller infarcts (224,225). Furthermore, Birnbaum et al. (225) have evidenced by histopathology (TTC staining) additive cardioprotective effects when combining AZD3366 infusion (at 1mg/kg) with intraperitoneal ticagrelor treatment prior to reperfusion. These benefits were reported at 24h post-MI in a rat model of open chest LAD coronary ligation that largely differs from the human setting (40). Within the last 4 decades, countless therapeutic interventions have failed to reach the clinical setting. One likely major reason for this failure to translate cardioprotection into patient benefit is the lack of a rigorous and systematic validation of those cardioprotective interventions shown to be effective in rodents in human-resembling animal models (226). The ESC-Working Group Cellular Biology of the Heart Position Paper (226) and the EU-Cardioprotection COST Action Criteria (227) have highlighted that preclinical studies in pig models of closed-chest complete LAD occlusion (i.e., a STEMI-like situation) with subsequent reperfusion are mandatory to determine the safety and efficacy of novel cardioprotective approaches before moving into clinical trials. Moreover, a scientific expert panel consensus document has recently recommended performing CMR imaging for identifying potential benefits associated with new

cardioprotective strategies in experimental and clinical trials (156). Indeed, CMR allows us to depict the protective effect of the different cardioprotective approaches more accurately on cardiac damage beyond tissue necrosis, and provide data on oedema, microvascular obstruction (no-reflow) and left ventricular contractibility and volumes (at rest and after dobutamine stress), parameters of key importance for further clinical translatability. In this regard, the extent of LGE as the CMR primary endpoint and LVEF and MVO as main secondary endpoints have shown to help in the diagnosis and risk stratification for future cardiovascular events (47,156).

With all this in mind, herein we evidence in a highly translatable STEMI preclinical approach and by serial CMR analyses, that infusion of AZD3366 at doses of 3mg/kg prior to reperfusion provides an additive cardioprotective effect to that of oral ticagrelor alone performing better in preventing oedema formation and myocyte death at 3 days post-MI and ultimately leading to a lower scar at day 42. These data support that increasing local adenosine availability by preventing its uptake (ticagrelor loading) and inducing its synthesis (by high-dose AZD3366 infusion) in the setting of MI lessens myocardial damage to a greater extent than ticagrelor alone. In contrast to studies performed in rodents (225,228) infusion of lower AZD3366 doses (1mg/kg) did not provide such additive cardioprotective effect highlighting the need to consider dose-related differences between small and large animal species prior to translation to the clinical setting.

Adenosine is known to exert a variety of beneficial effects in the context of cardioprotection including vasodilation, attenuation of the inflammatory processes, preservation of microvascular flow, reduction in the generation of reactive oxygen species, platelet inhibition, and enhanced cell viability. In this latter regard, Feliu et al. have recently demonstrated in endothelial cell cultures ticagrelor's ability to prevent apoptosis through adenosine signalling pathways (148). Moreover, multiple experimental studies have supported that adenosine affords cardioprotection in ischemic conditioning (pre-, post- and remote-) by interacting with adenosine receptors

(142,226) which, in turn, have shown to reduce oedema formation in humans (229). Of note, oedema is considered to contribute to cell death and accordingly to the final size of infarction (230). So far, clinical studies with adenosine in STEMI patients have yielded mixed results (40) some showing benefit (231,232) and others no beneficial effect (233). However, systemic infusion of exogenous adenosine with a very short half-life (only few seconds), may be quite different from a continuous enhancement of local endogenous adenosine concentration at sites of ischemia or tissue injury. In fact, this recombinant form of apyrase has shown to exhibit high adenosine diphosphatase activity and a longer (50 times) plasma half-life than did native apyrase (234).

Platelet function analyses in the setting of STEMI (acutely post-reperfusion) further supported AZD3366's ability to almost blunt platelet activation challenged by ADP (at all tested doses), an effect not reported by ticagrelor loading which diminished platelet activation by around 30%. This prominent platelet inhibitory effect was observed at both doses of AZD3366 (1 and 3 mg/kg) and persisted up to day 3 post-MI. Beyond inducing adenosine generation (with known antiplatelet properties), this recombinant apyrase has shown to block the interaction of ADP and ATP (likely released from α-granules upon ADP-induced platelet activation) to all three platelet P2 receptors (P2X1, P2Y1, and P2Y12) (235), thereby leading to a more pronounced platelet inhibition as compared to ticagrelor which only acts at the P2Y12 receptor.

Notably, this antiplatelet potential was not associated with a prolongation in bleeding time supporting AZD3366's powerful antithrombotic effectiveness in combination with a safe haemostatic profile, expanding on previously published data in a canine model of coronary thrombotic occlusion (234). These data seem promising considering that increased risk of bleeding has been a limiting issue in antiplatelet development and clinical implementation (236).

Nevertheless, the lack of a synergistic cardioprotective effect between ticagrelor and AZD3366 administered at 1mg/kg allow us

to speculate that AZD3366 exerts cardioprotection through platelet-independent mechanisms and that higher AZD3366 doses are required to protect against MI-related damage.

At a functional level, the enhanced reduction in myocardial damage provided by 3mg/kg AZD3366 was accompanied, at day 3, with a better preservation of LV volumes at rest and preserved LVESV and LVEF upon dobutamine stress as compared to non-treated pigs. These additional benefits on global cardiac function uniquely provided by the higher dose of AZD3366 were lost at a longer follow-up period (42 days). The limited scar size observed at day 42 in all animals may have hampered the ability to detect any global functional effect. Yet, we selected this moderate degree of cardiac damage to achieve infarct sizes in the order of magnitude of around 16% of the LV as obtained by modern reperfusion therapy and to thereby increase the clinical relevance of our experimental approach (92,237,238). In addition, by performing this approach, we also wanted to avoid overestimating the cardioprotective potential of AZD3366. Yet, regional functional analyses of the infarcted segments revealed a higher restoration in cardiac contractility in animals administered 3mg/kg AZD3366. The small scar size with low collagen content (less fibrosis) may partly explain this local functional recovery. It is important to note that previous studies in rodents have only assessed the impact of AZD3366 in the acute setting of MI and did not address whether these benefits translated into a better LV remodelling phase. Whether regular infusions of AZD336 beyond that of PCI may better preserve the cardiac tissue needs to be addressed.

At a molecular level and in agreement with our previous findings (177,237), ticagrelor treatment enhanced myocardial AMPK activation and preserved Cox2 expression up to day 42. Infusion of AZD3366 did not exert any synergistic effect on AMPK activity at this long-term follow up. Yet, taking into consideration that adenosine-related AMPK activation has shown to reduce both oedema formation and infarct size (135,136,138) we could speculate that administration of the higher dose of AZD3366 (3mg/kg) may have stimulated AMPK

activation during the acute phase post-MI likely contributing to the observed reduction in both oedema and myocardial death at day 3. Supporting this hypothesis, Birnbaum et al. (225) have demonstrated AZD3366 ability to attenuate inflammation, necrosis, necroptosis, and pyroptosis 24h post-MI. On the other hand, we observed an enhanced Cox2 expression in the infarcted myocardium of AZD3366 3mg/kg treated pigs as compared to ticagrelor and ticagrelor + AZD3366 1mg/kg treated pigs. Ticagrelor has shown to exert protective effects through adenosine-receptor activation with downstream upregulation of Cox2 activity (239). Consequently, whereas ticagrelor treatment may have preserved myocardial Cox2 levels in the setting of MI, increased adenosine concentrations after 3mg/kg AZD3366 infusion may have induced further Cox2 expression.

The following limitations should be acknowledged. The study was conducted in healthy normolipidemic pigs devoided of presence of comorbidities which are known to worsen cardiac damage and function upon acute coronary artery occlusion (240,241). Also, the acute ischaemic damage caused by coronary balloon inflation differs from coronary occlusion caused by atherothrombotic events.

In conclusion, despite the progress in prevention and treatment of AMI, post-STEMI survivors remain at high risk being the size of myocardial infarct, a critical determinant of survival and heart failure development (242,243). Infarct size develops during ischaemia and progresses upon reperfusion (176,178). Hence, cardioprotective agents with a rapid onset of action are needed. In the following study, we demonstrate that a single intravenous bolus of AZD3366 at 3mg/kg provides cardioprotection in the setting of STEMI on top of that provided by ticagrelor alone beyond a rapid, safe, and persistent inhibition of platelet activation. AZD3366 holds promise for emergency room treatment as well as pre-hospital use at any time after making the diagnosis of acute MI. The currently ongoing phase I clinical trial assessing AZD3366 pharmaceutical properties in healthy adults will provide us with valuable insights regarding its further translation to clinical use (244).

7. Conclusions

The conclusions of this thesis are the following:

1. Infusion of a soluble recombinant ADPase (AZD3366) on top of ticagrelor leads to enhanced and acute cardioprotection as compared to ticagrelor alone.

2. Left anterior descending (LAD) coronary ischaemia shows time-dependent features amenable to therapeutic interventions. As such, complete LAD coronary ischaemia for 30 minutes does not induce significant cardiac damage whereas 60-minute LAD coronary occlusion already induces cardiac structural and functional alterations. Longer coronary ischaemia times are needed to induce microvascular obstruction (90min) or adverse left ventricular remodeling (120 min).

3. Two independent CMR software tools (Medis Suite and CVI[42]) are interchangeable for biventricular volumes, oedema and MVO, yet, a single software tool is advised for serial LV mass and necrosis measurements. Preclinical studies need to validate their post-processing methods carefully to deliver reproducible results for a truly reliable bench-to- bedside translation.

8. Future directions and considerations

Cardioprotection will likely remain one of the major lines of translational and clinical research.

The main direction of future studies will fall into increasing translatability of pre-clinical results to clinical research. Two general lines, underlining rigorous study design, would aim to close the current translatability gap:

- A gradual approach (small animal models followed by large models) is mandatory to ensure early checkpoints of the feasibility of a novel therapeutic strategy. Only after robust results are achieved using this approach, clinical trials should be planned.
- Bedside-to-bench translation is recommended regarding the use of preclinical study imaging biomarkers, with appropriate assessment and validation of each method.

Specifically to the studies described in this work on healthy normolipidemic pigs, the presence of co-morbidities may increase cardiac damage and dysfunctional heart per- formance upon the acute coronary artery occlusion. Also, the damage caused by balloon inflation in this setting may differ from coronary occlusion in atherosclerosed human arteries. Further research in linking these settings would further help in translation.

Regarding the use of CMR, further studies expanding our knowledge on imaging biomarkers in translational studies – for example, further tissue characteristics, including novel tracers for myocardial inflammation and fibrosis, assessment of other markers of ventricular function such as strain and studying atrial involvement in cardiac remodelling – would be valuable.

9. Bibliography

1. Cardiovascular diseases (CVDs) [Internet]. [cited 2020 Jun 4]. Available from: https://www.who.int/news-room/fact-sheets/detail/cardiovascular-diseases-(cvds)

2. European Cardiovascular Disease Statistics 2017 [Internet]. [cited 2020 Jun 4]. Available from: https://www.bhf.org.uk/informationsupport/publications/statistics/european-cardiovascular-disease-statistics-2017

3. Virani Salim S., Alonso Alvaro, Benjamin Emelia J., Bittencourt Marcio S., Callaway Clifton W., Carson April P., et al. Heart Disease and Stroke Statistics—2020 Update: A Report From the American Heart Association. Circulation. 2020 Mar 3;141(9):e139–596.

4. Dai H, Much AA, Maor E, Asher E, Younis A, Xu Y, et al. Global, regional, and national burden of ischaemic heart disease and its attributable risk factors, 1990–2017: results from the Global Burden of Disease Study 2017. European Heart Journal - Quality of Care and Clinical Outcomes [Internet]. 2020 Oct 5 [cited 2021 Aug 6];(qcaa076). Available from: https://doi.org/10.1093/ehjqcco/qcaa076

5. Meyers HP, Bracey A, Lee D, Lichtenheld A, Li WJ, Singer DD, et al. Comparison of the ST-Elevation Myocardial Infarction (STEMI) vs. NSTEMI and Occlusion MI (OMI) vs. NOMI Paradigms of Acute MI. Journal of Emergency Medicine. 2021 Mar 1;60(3):273–84.

6. Thygesen K, Alpert JS, Jaffe AS, Chaitman BR, Bax JJ, Morrow DA, et al. Fourth universal definition of myocardial infarction (2018). Eur Heart J. 2019 Jan 14;40(3):237–69.

7. Libby P. History of Discovery: Inflammation in Atherosclerosis. Arterioscler Thromb Vasc Biol. 2012 Sep;32(9):2045–51.

8. Zaromitidou M, Siasos G, Papageorgiou N, Oikonomou E, Tousoulis D. Chapter 2 - Atherosclerosis and Coronary Artery Disease: From Basics to Genetics. In: Papageorgiou N, editor. Cardiovascular Diseases [Internet]. Boston: Academic Press; 2016 [cited 2021 Aug 6]. p. 3–24. Available from: https://www.sciencedirect.com/science/article/pii/B9780128033128000021

9. Libby P, Buring JE, Badimon L, Hansson GK, Deanfield J, Bittencourt MS, et al. Atherosclerosis. Nat Rev Dis Primers. 2019 Aug 16;5(1):1–18.

10. Libby P, Lichtman AH, Hansson GK. Immune effector mechanisms implicated in atherosclerosis: from mice to humans. Immunity. 2013 Jun 27;38(6):1092–104.

11. Llorente-Cortés V, Martínez-González J, Badimon L. LDL receptor-related protein mediates uptake of aggregated LDL in human

vascular smooth muscle cells. Arterioscler Thromb Vasc Biol. 2000 Jun;20(6):1572–9.

12. Jaiswal S, Natarajan P, Silver AJ, Gibson CJ, Bick AG, Shvartz E, et al. Clonal Hematopoiesis and Risk of Atherosclerotic Cardiovascular Disease. N Engl J Med. 2017 Jul 13;377(2):111–21.

13. Fuster JJ, MacLauchlan S, Zuriaga MA, Polackal MN, Ostriker AC, Chakraborty R, et al. Clonal hematopoiesis associated with TET2 deficiency accelerates atherosclerosis development in mice. Science. 2017 Feb 24;355(6327):842–7.

14. Huang H, Virmani R, Younis H, Burke AP, Kamm RD, Lee RT. The impact of calcification on the biomechanical stability of atherosclerotic plaques. Circulation. 2001 Feb 27;103(8):1051–6.

15. Criqui MH, Denenberg JO, Ix JH, McClelland RL, Wassel CL, Rifkin DE, et al. Calcium Density of Coronary Artery Plaque and Risk of Incident Cardiovascular Events. JAMA. 2014 Jan 15;311(3):271–8.

16. Schoenhagen P, Ziada KM, Kapadia SR, Crowe TD, Nissen SE, Tuzcu EM. Extent and Direction of Arterial Remodeling in Stable Versus Unstable Coronary Syndromes. Circulation. 2000 Feb 15;101(6):598–603.

17. Bittner DO, Mayrhofer T, Puchner SB, Lu MT, Maurovich-Horvat P, Ghemigian K, et al. Coronary Computed Tomography Angiography–Specific Definitions of High-Risk Plaque Features Improve Detection of Acute Coronary Syndrome. Circulation: Cardiovascular Imaging. 2018 Aug 1;11(8):e007657.

18. Arbustini E, Morbini P, Bello BD, Prati F, Specchia G. From plaque biology to clinical setting. American Heart Journal. 1999 Aug 1;138(2, Supplement):S55–60.

19. Dai J, Xing L, Jia H, Zhu Y, Zhang S, Hu S, et al. In vivo predictors of plaque erosion in patients with ST-segment elevation myocardial infarction: a clinical, angiographical, and intravascular optical coherence tomography study. Eur Heart J. 2018 Jun 7;39(22):2077–85.

20. Bagot CN, Arya R. Virchow and his triad: a question of attribution. British Journal of Haematology. 2008;143(2):180–90.

21. Chung I, Lip GYH. Virchow's Triad Revisited: Blood Constituents. PHT. 2003;33(5–6):449–54.

22. Koupenova M, Kehrel BE, Corkrey HA, Freedman JE. Thrombosis and platelets: an update. European Heart Journal. 2017 Mar 14;38(11):785–91.

23. Vilahur G, Gutiérrez M, Arzanauskaite M, Mendieta G, Ben-Aicha S, Badimon L. Intracellular platelet signalling as a target for drug development. Vascular Pharmacology. 2018 Dec 1;111:22–5.

24. Shin EK, Park H, Noh JY, Lim KM, Chung JH. Platelet Shape Changes and Cytoskeleton Dynamics as Novel Therapeutic Targets for Anti-Thrombotic Drugs. Biomol Ther (Seoul). 2017 May;25(3):223–30.

25. Badimon L, Vilahur G. Thrombosis formation on atherosclerotic lesions and plaque rupture. J Intern Med. 2014 Dec;276(6):618–32.

26. Torrent-Guasp F, Kocica MJ, Corno AF, Komeda M, Carreras-Costa F, Flotats A, et al. Towards new understanding of the heart structure and function. European Journal of Cardio-Thoracic Surgery. 2005 Feb 1;27(2):191–201.

27. Kilner PJ, McCarthy K, Murillo M, Ferreira P, Scott AD, McGill LA, et al. Histology of human myocardial laminar microstructure and consideration of its cyclic deformations with respect to interpretation of in vivo cardiac diffusion tensor imaging. Journal of Cardiovascular Magnetic Resonance. 2015 Feb 3;17(1):Q10.

28. Nielles-Vallespin S, Khalique Z, Ferreira PF, de Silva R, Scott AD, Kilner P, et al. Assessment of Myocardial Microstructural Dynamics by In Vivo Diffusion Tensor Cardiac Magnetic Resonance. Journal of the American College of Cardiology. 2017 Feb 14;69(6):661–76.

29. Buja LM. Myocardial ischemia and reperfusion injury. Cardiovascular Pathology. 2005 Jul 1;14(4):170–5.

30. Gutiérrez Gimeno M. Análisis de nuevas estrategias cardioprotectoras destinadas a modular el remodelado ventricular tras infarto agudo de miocardio : estudio preclínico y seguimiento mediante técnicas de imagen no invasiva de alta resolución [Internet]. 2020 [cited 2021 Aug 12]. Available from: https://ddd.uab.cat/record/233876

31. Maximilian Buja L. Mitochondria in Ischemic Heart Disease. Adv Exp Med Biol. 2017;982:127–40.

32. Wu MY, Yiang GT, Liao WT, Tsai APY, Cheng YL, Cheng PW, et al. Current Mechanistic Concepts in Ischemia and Reperfusion Injury. CPB. 2018;46(4):1650–67.

33. Braunwald E, Kloner RA. Myocardial reperfusion: a double-edged sword? J Clin Invest. 1985 Nov;76(5):1713–9.

34. Heusch G, Gersh BJ. The pathophysiology of acute myocardial infarction and strategies of protection beyond reperfusion: a continual challenge. Eur Heart J. 2017 Mar 14;38(11):774–84.

35. Kloner RA, Jennings RB. Consequences of brief ischemia: stunning, preconditioning, and their clinical implications: part 1. Circulation. 2001 Dec 11;104(24):2981–9.

36. Kloner RA, Jennings RB. Consequences of brief ischemia: stunning, preconditioning, and their clinical implications: part 2. Circulation. 2001 Dec 18;104(25):3158–67.

37. Ambrosio G, Betocchi S, Pace L, Losi MA, Perrone-Filardi P, Soricelli A, et al. Prolonged impairment of regional contractile function after resolution of exercise-induced angina. Evidence of myocardial stunning in patients with coronary artery disease. Circulation. 1996 Nov 15;94(10):2455–64.

38. Verma S, Fedak PWM, Weisel RD, Butany J, Rao V, Maitland A, et al. Fundamentals of Reperfusion Injury for the Clinical Cardiologist. Circulation. 2002 May 21;105(20):2332–6.

39. Abraham JM, Gibson CM, Pena G, Sanz R, AlMahameed A, Murphy SA, et al. Association of angiographic perfusion score following percutaneous coronary intervention for ST-elevation myocardial infarction with left ventricular remodeling at 6 weeks in GRACIA-2. J Thromb Thrombolysis. 2009 Apr;27(3):253–8.

40. Ibáñez B, Heusch G, Ovize M, Van de Werf F. Evolving Therapies for Myocardial Ischemia/Reperfusion Injury. Journal of the American College of Cardiology. 2015 Apr 14;65(14):1454–71.

41. Chiong M, Wang ZV, Pedrozo Z, Cao DJ, Troncoso R, Ibacache M, et al. Cardiomyocyte death: mechanisms and translational implications. Cell Death & Disease. 2011 Dec;2(12):e244–e244.

42. Heusch G, Kleinbongard P, Böse D, Levkau B, Haude M, Schulz R, et al. Coronary microembolization: from bedside to bench and back to bedside. Circulation. 2009 Nov 3;120(18):1822–36.

43. Gross GJ, O'Rourke ST, Pelc LR, Warltier DC. Myocardial and endothelial dysfunction after multiple, brief coronary occlusions: role of oxygen radicals. Am J Physiol. 1992 Dec;263(6 Pt 2):H1703-1709.

44. Sheridan FM, Dauber IM, McMurtry IF, Lesnefsky EJ, Horwitz LD. Role of leukocytes in coronary vascular endothelial injury due to ischemia and reperfusion. Circ Res. 1991 Dec;69(6):1566–74.

45. Higginson LA, White F, Heggtveit HA, Sanders TM, Bloor CM, Covell JW. Determinants of myocardial hemorrhage after coronary reperfusion in the anesthetized dog. Circulation. 1982 Jan;65(1):62–9.

46. Niccoli G, Burzotta F, Galiuto L, Crea F. Myocardial No-Reflow in Humans. Journal of the American College of Cardiology. 2009 Jul 21;54(4):281–92.

47. Niccoli G, Cosentino N, Spaziani C, Fracassi F, Tarantini G, Crea F. No-reflow: incidence and detection in the cath-lab. Curr Pharm Des. 2013;19(25):4564–75.

48. Prasad A, Gersh BJ, Mehran R, Brodie BR, Brener SJ, Dizon JM, et al. Effect of Ischemia Duration and Door-to-Balloon Time on Myocardial Perfusion in ST-Segment Elevation Myocardial Infarction: An Analysis From HORIZONS-AMI Trial (Harmonizing Outcomes with

Revascularization and Stents in Acute Myocardial Infarction). JACC Cardiovasc Interv. 2015 Dec 28;8(15):1966–74.

49. Reimer K A, Lowe J E, Rasmussen M M, Jennings R B. The wavefront phenomenon of ischemic cell death. 1. Myocardial infarct size vs duration of coronary occlusion in dogs. Circulation. 1977 Nov 1;56(5):786–94.

50. Ka R, Rb J. The "wavefront phenomenon" of myocardial ischemic cell death. II. Transmural progression of necrosis within the framework of ischemic bed size (myocardium at risk) and collateral flow. Lab Invest. 1979 Jun 1;40(6):633–44.

51. Gaudron P, Eilles C, Kugler I, Ertl G. Progressive left ventricular dysfunction and remodeling after myocardial infarction. Potential mechanisms and early predictors. Circulation. 1993 Mar;87(3):755–63.

52. Cohn JN, Ferrari R, Sharpe N. Cardiac remodeling--concepts and clinical implications: a consensus paper from an international forum on cardiac remodeling. Behalf of an International Forum on Cardiac Remodeling. J Am Coll Cardiol. 2000 Mar 1;35(3):569–82.

53. Fraccarollo D, Galuppo P, Bauersachs J. Novel therapeutic approaches to post-infarction remodelling. Cardiovasc Res. 2012 May 1;94(2):293–303.

54. Frangogiannis NG. The mechanistic basis of infarct healing. Antioxid Redox Signal. 2006 Dec;8(11–12):1907–39.

55. Shinde AV, Frangogiannis NG. Fibroblasts in myocardial infarction: A role in inflammation and repair. Journal of Molecular and Cellular Cardiology. 2014 May 1;70:74–82.

56. Sabbah HN, Stein PD, Kono T, Gheorghiade M, Levine TB, Jafri S, et al. A canine model of chronic heart failure produced by multiple sequential coronary microembolizations. Am J Physiol. 1991 Apr;260(4 Pt 2):H1379-1384.

57. Adams KF Jr. Pathophysiologic role of the renin-angiotensin-aldosterone and sympathetic nervous systems in heart failure. American Journal of Health-System Pharmacy. 2004 May 1;61(suppl_2):S4–13.

58. Floras JS. Clinical aspects of sympathetic activation and parasympathetic withdrawal in heart failure. J Am Coll Cardiol. 1993 Oct;22(4 Suppl A):72A-84A.

59. Mann DL, Kent RL, Parsons B, Cooper G. Adrenergic effects on the biology of the adult mammalian cardiocyte. Circulation. 1992 Feb;85(2):790–804.

60. Engelhardt S, Hein L, Wiesmann F, Lohse MJ. Progressive hypertrophy and heart failure in beta1-adrenergic receptor transgenic mice. Proc Natl Acad Sci U S A. 1999 Jun 8;96(12):7059–64.

61. Liu YH, Yang XP, Sharov VG, Nass O, Sabbah HN, Peterson E, et al. Effects of angiotensin-converting enzyme inhibitors and angiotensin II type 1 receptor antagonists in rats with heart failure. Role of kinins and angiotensin II type 2 receptors. J Clin Invest. 1997 Apr 15;99(8):1926–35.

62. Rocha R, Stier CT. Pathophysiological effects of aldosterone in cardiovascular tissues. Trends Endocrinol Metab. 2001 Sep;12(7):308–14.

63. Rocha R, Rudolph AE, Frierdich GE, Nachowiak DA, Kekec BK, Blomme EAG, et al. Aldosterone induces a vascular inflammatory phenotype in the rat heart. Am J Physiol Heart Circ Physiol. 2002 Nov;283(5):H1802-1810.

64. Brilla CG, Pick R, Tan LB, Janicki JS, Weber KT. Remodeling of the rat right and left ventricles in experimental hypertension. Circ Res. 1990 Dec;67(6):1355–64.

65. Verma A, Meris A, Skali H, Ghali JK, Arnold JMO, Bourgoun M, et al. Prognostic implications of left ventricular mass and geometry following myocardial infarction: the VALIANT (VALsartan In Acute myocardial iNfarcTion) Echocardiographic Study. JACC Cardiovasc Imaging. 2008 Sep;1(5):582–91.

66. Bolognese L, Neskovic AN, Parodi G, Cerisano G, Buonamici P, Santoro GM, et al. Left ventricular remodeling after primary coronary angioplasty: patterns of left ventricular dilation and long-term prognostic implications. Circulation. 2002 Oct 29;106(18):2351–7.

67. White HD, Norris RM, Brown MA, Brandt PW, Whitlock RM, Wild CJ. Left ventricular end-systolic volume as the major determinant of survival after recovery from myocardial infarction. Circulation. 1987 Jul;76(1):44–51.

68. Migrino RQ, Young JB, Ellis SG, White HD, Lundergan CF, Miller DP, et al. End-systolic volume index at 90 to 180 minutes into reperfusion therapy for acute myocardial infarction is a strong predictor of early and late mortality. The Global Utilization of Streptokinase and t-PA for Occluded Coronary Arteries (GUSTO)-I Angiographic Investigators. Circulation. 1997 Jul 1;96(1):116–21.

69. Solomon SD, Skali H, Anavekar NS, Bourgoun M, Barvik S, Ghali JK, et al. Changes in ventricular size and function in patients treated with valsartan, captopril, or both after myocardial infarction. Circulation. 2005 Jun 28;111(25):3411–9.

70. Chareonthaitawee P, Christian TF, Hirose K, Gibbons RJ, Rumberger JA. Relation of initial infarct size to extent of left ventricular remodeling in the year after acute myocardial infarction. Journal of the American College of Cardiology. 1995 Mar 1;25(3):567–73.

71. Orn S, Manhenke C, Anand IS, Squire I, Nagel E, Edvardsen T, et al. Effect of left ventricular scar size, location, and transmurality on left ventricular remodeling with healed myocardial infarction. Am J Cardiol. 2007 Apr 15;99(8):1109–14.

72. Larose E, Rodés-Cabau J, Pibarot P, Rinfret S, Proulx G, Nguyen CM, et al. Predicting late myocardial recovery and outcomes in the early hours of ST-segment elevation myocardial infarction traditional measures compared with microvascular obstruction, salvaged myocardium, and necrosis characteristics by cardiovascular magnetic resonance. J Am Coll Cardiol. 2010 Jun 1;55(22):2459–69.

73. Stone GW, Selker HP, Thiele H, Patel MR, Udelson JE, Ohman EM, et al. Relationship Between Infarct Size and Outcomes Following Primary PCI: Patient-Level Analysis From 10 Randomized Trials. J Am Coll Cardiol. 2016 Apr 12;67(14):1674–83.

74. Eapen Zubin J., Tang W.H. Wilson, Felker G. Michael, Hernandez Adrian F., Mahaffey Kenneth W., Lincoff A. Michael, et al. Defining Heart Failure End Points in ST-Segment Elevation Myocardial Infarction Trials. Circulation: Cardiovascular Quality and Outcomes. 2012 Jul 1;5(4):594–600.

75. Menees DS, Peterson ED, Wang Y, Curtis JP, Messenger JC, Rumsfeld JS, et al. Door-to-Balloon Time and Mortality among Patients Undergoing Primary PCI [Internet]. http://dx.doi.org/10.1056/NEJMoa1208200. Massachusetts Medical Society; 2013 [cited 2020 Jun 7]. Available from: https://www.nejm.org/doi/10.1056/NEJMoa1208200?url_ver=Z39.88-2003&rfr_id=ori%3Arid%3Acrossref.org&rfr_dat=cr_pub++0www.ncbi.nlm.nih.gov

76. Murry CE, Jennings RB, Reimer KA. Preconditioning with ischemia: a delay of lethal cell injury in ischemic myocardium. Circulation. 1986 Nov;74(5):1124–36.

77. Przyklenk K, Bauer B, Ovize M, Kloner RA, Whittaker P. Regional ischemic "preconditioning" protects remote virgin myocardium from subsequent sustained coronary occlusion. Circulation. 1993 Mar;87(3):893–9.

78. Liu GS, Thornton J, Van Winkle DM, Stanley AW, Olsson RA, Downey JM. Protection against infarction afforded by preconditioning is mediated by A1 adenosine receptors in rabbit heart. Circulation. 1991 Jul;84(1):350–6.

79. Laskey WK, Beach D. Frequency and clinical significance of ischemic preconditioning during percutaneous coronary intervention. Journal of the American College of Cardiology. 2003 Sep 17;42(6):998–1003.

80. Zhao ZQ, Corvera JS, Halkos ME, Kerendi F, Wang NP, Guyton RA, et al. Inhibition of myocardial injury by ischemic postconditioning during

reperfusion: comparison with ischemic preconditioning. Am J Physiol Heart Circ Physiol. 2003 Aug;285(2):H579-588.

81. Laskey WK. Brief repetitive balloon occlusions enhance reperfusion during percutaneous coronary intervention for acute myocardial infarction: a pilot study. Catheter Cardiovasc Interv. 2005 Jul;65(3):361–7.

82. Staat P, Rioufol G, Piot C, Cottin Y, Cung TT, L'Huillier I, et al. Postconditioning the human heart. Circulation. 2005 Oct 4;112(14):2143–8.

83. Bøtker HE, Kharbanda R, Schmidt MR, Bøttcher M, Kaltoft AK, Terkelsen CJ, et al. Remote ischaemic conditioning before hospital admission, as a complement to angioplasty, and effect on myocardial salvage in patients with acute myocardial infarction: a randomised trial. Lancet. 2010 Feb 27;375(9716):727–34.

84. Hahn JY, Song YB, Kim EK, Yu CW, Bae JW, Chung WY, et al. Ischemic postconditioning during primary percutaneous coronary intervention: the effects of postconditioning on myocardial reperfusion in patients with ST-segment elevation myocardial infarction (POST) randomized trial. Circulation. 2013 Oct 22;128(17):1889–96.

85. Engstrøm T, Kelbæk H, Helqvist S, Høfsten DE, Kløvgaard L, Clemmensen P, et al. Effect of Ischemic Postconditioning During Primary Percutaneous Coronary Intervention for Patients With ST-Segment Elevation Myocardial Infarction: A Randomized Clinical Trial. JAMA Cardiol. 2017 May 1;2(5):490–7.

86. Hausenloy DJ, Mwamure PK, Venugopal V, Harris J, Barnard M, Grundy E, et al. Effect of remote ischaemic preconditioning on myocardial injury in patients undergoing coronary artery bypass graft surgery: a randomised controlled trial. Lancet. 2007 Aug 18;370(9587):575–9.

87. Rentoukas I, Giannopoulos G, Kaoukis A, Kossyvakis C, Raisakis K, Driva M, et al. Cardioprotective Role of Remote Ischemic Periconditioning in Primary Percutaneous Coronary Intervention: Enhancement by Opioid Action. JACC: Cardiovascular Interventions. 2010 Jan 1;3(1):49–55.

88. Meybohm P, Bein B, Brosteanu O, Cremer J, Gruenewald M, Stoppe C, et al. A Multicenter Trial of Remote Ischemic Preconditioning for Heart Surgery. N Engl J Med. 2015 Oct 8;373(15):1397–407.

89. Hausenloy DJ, Candilio L, Evans R, Ariti C, Jenkins DP, Kolvekar S, et al. Remote Ischemic Preconditioning and Outcomes of Cardiac Surgery. N Engl J Med. 2015 Oct 8;373(15):1408–17.

90. Gaspar A, Lourenço AP, Pereira MÁ, Azevedo P, Roncon-Albuquerque R, Marques J, et al. Randomized controlled trial of remote ischaemic conditioning in ST-elevation myocardial infarction as adjuvant

to primary angioplasty (RIC-STEMI). Basic Res Cardiol. 2018 Mar 7;113(3):14.

91. Heusch G. 25 years of remote ischemic conditioning: from laboratory curiosity to clinical outcome. Basic Res Cardiol. 2018 Mar 7;113(3):15.

92. Francis R, Chong J, Ramlall M, Bucciarelli-Ducci C, Clayton T, Dodd M, et al. Effect of remote ischaemic conditioning on infarct size and remodelling in ST-segment elevation myocardial infarction patients: the CONDI-2/ERIC-PPCI CMR substudy. Basic Res Cardiol. 2021 Oct 14;116(1):59.

93. Meerson FZ, Gomzakov OA, Shimkovich MV. Adaptation to high altitude hypoxia as a factor preventing development of myocardial ischemic necrosis. The American Journal of Cardiology. 1973 Jan 1;31(1):30–4.

94. Mallet RT, Manukhina EB, Ruelas SS, Caffrey JL, Downey HF. Cardioprotection by intermittent hypoxia conditioning: evidence, mechanisms, and therapeutic potential. Am J Physiol Heart Circ Physiol. 2018 Aug 1;315(2):H216–32.

95. Guo Y, Chen J, Qiu H. Novel Mechanisms of Exercise-Induced Cardioprotective Factors in Myocardial Infarction. Frontiers in Physiology [Internet]. 2020 [cited 2022 Sep 13];11. Available from: https://www.frontiersin.org/articles/10.3389/fphys.2020.00199

96. Tao L, Bei Y, Lin S, Zhang H, Zhou Y, Jiang J, et al. Exercise Training Protects Against Acute Myocardial Infarction via Improving Myocardial Energy Metabolism and Mitochondrial Biogenesis. CPB. 2015;37(1):162–75.

97. Rodrigues F, Feriani DJ, Barboza CA, Abssamra MEV, Rocha LY, Carrozi NM, et al. Cardioprotection afforded by exercise training prior to myocardial infarction is associated with autonomic function improvement. BMC Cardiovascular Disorders. 2014 Jul 14;14(1):84.

98. Wojcik B, Knapp M, Gorski J. Non-ischemic heart preconditioning. J Physiol Pharmacol. 2018 Apr;69(2).

99. Marongiu E, Crisafulli A. Cardioprotection Acquired Through Exercise: The Role of Ischemic Preconditioning. Curr Cardiol Rev. 2014 Nov;10(4):336–48.

100. Heusch G. Molecular basis of cardioprotection: signal transduction in ischemic pre-, post-, and remote conditioning. Circ Res. 2015 Feb 13;116(4):674–99.

101. Hausenloy DJ, Barrabes JA, Bøtker HE, Davidson SM, Di Lisa F, Downey J, et al. Ischaemic conditioning and targeting reperfusion injury: a 30 year voyage of discovery. Basic Res Cardiol. 2016;111(6):70.

102. Bär FW, Tzivoni D, Dirksen MT, Fernández-Ortiz A, Heyndrickx GR, Brachmann J, et al. Results of the first clinical study of

adjunctive CAldaret (MCC-135) in patients undergoing primary percutaneous coronary intervention for ST-Elevation Myocardial Infarction: the randomized multicentre CASTEMI study. Eur Heart J. 2006 Nov;27(21):2516–23.

103. Kitakaze M, Asakura M, Kim J, Shintani Y, Asanuma H, Hamasaki T, et al. Human atrial natriuretic peptide and nicorandil as adjuncts to reperfusion treatment for acute myocardial infarction (J-WIND): two randomised trials. Lancet. 2007 Oct 27;370(9597):1483–93.

104. Lincoff AM, Roe M, Aylward P, Galla J, Rynkiewicz A, Guetta V, et al. Inhibition of delta-protein kinase C by delcasertib as an adjunct to primary percutaneous coronary intervention for acute anterior ST-segment elevation myocardial infarction: results of the PROTECTION AMI Randomized Controlled Trial. Eur Heart J. 2014 Oct 1;35(37):2516–23.

105. Najjar SS, Rao SV, Melloni C, Raman SV, Povsic TJ, Melton L, et al. Intravenous erythropoietin in patients with ST-segment elevation myocardial infarction: REVEAL: a randomized controlled trial. JAMA. 2011 May 11;305(18):1863–72.

106. Ibanez B, Macaya C, Sánchez-Brunete V, Pizarro G, Fernández-Friera L, Mateos A, et al. Effect of Early Metoprolol on Infarct Size in ST-Segment–Elevation Myocardial Infarction Patients Undergoing Primary Percutaneous Coronary Intervention. Circulation. 2013 Oct;128(14):1495–503.

107. Bulluck H, Sirker A, Loke YK, Garcia-Dorado D, Hausenloy DJ. Clinical benefit of adenosine as an adjunct to reperfusion in ST-elevation myocardial infarction patients: An updated meta-analysis of randomized controlled trials. International Journal of Cardiology. 2016 Jan 1;202:228–37.

108. Cung TT, Morel O, Cayla G, Rioufol G, Garcia-Dorado D, Angoulvant D, et al. Cyclosporine before PCI in Patients with Acute Myocardial Infarction. New England Journal of Medicine. 2015 Sep 10;373(11):1021–31.

109. Engstrøm T, Nepper-Christensen L, Helqvist S, Kløvgaard L, Holmvang L, Jørgensen E, et al. Danegaptide for primary percutaneous coronary intervention in acute myocardial infarction patients: a phase 2 randomised clinical trial. Heart. 2018 Oct;104(19):1593–9.

110. Dawson LP, Chen D, Dagan M, Bloom J, Taylor A, Duffy SJ, et al. Assessment of Pretreatment With Oral P2Y12 Inhibitors and Cardiovascular and Bleeding Outcomes in Patients With Non-ST Elevation Acute Coronary Syndromes: A Systematic Review and Meta-analysis. JAMA Network Open. 2021 Nov 19;4(11):e2134322.

111. Wiviott SD, Trenk D, Frelinger AL, O'Donoghue M, Neumann FJ, Michelson AD, et al. Prasugrel compared with high loading- and maintenance-dose clopidogrel in patients with planned percutaneous coronary intervention: the Prasugrel in Comparison to Clopidogrel for Inhibition of Platelet Activation and Aggregation-Thrombolysis in Myocardial Infarction 44 trial. Circulation. 2007 Dec 18;116(25):2923–32.

112. Montalescot G, Sideris G, Meuleman C, Bal-dit-Sollier C, Lellouche N, Steg PG, et al. A randomized comparison of high clopidogrel loading doses in patients with non-ST-segment elevation acute coronary syndromes: the ALBION (Assessment of the Best Loading Dose of Clopidogrel to Blunt Platelet Activation, Inflammation and Ongoing Necrosis) trial. J Am Coll Cardiol. 2006 Sep 5;48(5):931–8.

113. Hamilos M, Kanakakis J, Anastasiou I, Karvounis C, Vasilikos V, Goudevenos J, et al. Ticagrelor versus clopidogrel in patients with STEMI treated with thrombolysis: the MIRTOS trial [Internet]. EuroIntervention. [cited 2022 Aug 14]. Available from: https://eurointervention.pcronline.com/article/ticagrelor-versus-clopidogrel-in-patients-with-stemi-treated-with-thrombolysis-the-mirtos-trial

114. Elzanaty AM, Nazir S, Awad MT, Elsheikh E, Ahuja KR, Donato A, et al. Meta-Analysis of the Efficacy and Safety of P2Y12 Inhibitor Monotherapy After Short Course of Dual-Antiplatelet Therapy in Patients Undergoing Percutaneous Coronary Intervention. Cardiovasc Revasc Med. 2020 Dec;21(12):1500–6.

115. Badimon L, Padró T, Vilahur G. Atherosclerosis, platelets and thrombosis in acute ischaemic heart disease. Eur Heart J Acute Cardiovasc Care. 2012 Apr;1(1):60–74.

116. Wallentin L. P2Y(12) inhibitors: differences in properties and mechanisms of action and potential consequences for clinical use. Eur Heart J. 2009 Aug;30(16):1964–77.

117. Cohen MV, Downey JM. Combined cardioprotectant and antithrombotic actions of platelet P2Y12 receptor antagonists in acute coronary syndrome: just what the doctor ordered. J Cardiovasc Pharmacol Ther. 2014 Mar;19(2):179–90.

118. CAPRIE Steering Committee. A randomised, blinded, trial of clopidogrel versus aspirin in patients at risk of ischaemic events (CAPRIE). CAPRIE Steering Committee. Lancet. 1996 Nov 16;348(9038):1329–39.

119. Yusuf S, Zhao F, Mehta SR, Chrolavicius S, Tognoni G, Fox KK, et al. Effects of clopidogrel in addition to aspirin in patients with acute coronary syndromes without ST-segment elevation. N Engl J Med. 2001 Aug 16;345(7):494–502.

120. von Beckerath N, Taubert D, Pogatsa-Murray G, Schömig E, Kastrati A, Schömig A. Absorption, metabolization, and antiplatelet effects of 300-, 600-, and 900-mg loading doses of clopidogrel: results of the ISAR-CHOICE (Intracoronary Stenting and Antithrombotic Regimen: Choose Between 3 High Oral Doses for Immediate Clopidogrel Effect) Trial. Circulation. 2005 Nov 8;112(19):2946–50.

121. Vyas A, El Accaoui R, Blevins A, Karrowni W. Outcome comparison of 600 mg versus 300 mg loading dose of clopidogrel for patients with ST-elevation myocardial infarction: a meta-analysis. Postgrad Med. 2014 Sep;126(5):176–86.

122. Cuisset T, Frere C, Quilici J, Morange PE, Nait-Saidi L, Carvajal J, et al. Benefit of a 600-mg loading dose of clopidogrel on platelet reactivity and clinical outcomes in patients with non-ST-segment elevation acute coronary syndrome undergoing coronary stenting. J Am Coll Cardiol. 2006 Oct 3;48(7):1339–45.

123. Tokimasa S, Kitahara H, Nakayama T, Fujimoto Y, Shiba T, Shikama N, et al. Multicenter research of bleeding risk between prasugrel and clopidogrel in Japanese patients with coronary artery disease undergoing percutaneous coronary intervention. Heart Vessels. 2019 Oct;34(10):1581–8.

124. Gurbel PA, Bliden KP, Butler K, Tantry US, Gesheff T, Wei C, et al. Randomized double-blind assessment of the ONSET and OFFSET of the antiplatelet effects of ticagrelor versus clopidogrel in patients with stable coronary artery disease: the ONSET/OFFSET study. Circulation. 2009 Dec 22;120(25):2577–85.

125. Wallentin L, Becker RC, Budaj A, Cannon CP, Emanuelsson H, Held C, et al. Ticagrelor versus Clopidogrel in Patients with Acute Coronary Syndromes. New England Journal of Medicine. 2009 Sep 10;361(11):1045–57.

126. Bonaca MP, Bhatt DL, Cohen M, Steg PG, Storey RF, Jensen EC, et al. Long-Term Use of Ticagrelor in Patients with Prior Myocardial Infarction. New England Journal of Medicine. 2015 May 7;372(19):1791–800.

127. Akers WS, Oh JJ, Oestreich JH, Ferraris S, Wethington M, Steinhubl SR. Pharmacokinetics and pharmacodynamics of a bolus and infusion of cangrelor: a direct, parenteral P2Y12 receptor antagonist. J Clin Pharmacol. 2010 Jan;50(1):27–35.

128. Steg PG, Bhatt DL, Hamm CW, Stone GW, Gibson CM, Mahaffey KW, et al. Effect of cangrelor on periprocedural outcomes in percutaneous coronary interventions: a pooled analysis of patient-level data. The Lancet. 2013 Dec 14;382(9909):1981–92.

129. Franchi F, Rollini F, Rivas A, Wali M, Briceno M, Agarwal M, et al. Platelet Inhibition With Cangrelor and Crushed Ticagrelor in Patients With ST-Segment–Elevation Myocardial Infarction Undergoing Primary Percutaneous Coronary Intervention. Circulation. 2019 Apr 2;139(14):1661–70.

130. Gargiulo G, Esposito G, Avvedimento M, Nagler M, Minuz P, Campo G, et al. Cangrelor, Tirofiban, and Chewed or Standard Prasugrel Regimens in Patients With ST-Segment–Elevation Myocardial Infarction. Circulation. 2020 Aug 4;142(5):441–54.

131. De Luca L, Steg PG, Bhatt DL, Capodanno D, Angiolillo DJ. Cangrelor: Clinical Data, Contemporary Use, and Future Perspectives. J Am Heart Assoc. 2021 Jul 6;10(13):e022125.

132. Cohen MV, Yang XM, White J, Yellon DM, Bell RM, Downey JM. Cangrelor-Mediated Cardioprotection Requires Platelets and Sphingosine Phosphorylation. Cardiovasc Drugs Ther. 2016 Apr;30(2):229–32.

133. Vilahur G, Gutiérrez M, Casani L, Varela L, Capdevila A, Pons-Lladó G, et al. Protective Effects of Ticagrelor on Myocardial Injury After Infarction. Circulation. 2016 Nov 29;134(22):1708–19.

134. Mendieta G, Vilahur G, Gutierrez M, Casani L, Lambert C, Ben-Aicha S, et al. 3110Ticagrelor improves cardiac function and post-myocardial infarction healing: cardiac magnetic resonance imaging assessment of functional, anatomical and remodeling parameters. European Heart Journal [Internet]. 2017 Aug 1 [cited 2021 Jul 16];38(suppl_1). Available from: https://doi.org/10.1093/eurheartj/ehx504.3110

135. Kim AS, Miller EJ, Wright TM, Li J, Qi D, Atsina K, et al. A small molecule AMPK activator protects the heart against ischemia-reperfusion injury. J Mol Cell Cardiol. 2011 Jul;51(1):24–32.

136. Castanares-Zapatero D, Bouleti C, Sommereyns C, Gerber B, Lecut C, Mathivet T, et al. Connection between cardiac vascular permeability, myocardial edema, and inflammation during sepsis: role of the α1AMP-activated protein kinase isoform. Crit Care Med. 2013 Dec 1;41(12):e411-22.

137. Daskalopoulos EP, Dufeys C, Beauloye C, Bertrand L, Horman S. AMPK in Cardiovascular Diseases. Exp Suppl. 2016;107:179–201.

138. Noppe G, Dufeys C, Buchlin P, Marquet N, Castanares-Zapatero D, Balteau M, et al. Reduced scar maturation and contractility lead to exaggerated left ventricular dilation after myocardial infarction in mice lacking AMPKα1. J Mol Cell Cardiol. 2014 Sep;74:32–43.

139. Escobar DA, Botero-Quintero AM, Kautza BC, Luciano J, Loughran P, Darwiche S, et al. AMPK Activation Protects Against Sepsis-Induced Organ Injury and Inflammation. J Surg Res. 2015 Mar;194(1):262–72.

140. Triska J, Maitra N, Deshotels MR, Haddadin F, Angiolillo DJ, Vilahur G, et al. A Comprehensive Review of the Pleiotropic Effects of Ticagrelor. Cardiovasc Drugs Ther [Internet]. 2022 Aug 24 [cited 2022 Aug 26]; Available from: https://doi.org/10.1007/s10557-022-07373-5

141. Kaczmarek E, Koziak K, Sévigny J, Siegel JB, Anrather J, Beaudoin AR, et al. Identification and characterization of CD39/vascular ATP diphosphohydrolase. J Biol Chem. 1996 Dec 20;271(51):33116–22.

142. Borea PA, Gessi S, Merighi S, Vincenzi F, Varani K. Pharmacology of Adenosine Receptors: The State of the Art. Physiol Rev. 2018 Jul 1;98(3):1591–625.

143. Mazzola A, Amoruso E, Beltrami E, Lecca D, Ferrario S, Cosentino S, et al. Opposite effects of uracil and adenine nucleotides on the survival of murine cardiomyocytes. J Cell Mol Med. 2008 Apr;12(2):522–36.

144. Headrick JP, Hack B, Ashton KJ. Acute adenosinergic cardioprotection in ischemic-reperfused hearts. Am J Physiol Heart Circ Physiol. 2003 Nov;285(5):H1797-1818.

145. Vinten-Johansen J, Thourani VH, Ronson RS, Jordan JE, Zhao ZQ, Nakamura M, et al. Broad-spectrum cardioprotection with adenosine. Ann Thorac Surg. 1999 Nov;68(5):1942–8.

146. Zhao ZQ, Budde JM, Morris C, Wang NP, Velez DA, Muraki S, et al. Adenosine attenuates reperfusion-induced apoptotic cell death by modulating expression of Bcl-2 and Bax proteins. J Mol Cell Cardiol. 2001 Jan;33(1):57–68.

147. Caen JP, Jenkins CS, Michel H, Bellanger R. Adenosine inhibition of human platelet aggregation by ADP. Nat New Biol. 1972 Oct 18;239(94):211–3.

148. Feliu C, Peyret H, Brassart-Pasco S, Oszust F, Poitevin G, Nguyen P, et al. Ticagrelor Prevents Endothelial Cell Apoptosis through the Adenosine Signalling Pathway in the Early Stages of Hypoxia. Biomolecules. 2020 May 9;10(5):E740.

149. Eckle T, Krahn T, Grenz A, Köhler D, Mittelbronn M, Ledent C, et al. Cardioprotection by ecto-5'-nucleotidase (CD73) and A2B adenosine receptors. Circulation. 2007 Mar 27;115(12):1581–90.

150. Köhler D, Eckle T, Faigle M, Grenz A, Mittelbronn M, Laucher S, et al. CD39/ectonucleoside triphosphate diphosphohydrolase 1 provides myocardial protection during cardiac ischemia/reperfusion injury. Circulation. 2007 Oct 16;116(16):1784–94.

151. Jeong SS, Broekman MJ, Mitsky TA, Chen R, Marcus AJ. Antithrombotic Activity of a Novel Engineered Human Apyrase. Enzymatic Profile, Ex Vivo and In Vivo Properties. Blood. 2004 Nov 16;104(11):530.

152. Moeckel D, Jeong SS, Sun X, Broekman MJ, Nguyen A, Drosopoulos JHF, et al. Optimizing human apyrase to treat arterial thrombosis

and limit reperfusion injury without increasing bleeding risk. Sci Transl Med. 2014 Aug 6;6(248):248ra105.

153. Ji Y, Adeola O, Strawn TL, Jeong SS, Chen R, Fay WP. Recombinant soluble apyrase APT102 inhibits thrombosis and intimal hyperplasia in vein grafts without adversely affecting hemostasis or re-endothelialization. J Thromb Haemost. 2017 Apr;15(4):814–25.

154. Pennell DJ, Sechtem UP, Higgins CB, Manning WJ, Pohost GM, Rademakers FE, et al. Clinical indications for cardiovascular magnetic resonance (CMR): Consensus Panel report. Eur Heart J. 2004 Nov 1;25(21):1940–65.

155. Hendel RC, Patel MR, Kramer CM, Poon M, Hendel RC, Carr JC, et al. ACCF/ACR/SCCT/SCMR/ASNC/NASCI/SCAI/SIR 2006 appropriateness criteria for cardiac computed tomography and cardiac magnetic resonance imaging: a report of the American College of Cardiology Foundation Quality Strategic Directions Committee Appropriateness Criteria Working Group, American College of Radiology, Society of Cardiovascular Computed Tomography, Society for Cardiovascular Magnetic Resonance, American Society of Nuclear Cardiology, North American Society for Cardiac Imaging, Society for Cardiovascular Angiography and Interventions, and Society of Interventional Radiology. J Am Coll Cardiol. 2006 Oct 3;48(7):1475–97.

156. Ibanez B, Aletras AH, Arai AE, Arheden H, Bax J, Berry C, et al. Cardiac MRI Endpoints in Myocardial Infarction Experimental and Clinical Trials: JACC Scientific Expert Panel. Journal of the American College of Cardiology. 2019 Jul 16;74(2):238–56.

157. Vassiliou VS, Cameron D, Prasad SK, Gatehouse PD. Magnetic resonance imaging: Physics basics for the cardiologist. JRSM Cardiovascular Disease. 2018 Jan 1;7:2048004018772237.

158. Leiner T, Bogaert J, Friedrich MG, Mohiaddin R, Muthurangu V, Myerson S, et al. SCMR Position Paper (2020) on clinical indications for cardiovascular magnetic resonance. Journal of Cardiovascular Magnetic Resonance. 2020 Nov 9;22(1):76.

159. Eitel I, de Waha S, Wöhrle J, Fuernau G, Lurz P, Pauschinger M, et al. Comprehensive prognosis assessment by CMR imaging after ST-segment elevation myocardial infarction. J Am Coll Cardiol. 2014 Sep 23;64(12):1217–26.

160. Bulluck H, Dharmakumar R, Arai AE, Berry C, Hausenloy DJ. Cardiovascular Magnetic Resonance in Acute ST-Segment-Elevation Myocardial Infarction: Recent Advances, Controversies, and Future Directions. Circulation. 2018 May 1;137(18):1949–64.

161. Bellenger NG, Burgess MI, Ray SG, Lahiri A, Coats AJ, Cleland JG, et al. Comparison of left ventricular ejection fraction and volumes in

heart failure by echocardiography, radionuclide ventriculography and cardiovascular magnetic resonance; are they interchangeable? Eur Heart J. 2000 Aug;21(16):1387–96.

162. Eitel I, Friedrich MG. T2-weighted cardiovascular magnetic resonance in acute cardiac disease. J Cardiovasc Magn Reson. 2011 Feb 18;13(1):13.

163. Eitel I, Desch S, Fuernau G, Hildebrand L, Gutberlet M, Schuler G, et al. Prognostic significance and determinants of myocardial salvage assessed by cardiovascular magnetic resonance in acute reperfused myocardial infarction. J Am Coll Cardiol. 2010 Jun 1;55(22):2470–9.

164. Kim RJ, Wu E, Rafael A, Chen EL, Parker MA, Simonetti O, et al. The use of contrast-enhanced magnetic resonance imaging to identify reversible myocardial dysfunction. N Engl J Med. 2000 Nov 16;343(20):1445–53.

165. Kramer CM, Barkhausen J, Bucciarelli-Ducci C, Flamm SD, Kim RJ, Nagel E. Standardized cardiovascular magnetic resonance imaging (CMR) protocols: 2020 update. Journal of Cardiovascular Magnetic Resonance. 2020 Feb 24;22(1):17.

166. Lecour S, Bøtker HE, Condorelli G, Davidson SM, Garcia-Dorado D, Engel FB, et al. ESC working group cellular biology of the heart: position paper: improving the preclinical assessment of novel cardioprotective therapies. Cardiovasc Res. 2014 Dec 1;104(3):399–411.

167. Liao J, Huang W, Liu G. Animal models of coronary heart disease. J Biomed Res. 2017 Jan;31(1):3–10.

168. Badimon L, Mendieta G, Ben-Aicha S, Vilahur G. Post-Genomic Methodologies and Preclinical Animal Models: Chances for the Translation of Cardioprotection to the Clinic. Int J Mol Sci. 2019 Jan 25;20(3):E514.

169. Schaper W, Görge G, Winkler B, Schaper J. The collateral circulation of the heart. Prog Cardiovasc Dis. 1988 Aug;31(1):57–77.

170. Yang XM, Liu Y, Liu Y, Tandon N, Kambayashi J, Downey JM, et al. Attenuation of infarction in cynomolgus monkeys: preconditioning and postconditioning. Basic Res Cardiol. 2010 Jan;105(1):119–28.

171. Lilley E, Stanford SC, Kendall DE, Alexander SPH, Cirino G, Docherty JR, et al. ARRIVE 2.0 and the British Journal of Pharmacology: Updated guidance for 2020. British Journal of Pharmacology. 2020;177(16):3611–6.

172. Ji Y, Adeola O, Strawn TL, Jeong SS, Chen R, Fay WP. Recombinant soluble apyrase APT102 inhibits thrombosis and intimal hyperplasia in vein grafts without adversely affecting hemostasis or re-endothelialization. J Thromb Haemost. 2017 Apr;15(4):814–25.

173. Vilahur G, Casaní L, Badimon L. A thromboxane A2/prostaglandin H2 receptor antagonist (S18886) shows high antithrombotic efficacy in an experimental model of stent-induced thrombosis. Thromb Haemost. 2007 Sep;98(3):662–9.

174. Mendieta G, Ben-Aicha S, Gutiérrez M, Casani L, Aržanauskaitė M, Carreras F, et al. Intravenous Statin Administration During Myocardial Infarction Compared With Oral Post-Infarct Administration. J Am Coll Cardiol. 2020 Mar 23;75(12):1386–402.

175. Vilahur G, Gutiérrez M, Casani L, Lambert C, Mendieta G, Ben-Aicha S, et al. P2Y12 antagonists and cardiac repair post-myocardial infarction: global and regional heart function analysis and molecular assessments in pigs. Cardiovasc Res. 2018 Dec 1;114(14):1860–70.

176. Mendieta G, Ben-Aicha S, Casani L, Badimon L, Sabate M, Vilahur G. Molecular pathways involved in the cardioprotective effects of intravenous statin administration during ischemia. Basic Res Cardiol. 2019 Nov 28;115(1):2.

177. Vilahur G, Gutiérrez M, Casani L, Varela L, Capdevila A, Pons-Lladó G, et al. Protective Effects of Ticagrelor on Myocardial Injury After Infarction. Circulation. 2016 Nov 29;134(22):1708–19.

178. Kim TT, Dyck JRB. Is AMPK the savior of the failing heart? Trends Endocrinol Metab. 2015 Jan;26(1):40–8.

179. Radike M, Sutelman P, Ben-Aicha S, Gutiérrez M, Mendieta G, Alcover S, et al. A comprehensive and longitudinal cardiac magnetic resonance imaging study of the impact of coronary ischemia duration on myocardial damage in a highly translatable animal model. Eur J Clin Investigation [Internet]. 2022 Aug 20 [cited 2022 Aug 22]; Available from: https://onlinelibrary.wiley.com/doi/10.1111/eci.13860

180. Radiké M, Ben-Aicha S, Gutiérrez M, Hidalgo A, Badimón L, Vilahur G. Comparison of two cardiac magnetic resonance imaging postprocessing software tools in a pig model of myocardial infarction. Revista Española de Cardiología (English Edition) [Internet]. 2022 Jul 6 [cited 2022 Jul 12]; Available from: https://www.sciencedirect.com/science/article/pii/S1885585722001803

181. Triska J, Maitra N, Deshotels MR, Haddadin F, Angiolillo DJ, Vilahur G, et al. A Comprehensive Review of the Pleiotropic Effects of Ticagrelor. Cardiovasc Drugs Ther [Internet]. 2022 Aug 24 [cited 2022 Aug 26]; Available from: https://doi.org/10.1007/s10557-022-07373-5

182. Xu Z, Chen W, Zhang R, Wang L, Chen R, Zheng J, et al. Human Recombinant Apyrase Therapy Protects Against Myocardial Ischemia/Reperfusion Injury and Preserves Left Ventricular Systolic Function in Rats, as Evaluated by 7T Cardiovascular Magnetic Resonance Imaging. Korean J Radiol. 2020 Jun;21(6):647–59.

183. Birnbaum Y, Ye R, Chen H, Carlsson L, Whatling C, Fjellström O, et al. Recombinant Apyrase (AZD3366) Against Myocardial Reperfusion Injury. Cardiovasc Drugs Ther [Internet]. 2022 Feb 22 [cited 2022 Aug 29]; Available from: https://doi.org/10.1007/s10557-022-07329-9

184. Lecour S, Bøtker HE, Condorelli G, Davidson SM, Garcia-Dorado D, Engel FB, et al. ESC working group cellular biology of the heart: position paper: improving the preclinical assessment of novel cardioprotective therapies. Cardiovasc Res. 2014 Dec 1;104(3):399–411.

185. Lecour S, Andreadou I, Bøtker HE, Davidson SM, Heusch G, Ruiz-Meana M, et al. IMproving Preclinical Assessment of Cardioprotective Therapies (IMPACT) criteria: guidelines of the EU-CARDIOPROTECTION COST Action. Basic Res Cardiol. 2021 Sep 13;116(1):52.

186. Xu Z, Chen W, Zhang R, Wang L, Chen R, Zheng J, et al. Human Recombinant Apyrase Therapy Protects Against Myocardial Ischemia/Reperfusion Injury and Preserves Left Ventricular Systolic Function in Rats, as Evaluated by 7T Cardiovascular Magnetic Resonance Imaging. Korean J Radiol. 2020 Jun;21(6):647–59.

187. Thuny F, Lairez O, Roubille F, Mewton N, Rioufol G, Sportouch C, et al. Post-conditioning reduces infarct size and edema in patients with ST-segment elevation myocardial infarction. J Am Coll Cardiol. 2012 Jun 12;59(24):2175–81.

188. Piper HM, García-Dorado D. Prime causes of rapid cardiomyocyte death during reperfusion. Ann Thorac Surg. 1999 Nov;68(5):1913–9.

189. Kloner RA, Jennings RB. Consequences of brief ischemia: stunning, preconditioning, and their clinical implications: part 1. Circulation. 2001 Dec 11;104(24):2981–9.

190. Bulluck H, Dharmakumar R, Arai AE, Berry C, Hausenloy DJ. Cardiovascular Magnetic Resonance in Acute ST-Segment-Elevation Myocardial Infarction: Recent Advances, Controversies, and Future Directions. Circulation. 2018 May 1;137(18):1949–64.

191. Desmet W, Bogaert J, Dubois C, Sinnaeve P, Adriaenssens T, Pappas C, et al. High-dose intracoronary adenosine for myocardial salvage in patients with acute ST-segment elevation myocardial infarction. Eur Heart J. 2011 Apr;32(7):867–77.

192. Moeckel D, Jeong SS, Sun X, Broekman MJ, Nguyen A, Drosopoulos JHF, et al. Optimizing human apyrase to treat arterial thrombosis and limit reperfusion injury without increasing bleeding risk. Sci Transl Med. 2014 Aug 6;6(248):248ra105.

193. Gachet C. P2 receptors, platelet function and pharmacological implications. Thromb Haemost. 2008 Mar;99(3):466–72.

194. Barriuso I, Worner F, Vilahur G. Novel Antithrombotic Agents in Ischemic Cardiovascular Disease: Progress in the Search for the Optimal Treatment. J Cardiovasc Dev Dis. 2022 Nov 16;9(11):397.

195. Hjortbak MV, Olesen KKW, Seefeldt JM, Lassen TR, Jensen RV, Perkins A, et al. Translation of experimental cardioprotective capability of P2Y12 inhibitors into clinical outcome in patients with ST-elevation myocardial infarction. Basic Res Cardiol. 2021 May 26;116(1):36.

196. Busk M, Kaltoft A, Nielsen SS, Bøttcher M, Rehling M, Thuesen L, et al. Infarct size and myocardial salvage after primary angioplasty in patients presenting with symptoms for <12 h vs. 12-72 h. Eur Heart J. 2009 Jun;30(11):1322–30.

197. Nanhwan MK, Ling S, Kodakandla M, Nylander S, Ye Y, Birnbaum Y. Chronic treatment with ticagrelor limits myocardial infarct size: an adenosine and cyclooxygenase-2-dependent effect. Arterioscler Thromb Vasc Biol. 2014 Sep;34(9):2078–85.

198. Vilahur G, Casani L, Juan-Babot O, Guerra JM, Badimon L. Infiltrated cardiac lipids impair myofibroblast-induced healing of the myocardial scar post-myocardial infarction. Atherosclerosis. 2012 Oct;224(2):368–76.

199. Andreadou I, Schulz R, Badimon L, Adameová A, Kleinbongard P, Lecour S, et al. Hyperlipidaemia and cardioprotection: Animal models for translational studies. Br J Pharmacol. 2020 Dec;177(23):5287–311.

200. Chi GC, Kanter MH, Li BH, Qian L, Reading SR, Harrison TN, et al. Trends in Acute Myocardial Infarction by Race and Ethnicity. J Am Heart Assoc. 2020 Mar 3;9(5):e013542.

201. De Luca G, Suryapranata H, Ottervanger JP, Antman EM. Time delay to treatment and mortality in primary angioplasty for acute myocardial infarction: every minute of delay counts. Circulation. 2004 Mar 16;109(10):1223–5.

202. AstraZeneca. A Phase 1, Randomized, Single-blind, Placebo-controlled Study to Assess the Safety, Tolerability, Pharmacokinetics and Pharmacodynamics of AZD3366 in Healthy Men and Women of Non-Childbearing Potential Following: Part A: Single Ascending Dose Administration (Including Populations of Japanese and Chinese Subjects) Part B: Single Dose Administration of AZD3366 at One Dose Level or Placebo With Concomitant Repeated Dosing of Ticagrelor and Acetylsalicylic Acid [Internet]. clinicaltrials.gov; 2022 May [cited 2022 Aug 28]. Report No.: NCT04588727. Available from: https://clinicaltrials.gov/ct2/show/NCT04588727

203. Heusch G, Skyschally A, Kleinbongard P. Translation, Translation, Translation. Circulation Research. 2018 Sep 28;123(8):931–3.

204. Heusch G, Gersh BJ. Is Cardioprotection Salvageable? Circulation. 2020 Feb 11;141(6):415–7.

205. Heusch G. Myocardial ischaemia-reperfusion injury and cardioprotection in perspective. Nat Rev Cardiol. 2020 Dec;17(12):773–89.

206. Bøtker HE, Hausenloy D, Andreadou I, Antonucci S, Boengler K, Davidson SM, et al. Practical guidelines for rigor and reproducibility in preclinical and clinical studies on cardioprotection. Basic Res Cardiol. 2018 Aug 17;113(5):39.

207. Heusch G. Cardioprotection research must leave its comfort zone. European Heart Journal. 2018 Sep 21;39(36):3393–5.

208. Reimer KA, Vander Heide RS, Richard VJ. Reperfusion in acute myocardial infarction: effect of timing and modulating factors in experimental models. Am J Cardiol. 1993 Dec 16;72(19):13G-21G.

209. Fujiwara H, Matsuda M, Fujiwara Y, Ishida M, Kawamura A, Takemura G, et al. Infarct size and the protection of ischemic myocardium in pig, dog and human. Jpn Circ J. 1989 Sep;53(9):1092–7.

210. Näslund U, Häggmark S, Johansson G, Pennert K, Reiz S, Marklund SL. Effects of reperfusion and superoxide dismutase on myocardial infarct size in a closed chest pig model. Cardiovasc Res. 1992 Feb;26(2):170–8.

211. Silvis MJM, van Hout GPJ, Fiolet ATL, Dekker M, Bosch L, van Nieuwburg MMJ, et al. Experimental parameters and infarct size in closed chest pig LAD ischemia reperfusion models; lessons learned. BMC Cardiovasc Disord. 2021 Apr 12;21(1):171.

212. Bulluck H, Hammond-Haley M, Weinmann S, Martinez-Macias R, Hausenloy DJ. Myocardial Infarct Size by CMR in Clinical Cardioprotection Studies: Insights From Randomized Controlled Trials. JACC Cardiovasc Imaging. 2017 Mar;10(3):230–40.

213. Fernández-Jiménez R, Barreiro-Pérez M, Martin-García A, Sánchez-González J, Agüero J, Galán-Arriola C, et al. Dynamic Edematous Response of the Human Heart to Myocardial Infarction. Circulation. 2017 Oct 3;136(14):1288–300.

214. Heusch G. Coronary microvascular obstruction: the new frontier in cardioprotection. Basic Res Cardiol. 2019 Oct 15;114(6):45.

215. de Waha S, Patel MR, Granger CB, Ohman EM, Maehara A, Eitel I, et al. Relationship between microvascular obstruction and adverse events following primary percutaneous coronary intervention for ST-segment elevation myocardial infarction: an individual patient data pooled analysis from seven randomized trials. Eur Heart J. 2017 Dec 14;38(47):3502–10.

216. Redfield MM, Jacobsen SJ, Burnett JC, Mahoney DW, Bailey KR, Rodeheffer RJ. Burden of systolic and diastolic ventricular dysfunction in

the community: appreciating the scope of the heart failure epidemic. JAMA. 2003 Jan 8;289(2):194–202.

217. McKay RG, Pfeffer MA, Pasternak RC, Markis JE, Come PC, Nakao S, et al. Left ventricular remodeling after myocardial infarction: a corollary to infarct expansion. Circulation. 1986 Oct;74(4):693–702.

218. Legallois D, Hodzic A, Alexandre J, Dolladille C, Saloux E, Manrique A, et al. Definition of left ventricular remodelling following ST-elevation myocardial infarction: a systematic review of cardiac magnetic resonance studies in the past decade. Heart Fail Rev. 2022 Jan;27(1):37–48.

219. Campbell SE, Gerdes AM, Smith TD. Comparison of regional differences in cardiac myocyte dimensions in rats, hamsters, and guinea pigs. Anat Rec. 1987 Sep;219(1):53–9.

220. Ruijsink B, Puyol-Antón E, Oksuz I, Sinclair M, Bai W, Schnabel JA, et al. Fully Automated, Quality-Controlled Cardiac Analysis From CMR: Validation and Large-Scale Application to Characterize Cardiac Function. JACC: Cardiovascular Imaging. 2020 Mar 1;13(3):684–95.

221. Bhuva Anish N., Bai Wenjia, Lau Clement, Davies Rhodri H., Ye Yang, Bulluck Heeraj, et al. A Multicenter, Scan-Rescan, Human and Machine Learning CMR Study to Test Generalizability and Precision in Imaging Biomarker Analysis. Circulation: Cardiovascular Imaging. 2019 Oct 1;12(10):e009214.

222. Flett AS, Hasleton J, Cook C, Hausenloy D, Quarta G, Ariti C, et al. Evaluation of Techniques for the Quantification of Myocardial Scar of Differing Etiology Using Cardiac Magnetic Resonance. JACC: Cardiovascular Imaging. 2011 Feb;4(2):150–6.

223. Suinesiaputra A, Bluemke DA, Cowan BR, Friedrich MG, Kramer CM, Kwong R, et al. Quantification of LV function and mass by cardiovascular magnetic resonance: multi-center variability and consensus contours. Journal of Cardiovascular Magnetic Resonance. 2015 Jul 28;17(1):63.

224. Zange L, Muehlberg F, Blaszczyk E, Schwenke S, Traber J, Funk S, et al. Quantification in cardiovascular magnetic resonance: agreement of software from three different vendors on assessment of left ventricular function, 2D flow and parametric mapping. Journal of Cardiovascular Magnetic Resonance. 2019 Feb 21;21(1):12.

225. Handayani A, Sijens PE, Lubbers DD, Triadyaksa P, Oudkerk M, van Ooijen PMA. Influence of the Choice of Software Package on the Outcome of Semiquantitative MR Myocardial Perfusion Analysis. Radiology. 2013 Mar 1;266(3):759–65.

226. Messalli G, Palumbo A, Maffei E, Martini C, Seitun S, Aldrovandi A, et al. Assessment of left ventricular volumes with cardiac MRI:

comparison between two semiautomated quantitative software packages. Radiol med. 2009 Aug 1;114(5):718–27.

227. Mooij CF, de Wit CJ, Graham DA, Powell AJ, Geva T. Reproducibility of MRI Measurements of Right Ventricular Size and Function in Patients with Normal and Dilated Ventricles. J Magn Reson Imaging. 2008 Jul;28(1):67–73.

228. Germain P, Roul G, Kastler B, Mossard JM, Bareiss P, Sacrez A. Inter-study variability in left ventricular mass measurement Comparison between M-mode echography and MRI. Eur Heart J. 1992 Aug 1;13(8):1011–9.

229. Semelka RC, Tomei E, Wagner S, Mayo J, Kondo C, Suzuki J, et al. Normal left ventricular dimensions and function: interstudy reproducibility of measurements with cine MR imaging. Radiology. 1990 Mar 1;174(3):763–8.

230. Matheijssen NAA, Baur LHB, Reiber JHC, van der Velde EA, van Dijkman PRM, van der Geest RJ, et al. Assessment of left ventricular volume and mass by cine magnetic resonance imaging in patients with anterior myocardial infarction intra-observer and inter-observer variability on contour detection. Int J Cardiac Imag. 1996 Mar 1;12(1):11–9.

231. Clay S, Alfakih K, Messroghli DR, Jones T, Ridgway JP, Sivananthan MU. The reproducibility of left ventricular volume and mass measurements: a comparison between dual-inversion-recovery black-blood sequence and SSFP. Eur Radiol. 2006 Jan;16(1):32–7.

232. Karamitsos TD, Hudsmith LE, Selvanayagam JB, Neubauer S, Francis JM. Operator induced variability in left ventricular measurements with cardiovascular magnetic resonance is improved after training. J Cardiovasc Magn Reson. 2007;9(5):777–83.

233. Fieno DS, Kim RJ, Chen EL, Lomasney JW, Klocke FJ, Judd RM. Contrast-enhanced magnetic resonance imaging of myocardium at risk: Distinction between reversible and irreversible injury throughout infarct healing. Journal of the American College of Cardiology. 2000 Nov 15;36(6):1985–91.

234. Fernández-Jiménez Rodrigo, Barreiro-Pérez Manuel, Martin-García Ana, Sánchez-González Javier, Agüero Jaume, Galán-Arriola Carlos, et al. Dynamic Edematous Response of the Human Heart to Myocardial Infarction. Circulation. 2017 Oct 3;136(14):1288–300.

235. Goldman M R, Brady T J, Pykett I L, Burt C T, Buonanno F S, Kistler J P, et al. Quantification of experimental myocardial infarction using nuclear magnetic resonance imaging and paramagnetic ion contrast enhancement in excised canine hearts. Circulation. 1982 Nov 1;66(5):1012–6.

236. Wesbey GE, Higgins CB, McNamara MT, Engelstad BL, Lipton MJ, Sievers R, et al. Effect of gadolinium-DTPA on the magnetic relaxation times of normal and infarcted myocardium. Radiology. 1984 Oct;153(1):165–9.

237. Wesbey G, Higgins C B, Lanzer P, Botvinick E, Lipton M J. Imaging and characterization of acute myocardial infarction in vivo by gated nuclear magnetic resonance. Circulation. 1984 Jan 1;69(1):125–30.

238. Kim Raymond J., Fieno David S., Parrish Todd B., Harris Kathleen, Chen Enn-Ling, Simonetti Orlando, et al. Relationship of MRI Delayed Contrast Enhancement to Irreversible Injury, Infarct Age, and Contractile Function. Circulation. 1999 Nov 9;100(19):1992–2002.

239. Selvanayagam Joseph B., Kardos Attila, Francis Jane M., Wiesmann Frank, Petersen Steffen E., Taggart David P., et al. Value of Delayed-Enhancement Cardiovascular Magnetic Resonance Imaging in Predicting Myocardial Viability After Surgical Revascularization. Circulation. 2004 Sep 21;110(12):1535–41.

240. Choi Kelly M., Kim Raymond J., Gubernikoff George, Vargas John D., Parker Michelle, Judd Robert M. Transmural Extent of Acute Myocardial Infarction Predicts Long-Term Improvement in Contractile Function. Circulation. 2001 Sep 4;104(10):1101–7.

241. Kwong Raymond Y., Chan Anna K., Brown Kenneth A., Chan Carmen W., Reynolds H. Glenn, Tsang Sui, et al. Impact of Unrecognized Myocardial Scar Detected by Cardiac Magnetic Resonance Imaging on Event-Free Survival in Patients Presenting With Signs or Symptoms of Coronary Artery Disease. Circulation. 2006 Jun 13;113(23):2733–43.

242. Wu E, Ortiz JT, Tejedor P, Lee DC, Bucciarelli-Ducci C, Kansal P, et al. Infarct size by contrast enhanced cardiac magnetic resonance is a stronger predictor of outcomes than left ventricular ejection fraction or end-systolic volume index: prospective cohort study. Heart. 2008 Jun 1;94(6):730–6.

243. Gräni C, Eichhorn C, Bière L, Kaneko K, Murthy VL, Agarwal V, et al. Comparison of myocardial fibrosis quantification methods by cardiovascular magnetic resonance imaging for risk stratification of patients with suspected myocarditis. Journal of Cardiovascular Magnetic Resonance. 2019 Feb 28;21(1):14.

244. Gho JMIH, van Es R, van Slochteren FJ, Jansen of Lorkeers SJ, Hauer AJ, van Oorschot JWM, et al. A systematic comparison of cardiovascular magnetic resonance and high resolution histological fibrosis quantification in a chronic porcine infarct model. Int J Cardiovasc Imaging. 2017 Nov 1;33(11):1797–807.